NORTHWESTERN UNIVERSITY

The Refinement of Control Strategies for Cortically-Controlled Functional Electrical Stimulation

A DISSERTATION

SUBMITTED TO THE GRADUATE SCHOOL
IN PARTIAL FULFILLMENT OF THE REQUIREMENTS

For the degree

DOCTOR OF PHILOSOPHY

Field of Biomedical Engineering

By

Stephanie Naufel Naufel

EVANSTON, ILLINOIS

September 2017

Abstract

Paralysis resulting from spinal cord injury (SCI) is devastating, dramatically reducing the independence of affected individuals. Currently, functional electrical stimulation (FES), controlled by a patient's residual movements, is used clinically to restore a limited range of voluntary movement. However, if FES could be controlled using signals recorded from the brain, it might allow patients with high-level SCI to regain even more natural and sophisticated movements. Cortically-controlled FES has been successfully used in animal experiments and in preliminary human clinical trials, but it needs refinement before it can be fully translated to the clinic. Here I present three distinct studies, each of which addresses the improvement of a system control strategy. Taken together, my three studies offer insights that will improve the future implementation of cortically-controlled FES.

In my first study, I evaluated the ability to use peripheral nerve stimulation to selectively activate muscles for FES. I demonstrated that the Flat Interface Nerve Electrode (FINE) can selectively stimulate a subset of wrist and hand muscles, and that this stimulation is stable over a period of 4 months. In future implementations of FES, nerve stimulation can therefore be used to selectively stimulate a subset of muscles without the need to implant these muscles individually. This method may be especially useful for muscles which are difficult to individually implant and stimulate intramuscularly without current spillover.

Cortically-controlled FES also relies on the ability to accurately predict muscle signals (EMG) from neural activity in motor cortex (M1) using a mathematical algorithm, or neural "decoder". In my second and third studies, I address the question of how accurate a decoder needs to be, both for making accurate EMG predictions across behaviors, and for facilitating intuitive user control. No decoder can be expected to be perfect, but I also evaluate the brain's ability to adapt to imperfect decoders, which may ultimately enable the successful restoration of movement. I first examine the accuracy of a single decoder for predicting actual wrist EMG across three highly varied dynamical conditions: isometric forces, unloaded movements, and movements against an elastic load. To allow a decoder to perform well across these tasks, it needs to be trained on data from all three, and furthermore, needs to be nonlinear. Second, I evaluate the ability of monkeys to learn two different kinds of altered decoders: one that preserved the natural coactivation

patterns of muscles, and one that didn't. The monkeys are better able to learn to use the former decoder, and never accomplish all task goals in the latter case. Taken together, my results suggest that neural decoders should include robust multi-task training, and should account for nonlinearities in the motor system. They also suggest that imperfect EMG decoders can be learned, as long as they take into account the natural activation patterns of muscles. Overall, the results presented in this dissertation offer insights and tools that will improve the future implementation of cortically-controlled FES.

Acknowledgements

In my time at Northwestern, I have worked in many different teams, and have been inspired by the excellent scientists and clinicians that I've met and worked with over the past six years. I would first like to thank my committee members, Dr. Nicho Hatsopoulos, Dr. Eric Perreault, and Dr. Sandro Mussa-Ivaldi for their valuable feedback on my projects, as well as for their encouragement. I enjoyed consulting with them on my specific projects as well as on general scientific ideas. I would also like to thank Dr. Sara Solla, though she was not an official committee member, for serving as a mentor figure and role model for me. She approached every topic with enthusiasm, and was an expert at clearly and comprehensively explaining complicated topics – a skill that should be bottled and sold. I also thank my doctoral advisor, Dr. Lee Miller, for the resources and scientific advice he provided to me over the years. He was always ready and available to discuss new results and experimental plans, and was a role model of responsibility.

I would also like to thank my colleagues in the Miller lab for their helpful feedback on my projects, their collaboration, and for their general camaraderie. I especially thank Drs. Christian Ethier and Nicholas Sachs, who were patient mentors to me in my early years of graduate school. I also give my earnest thanks to Matt Perich, who was my main cheerleader for many years during this graduate adventure, for which I will forever be grateful.

I would like to thank our veterinary staff, especially Dr. Charlette Cain, Dr. Tracy Gluckman, and Dr. Rebecca Erickson, along with Carey Nichols, Danielle Stephens, Katie Mahoney, and Kourtney Wallace. These individuals all showed an earnest care for our animal subjects, and were quick and capable responders during emergencies. They were also patient with us when procedures ran long, which we sincerely appreciated. I would furthermore like to thank the plastic surgery residents who volunteered their time to help us with these long and complicated surgical procedures, which at times lasted up to 11 hours: Dr. Jennie Cheesborough, Dr. Michael Gart, Dr. Chad Purnell, Dr. Steve Lanier, and Dr. Elbert Vaca.

My research also included collaborations with a number of labs. I would first like to acknowledge Dr. Konrad Kording and Joshua Glaser. They both provided me with useful comments for how to write compelling scientific papers, and Josh's perseverance in trying so many different analyses was wonderful to behold, and greatly benefitted our joint project.

For their help and support for my rat experiments, I would like to thank Dr. Matt Tresch and Dr. Ben Rellinger. Matt very graciously let me use his lab setup for these experiments, and Ben patiently taught me how to conduct rat surgeries in general, as well as the specifics of implanting EMG wires in rat hindlimb muscles.

I would like to thank Dr. Mitra Hartmann, who was very kind to allow me to collaborate with her team on a somatosensory project. I really appreciated the opportunity to be involved in sensory research again, and I was inspired by Mitra's enduring and contagious excitement for science.

I would like to thank my colleagues at Case Western Reserve University, with whom we collaborated on the nerve stimulation experiments described in Chapter 2: Drs. Dustin Tyler, Natalie Brill, and Katherine Polasek. I found their nerve cuffs very exciting, and I was thankful to be a part of this project with them. I also thank Dr. Kate Murray and Rebecca Moore for assisting with the chronic nerve stimulation experiments we performed.

I would also like to acknowledge Drs. Steve Helms Tillery, Veronica Santos, and Jason Robert for being my mentors during my formative years as a researcher, and for their continued friendship and encouragement throughout my doctoral studies. I particularly thank Steve and Jason for believing in my idea to have graduate students in ethics to do a semester-long rotation in research labs. Not only did they procure the funding to make these ideas a reality, they also facilitated my ability to help oversee the pilot implementation of the program, even while I was at Northwestern.

I also thank my husband Jon, who has been a friend and confidant since Day 0, when we both arrived in Chicago for recruitment weekend, wondering if Northwestern was in our future. I also thank my supportive family members for their encouragement. I additionally extend my thanks to my friends, some of whom have navigated through graduate school with me, for their encouragement and exemplary resilience to life's obstacles. I feel lucky to be surrounded by such admirable people.

Finally, I would like to explicitly acknowledge my research subjects – Fish, Jaco, Jango, Kevin, Nacho, and Spike – for their cooperation and their contribution to science. Successful experiments required a trusting and tacit agreement between trainer and subject, and it was meaningful to me to build and maintain a relationship with each of these animals. Even after nearly a decade of primate research, the excitement of seeing a task "click" with a monkey has never faded for me. I took my responsibility to be an ethical researcher seriously, and sincerely hope the sacrifice of these animals has served to benefit a greater good.

Preface

In 1818, Mary Shelley published her famed novel Frankenstein, detailing the story of a scientist who creates a fearsome living being out of cadaver parts and a "spark" (Shelley 1818). While fantastical, some of her ideas were not completely foreign for the time. A few decades prior, Luigi Galvani had successfully elicited muscle contractions from dissected frog legs using electric current (Galvani 1791). His experiments were purportedly the inspiration behind Shelley's story, but even more importantly, they set the stage for a future of electrical stimulation to medically treat the human body. Today, as we rapidly approach the bicentennial of Frankenstein's publication, and are more than 200 years past Galvani's frog studies, several medical devices exist in the market that electrically stimulate the body, either to provide and restore functionality, or to treat illness. These devices include cochlear implants, which electrically stimulate the auditory nerve to provide a mode of hearing to the profoundly deaf (Wilson and Dorman 2017), and deep brain stimulation, which can treat the symptoms of Parkinson's disease, dystonia and even obsessive-compulsive disorder (Perlmutter and Mink 2006). There is also functional electrical stimulation (FES), a technique that uses electrical stimulation to activate muscles that have been paralyzed by spinal cord injury, or other movement disorders. Researchers have recently developed a cortically-controlled FES system, which promises to allow paralyzed individuals to control muscle stimulation directly from their own neural activity (Moritz, Perlmutter, and Fetz 2008; Pohlmeyer et al. 2008; C Ethier et al. 2012). Such a system has recently been demonstrated in human clinical trials with some degree of success (Bouton et al. 2016; Ajiboye et al. 2017), but control strategies need to be refined before this technology can completely translate into the clinic. In this thesis, I address ideas for improving the implementation of cortically-controlled FES, with the hope that it may one day join the ranks of the remarkable neurostimulation devices currently in the market.

List of Abbreviations

AI	Artificial intelligence
ASU	Arizona State University
BMI	Brain-machine interface
cFINE	Composite Flat Interface Nerve Electrode
CWRU	Case Western Reserve University
DBS	Deep brain stimulation
DoF	Degree of freedom
EEG	Electroencephalogram
ECoG	Electrocochleography
EMG	Electromyography
FES	Functional electrical stimulation
FINE	Flat Interface Nerve Electrode
FMA	Floating microelectrode array
ICMS	Intracortical microstimulation
LIFE	Longitudinal Intrafascicular Electrode
LFP	Local field potential(s)
LMA	Linear microelectrode array
LSTM	Long Short-term Memory
MUA	Multi-unit activity
M1	Motor cortex
PAM	Pulse-amplitude modulation
PIC	Persistent inward current
PD	Preferred direction
PTN	Pyramidal tract neuron
PWM	Pulse-width modulation
RNN	Recurrent neural network

S1	Primary somatosensory cortex
SCI	Spinal cord injury
SUA	Single-unit activity
TIME	Transverse intrafascicular multi-channel electrode
NHP	Non-human primate
UC	University of Chicago
USEA	Utah slant-electrode array

Dedication

I dedicate this thesis to my late lab colleague and friend, Kevin Bair. He was dedicated, optimistic, well-rounded, and an excellent role model to his fellow graduate students.

Table of Contents

Table of Figures

Table of Tables

1 Introduction

1.1 Functional Electrical Stimulation

Functional electrical stimulation (FES) is a technique that is used to electrically activate paralyzed muscles (Lynch and Popovic 2008). This technique can be used for a variety of rehabilitation purposes, such as for restoring bladder and respiratory control, relieving pressure sores, to counter muscle atrophy, and for the general restoration of movement. FES can be a viable option for individuals with spinal cord injury, stroke, or other movement disorders. It typically works by stimulating the nerves that innervate muscles, rather than the actual muscle fibers themselves. During FES, an electrical pulse is delivered to the nerve, which causes an action potential to propagate down the nerve to the neuromuscular junction – where the motor neuron synapses onto muscle – mimicking the process that occurs during the normal control of muscle contraction. For individuals who do have denervation, FES is technically possible, but it would have to be used to stimulate the individual muscle fibers directly. This would require high levels of current that would be unsafe, especially with prolonged FES use (Lynch and Popovic 2008).

During natural movement, the nervous system sequentially activates motor units to cause a single muscle to contract, and this asynchronous recruitment works to prevent the muscle from fatiguing quickly. FES systems, however, cannot stimulate muscle fibers in this asynchronous pattern. Frequencies between 20-40 Hz are typically required to stimulate all the fibers synchronously and produce a sustained contraction (Lynch and Popovic 2008). While effective, this method also leads to rapid muscle fatigue, which remains a major challenge for FES. Fatigue is also difficult to avoid because FES reportedly recruits fast-twitch fibers before slow-twitch fibers, opposite to the natural order of recruitment. This is because fast-twitch fibers, which fatigue more rapidly than their slow-twitch counterparts, are innervated by larger axons, and therefore easier to stimulate.

The main components of an FES system includes a power source, a control unit, sensors, a stimulator, and stimulating electrodes (Ragnarsson 2008). The stimulating electrodes can either be placed on the surface of the skin, implanted on the surface of the actual muscle, or implanted in the muscle belly. Muscles can also be stimulated using electrodes that interface with a major nerve trunk, either by wrapping around the nerve, or by penetrating nerve fascicles (see *BMI methodology*). The two major methods for stimulation

include pulse width modulation (PWM) and pulse amplitude modulation (PAM). Both methods are used for eliciting muscle contraction in this dissertation (Chapter 2).

1.2 FES for grasp

According to a national survey, the highest priority for quadriplegics is the restoration of hand and arm function (Anderson 2004). The first FDA-approved FES system for grasp was the Freehand System, which received FDA approval in 1997 (Peckham et al. 2001). This system restored muscle activity to individuals with C5-C6 level spinal cord injury. Shoulder muscles are not affected at this level of spinal cord injury, and were therefore used as a control signal for the system. An external position sensor was placed over the contralateral shoulder, requiring the user to move the shoulder to activate two types of grasp. The first grasp type, lateral pinch, allows the thumb to press down against the index finger in such a way that could allow the hand to grasp a tool, such as a spoon or a pen. The second grasp type, called palmar prehension or palmar grasp, brings the thumb to meet the fingers in a way that allows for a wider grasp, as might be employed to pick up a block, or a glass of water. For various reasons, the Freehand System eventually went off the market in 2001.

The next generation version of the Freehand System is the Implanted Stimulator Telemeter Twelve-channel System (IST-12) (Kilgore et al. 2008). This system improves upon the original design by including more stimulating electrodes, and gets rid of the external shoulder position sensor in favor of implanted recording electrodes. Depending on the subject, these electrodes are implanted in residual shoulder, neck, or face muscles, and are implanted on the same side of the body as the device. In addition to the two types of grasp described above, the IST-12 could also stimulate the arm to produce forearm pronation and elbow extension.

In addition to the Freehand System and the IST-12 system, both of which were developed at Case Western University, other FES systems have been developed in the past few decades. One such system is the Bionic Glove, which was developed at the University of Alberta in 1989 to serve level C6-C7 spinal cord injury patients (Prochazka et al., 1997). This technology consists of a fingerless glove that uses surface muscle stimulation to produce grasp. It is currently marketed by Rehabtronics, Inc as the ReGrasp

stimulator system, and uses residual wrist movement as a control signal to stimulate finger extensors and flexors. Yet another FES for grasp device is the NESS H200, or Handmaster, which is currently marketed by Bioness, Inc. in southern California (Snoek et al. 2000; Venugopalan et al. 2015). This device consists of a forearm splint, which is used to hold surface electrodes in place over forearm muscles. The system can activate three different exercise modes for rehabilitation, as well as the usual key/pinch and palmar grasp to restore functional capabilities. Stimulation is controlled by a remote with push buttons that are controlled by the user. The Handmaster is best suited for SCI users with C4-C6 injury levels, as well as victims of stroke or other movement disorders that cause impairment of grasp.

Shortcomings of current FES systems and how to move forward

Despite the development of a number of FES systems for grasp, these systems generally share similar shortcomings. All of these systems, for example, provide only a few grasp possibilities to the user – typically a pinch grasp, a palmar grasp, and sometimes other types of muscle activation such as elbow extension or forearm pronation. Unfortunately, systems do not facilitate individuated finger movements. This may in large part be due to the difficulty in stimulating the intrinsic muscles of the hand. The small size of these muscles make them difficult to implant, and furthermore difficult to stimulate individually without current spillover to adjacent muscles. Another reason may be the limitations of the FES controller, which at present is very simple. In many systems, a simple control signal activates a preprogrammed grasp. This single degree-of-freedom control does not allow for the sophistication required to activate fingers individually.

Other FES system shortcomings include the unintuitive methods of control. Actions such as a shrugging the shoulder to activate the hand, for example, impose unusual cognitive load on the user, who has to adopt new patterns of movement in order to restore simple grasp. For systems that require control of a push button on a remote, this adds extra steps to the production of simple grasp. Furthermore, the users must still have enough residual abilities to control the remote. These types of controllers are therefore impractical for patients with very high-level SCI, who may not have any residual limb or even neck movements. For these patients, the brain is the remaining practical and natural controller post-injury.

Recording from the brain, however, allows for a natural and sophisticated controller, and using neural signals for control can potentially direct a wider range of movements for the patient. Neuroscience research in fact has demonstrated the ability to make predictions of individual muscle activity based on neural activity in motor cortex (M1). These principles have recently been used to develop cortically-control FES systems (Moritz, Perlmutter, and Fetz 2008; Pohlmeyer, Oby, et al. 2009; Ethier et al. 2012). In these systems, neural activity in M1 is decoded to predict intended EMG activity, and these predictions are translated into stimulation commands that in turn activate the muscles (**Figure 1-1**). These FES systems have been used to restore functional grasp in monkeys (C Ethier et al. 2012), and are now also being tested in paralyzed human subjects (Bouton et al. 2016; Ajiboye et al. 2017). This early success is promising, but there is still a need for the refinement of the control strategies that are currently being used for cortically-controlled FES. This includes improving ways to activate individual muscles, and improving the decoding methods for predicting EMG activity. These are the main topics that will be addressed in this dissertation. However, to understand how to refine a cortically-controlled FES system, which serves as a substitute for the motor system, one must first understand how motor cortex controls movement.

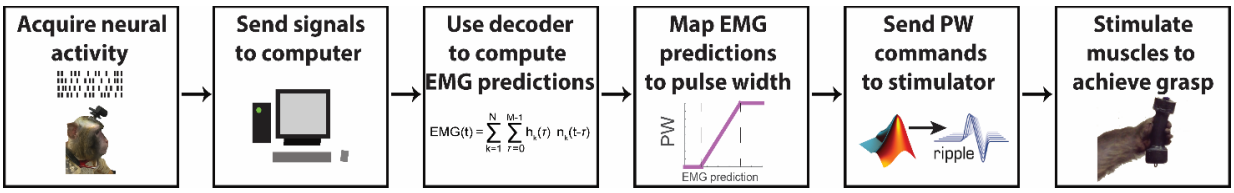

Figure 1-1. Cortically-controlled FES system. Signals recorded from motor cortex are routed to a computer, which using an algorithm, called a neural "decoder" to translate signals into predictions of muscle activity. These predictions are then mapped to pulse width parameters, which are used to stimulate the muscles to produce grasp.

1.3 How motor cortex controls movement

Despite decades of research and a variety of experimental paradigms, a conclusive understanding of how motor cortex produces movement remains elusive. In recent decades, different camps of thought have arisen, each with their own ideas on how neural activity in motor cortex relates to movement. Most of these groups employ similar physiological methods for recording signals, but vary with regard to the movement variables they focus on. Some experiments examine the relationship between neurons and kinematic variables such as limb position and velocity. Others aim to describe how neural activity correlates

to individual muscle activity or force. A seminal study, which evaluated the relationship of M1 to movement variables, was performed by Evarts in 1968. He recorded from individual pyramidal tract neurons (PTNs) in monkeys while they performed a task that required making flexion and extension movements about the wrist. The force that the monkeys had to exert was dissociated from movement direction, in order to separate out the variables (Evarts 1968). Overall, Evarts found that PTNs correlated more strongly to force and dF/dt than to displacement.

Similar studies over the next few decades added to this general finding. In 1970, Humphrey and colleagues repeated the general premise of the Evarts experiment, but with the ability to record from more than one neuron simultaneously (Humphrey, Schmidt, and Thompson 1970). This allowed them to compute simple relationships between neural activity and movement variables using linear regression. They predicted position, velocity, force, and dF/dt, and found that they could best predict force from their small population of neurons, though the other three variables could also be predicted, just with less accuracy. A few years later, Thach revisited the general Evarts and Humphrey experimental paradigm to evaluate the relationship of neurons in M1 and the cerebellum to muscle activity, wrist joint position, and intended movement direction. He reported that M1 cells could be split into three categories, each relating to a different movement variable. However, M1 cells that were related to wrist joint position were often also related to movement direction, and vice versa (Thach 1978). Other notable studies from this era include an experiment by Cheney and Fetz to characterize the relationship of corticomotoneural (CM) cells to active force (Cheney and Fetz 1980). They reported correlations between CM discharge and active torque during an isometric task and movements against an elastic load, and also described the different firing rate characteristics of the CM cells. While some cells fired tonically in relation to ramp-and-hold torque, for example, others ramped their firing, while others still fired with a phasic burst, followed by tonic or ramp activity. Taken together, these studies demonstrate the ability of M1 firing to correlate to a variety of movement variables, such as EMG, position, and principally force and torque.

A new theory on how motor cortex encodes movement arose in the 1980s, which for many introduced a significant shift of thought (a P. Georgopoulos et al. 1982; A. Georgopoulos et al. 1983; A. P. Georgopoulos, Schwartz, and Kettner 1986). The seminal study came from Georgopoulos and colleagues,

who evaluated M1 firing rates while monkeys made arm movements in eight directions, spaced equally at 45 degree intervals. For 75% of their 241 task-relevant neurons, they were able to identify a "preferred direction", or PD (A. P. Georgopoulos et al. 1982). This preferred direction could be described by the equation, Firing Rate = $b_0 + c_1*\cos(\theta - \theta_0)$, where b_0 and c_1 are regression coefficients, θ is the direction of movement, and θ_0 is the preferred direction, or the direction at which the neuron fired maximally. This study promulgated the idea that cells could change their firing rates in an orderly fashion with movement direction, and furthermore, that cells fired maximally for a particular movement direction.

Following the introduction of the preferred direction theory, a number of studies began to highlight the relationship between neural activity in motor cortex and kinematic variables. Several of these early studies came from Schwartz and colleagues, who demonstrated the correlation between M1 firing rates and both speed and direction (Moran and Schwartz 1999; Schwartz 1993; Schwartz and Moran 2000; Schwartz 1992), though many other groups have also demonstrated M1's relationship to kinematic variables (i.e. Alexander and Crutcher 1990; Caminiti, Johnson, and Urbano 1990; Fu et al. 1995; Paninski et al. 2004) These kinematic studies, taken into consideration with the number of experiments that relate M1 activity to force and EMG, demonstrate the ability of M1 to encode a number of movement variables. There remains no unanimous consensus on which variable may be the most reliably represented in M1, though some studies have demonstrated the superior robustness of the M1 to EMG relationship over kinematics across both workspaces and loads (Morrow, Jordan, and Miller 2007; Cherian, Krucoff, and Miller 2011).

While researchers may not completely agree on which movement variable is more reliably encoded by M1, the fact that many variables can be decoded is advantageous for the development of medical devices that restore movement. By using M1 to predict endpoint position and velocity, for example, a system can be developed that controls a cursor or a robot using a person's neural activity alone. These types of devices would be useful for people with paralysis or amputees, either to complete tasks using a computer, or by using a robotic limb to interact with the world. Alternatively, by using M1 to predict muscle activity, an FES system can be developed that allows individuals to control muscle stimulation using neural activity. All of these types of devices are in fact currently in development, and are referred to as motor brain-machine

interfaces (BMIs). They offer enormous potential for helping individuals with movement disorders resume activities of daily living, and future research will continue to increase their clinical viability in coming years.

1.4 Motor brain-machine interfaces

Motor BMIs involve computing a "neural decoder", the term used to describe any algorithm that correlates neural activity to an external movement variable, such as force, muscle activity, joint angles, or endpoint position, velocity, or acceleration. In many of the BMI studies performed in monkeys, researchers develop the neural decoders by first having the monkey complete a task with its arm or hand, and simultaneously collecting neural and movement data (force, kinematics, muscle activity). Other experiments use compute "observation-based decoders", where the subject typically observes the motion of a computer cursor as it acquires targets on a screen. In all cases, neural activity as well as movement data is simultaneously recorded during this training period in order to compute the neural decoder. In the next step of the experiment, the subject is asked to modulate its neural activity in order to use the decoder to complete a task, such as controlling a computer cursor, a robot, or muscle stimulation for FES.

The earliest demonstration of a real-time motor BMI was shown in rats, in a simple experiment where rats were able to activate neurons in order to control the proportional 1D movement of a lever (Chapin et al. 1999). The same group followed up this experiment with a study in monkeys, where they demonstrated that three-dimensional signals could be used to control the endpoint position of robotic arms (Wessberg et al. 2000). While in this experiment, the monkey did not see the predicted robot movements, Serruya et al. (Serruya et al. 2002), as well as Taylor, Helms Tillery, and Schwartz subsequently demonstrated the importance of a "closed-loop" BMI paradigm where visual feedback about predictions are provided, allowing the monkey to make corrective movements and adapt (Taylor, Helms Tillery, and Schwartz 2002). Schwartz subsequently followed up this study with an experiment that demonstrated the cortically-controlled use of a robotic arm for self-feeding (Velliste et al. 2008).

Not long after the initial BMI successes in monkeys, researchers at Brown University began piloting experiments in human subjects using a BMI system dubbed BrainGate. In 2004, Matthew Nagle became the first human subject to test the system. Nagle had suffered a spinal cord injury three years prior to the

clinical trial, the result of a knife wound between the C3 and C4 vertebrae. Despite this injury, he was able to successfully modulate neurons in motor cortex to control the position of a cursor on a computer (Hochberg et al. 2006). This opened a new world of control for him, enabling him to check email, operate a television, and even play the classic computer game Pong. He was further able to demonstrate the ability to open and close a robot hand using one-dimensional proportional control, and could use a simple robot to move objects from point A to point B.

Since Nagle, BMIs have increased in sophistication. In the BrainGate2 clinical trials, two human subjects with tetraplegia due to brainstem stroke were able to use a BMI to control two-different types of robotic arms to perform a reach-to-grasp task (Hochberg et al. 2012). One subject was further able to demonstrate to ability to feed herself by moving the robot to bring a cup of coffee to her mouth, which she was able to drink from using a straw. While this study used velocity-predictions to translate the robotic hand in space, other clinical trials extended the capabilities of a BMI to predicting orientation as well as translation. In a trial performed at the University of Pittsburgh, a 52-year old tetraplegic with spinocerebellar degeneration was able to control 7 degrees of freedom (DoF) of a robot arm (Collinger et al. 2013). This included the ability to control three dimensions of translation, three dimensions of orientation, and one-dimension for hand grasp. This subject was later able to control 10 DoF, where the one-dimensional grasp was replaced with four types of hand shapes: pinch, scoop, finger abduction, and thumb opposition (Wodlinger et al. 2015).

While the above BMIs are centered on predicting kinematic variables such as position and velocity, BMI use has also been successful for FES applications. The first example of a BMI for FES came from the University of Washington, where researchers demonstrated the ability to use single cells from motor cortex to control the stimulation of temporarily paralyzed wrist extensors (Moritz, Perlmutter, and Fetz 2008). Pohlmeyer and colleagues at Northwestern University subsequently published a study that further established the viability of neural decoders for FES (Pohlmeyer, Oby, et al. 2009) In this study, they demonstrated the ability of monkeys to control the stimulation of four wrist muscles. Later, the same lab extended the use of cortically-controlled FES to the restoration of functional grasp (Ethier et al. 2012). In this experiment, the monkeys were able to use neural decoders to control stimulation of wrist and finger

flexors in order to grasp and drop a ball down a tube. They were further able to control varying and distinct levels of grasp force.

Aside from monkey experiments, human clinical trials for cortically-controlled FES have also recently begun. One collaboration between Ohio State University and the research firm Battelle in Ohio demonstrated successful FES use in a 24-year old patient with a C5/C6 level spinal cord injury (Bouton et al. 2016). They used a flexible sleeve of surface stimulation electrodes that wrapped around the forearm to activate muscles, and the subject was able to able to control wrist and isolated finger movements, and could complete several functional tasks, such as grasping objects, and pouring from a bottle. In another experiment, researchers at Case Western Reserve University have recently demonstrated BMI use for FES in a BrainGate2 clinical trial (Ajiboye et al. 2017). Their subject was a 53-year old man with a level C4 spinal cord injury. While he maintained residual shoulder girdle movement, he was paralyzed below the shoulder with no sensory feedback. Using his BMI, he was able to cortically-control muscle activation patterns and could complete functional activities, such as drinking a beverage and self-feeding.

1.5 Neural decoders for BMIs

In addition to the impressive demonstrations of BMI use above, countless studies have been performed, primarily in monkeys, to further develop these systems. As described above, neural decoders for BMI translate neural activity into movement variables, such as position, velocity, force, or muscle activity. Most decoders typically use neural activity from M1 as their input, but others use activity from other brain areas such as premotor cortex, particularly dorsal premotor cortex (PMd) (i.e. Wessberg et al. 2000; Carmena et al. 2003). Decoder algorithms may be linear filters, such as the Wiener or Kalman filter, or may involve more advanced machine learning, such as artificial or recurrent neural networks. Rather than directly predicting movement variables such as position or EMG, some groups also implement musculoskeletal models into their decoders that may account for the dynamics of the arm (i.e. Héliot et al. 2010; Chhatbar and Francis 2013).

Other decoder considerations include the fact that neural decoders are not perfect, and often require user adaptation. Several BMI studies have studied the ability to adapt to various types of decoders. For

example, monkeys can better learn to use BMIs to control velocity over time (Lebedev et al. 2005), and can also improve kinematic control of a robot arm and gripper across experiment sessions (Carmena et al. 2003). Monkeys can even learn to adapt to nonbiomimetic decoders. For example, Ganguly and Carmena demonstrated that monkeys could adapt to a BMI where the decoder weights were shuffled among neurons (Ganguly and Carmena 2009). In another example, Jarosiewicz and colleagues show monkeys can learn to use altered decoders, where the relationship between M1 and kinematics is rotated for only a subset of the BMI neurons used for control (Jarosiewicz et al. 2008)

Despite these apparent abilities to learn to use nonbiomimetic decoders, recent work has also demonstrated that there do exist limitations to the ability to readily adapt to decoders. In a seminal BMI study on the neural constraints of learning, Sadtler and colleagues recently demonstrated that some decoders are more difficult to learn that others, and that these difficult decoders explicitly require neurons to co-modulate in abnormal ways (Sadtler et al. 2014). Various groups are currently following up this study in order to further evaluate the extent of these limitations on learning.

Finally, in addition to user adaptation, the decoders methods themselves can be designed to adapt or otherwise facilitate improved use (Shenoy and Carmena 2014). In one example, the user is eased into 100% brain control of a BMI through a process called “assistive training”. Here, the user begins by controlling a plant, such as a computer cursor, using brain-control mixed in with external assistance that helps the cursor move toward the target. As the user becomes more proficient at using the BMI, the percentage of assistive training is gradually reduced to zero. This type of facilitated adaptation has been primarily used in studies by researchers at the University of Pittsburgh (Velliste et al. 2008; Collinger et al. 2013). Another example is the SmoothBatch closed-loop decoder adaptation algorithm, developed at the University of California, Berkeley. This algorithm updates decoders on a 1-2 minute time scale using a weighted average, and improves decoder performance even with shuffled initial weights (Orsborn et al. 2012). Adaptation has also been built into EMG decoders that may be directly applicable for FES. For example, an adaptive EMG decoder designed by Ethier and colleagues used a starting template of muscle pulling directions, and updated decoder weights using gradient descent as monkeys went through trial and error to use the BMI to control force (Ethier et al. 2016).

1.6 BMI methodology

Beyond neural decoder development, there are many other facets involved in implementing a BMI system for FES, including implanting electrodes to record from the brain and stimulate muscles, and simulating temporary paralysis in order to test the system in intact animals. The sections below describe various methods for both general neurophysiology and the development of BMI systems.

Intracortical Neural Recording for Systems Neuroscience

Single-unit recording: Single-unit recording is typically hailed as the "gold standard" of neural recording. This method involves using a drive to move individual electrodes into the brain to find individual neurons, which are recorded extracellularly. The electrodes used for this type of recording often have a single recording site at the tip of the electrode, but other designs also include multiple recording sites along the shank of a single electrode. While this type of recording is useful for neurophysiology experiments, and even single neurons can be used to simple control of muscle stimulation (Moritz, Perlmutter, and Fetz 2008), it is not practical for implementing an effective BMI system, which usually relies on a population of neurons for sophisticated control.

Multi-unit recording: Recording multi-unit activity (MUA) typically involves implanting an electrode array into the brain, and recording from a population of neurons from many electrodes at once. There are various types of electrode arrays that provide for multi-unit recording. The most well-established electrode in the BMI field is arguably the "Utah array", which was developed by Richard Normann's laboratory at the University of Utah (Campbell et al. 1991). This array is currently commercialized by Blackrock Microsystems in Salt Lake City, Utah, and is a silicon-based, 96-electrode implant that is pneumatically inserted into the brain. Other types of electrodes include floating microelectrode arrays (FMAs), which allow the customization of individual electrode-lengths up to 10mm for reaching deeper structures. Other arrays still, such as the "Michigan probe", now commercialized by NeuroNexus, or Linear Microelectrode Arrays (Microprobes for Life Science, Gaithersburg, Maryland), include multiple recording sites spaced out along each electrode shank. **Figure 1-2** shows examples of three types of cortical arrays implanted in M1.

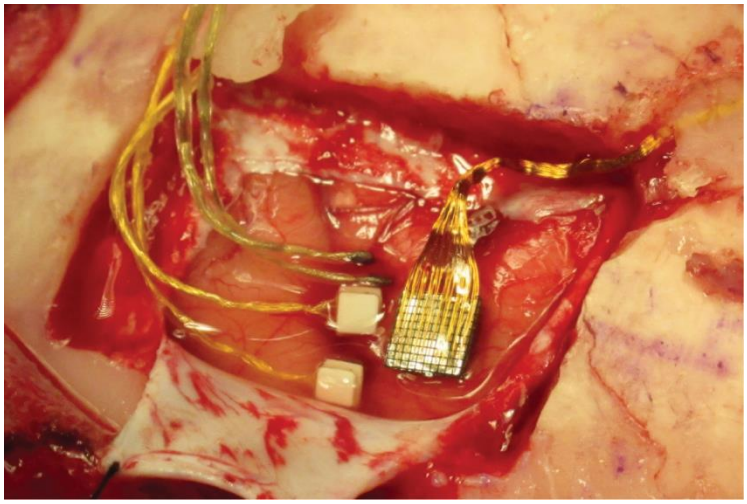

Figure 1-2. Cortical arrays implanted in M1. This intraoperative photo shows a multi-unit electrode Utah array, two FMAs, and two pairs of LMAs implanted in the motor cortex of a rhesus macaque.

Local Field Potentials: Local field potentials (LFPs) are brain signals that are collected below a certain frequency, typically 200-300Hz. These signals exclude action potentials from single neurons, but still carry information that can be used for decoding both kinematic variables and EMG (Flint, Wright, and Slutzky 2012; Flint et al. 2017). LFPs can also provide long-term stable recordings that may be used for decoding once an electrode array old, and is no longer recording discernable spikes from individual neurons (Flint et al. 2012; Flint et al. 2013).

Sorting Neurons

While single-unit recording is considered the “gold-standard” of neural recording, BMI studies do not necessarily require the use of discriminable neurons. In fact, many studies use a combination of single and multi-unit activity for decoding. Furthermore, BMI researchers have reported that spike-sorting is not necessary for quality neuroprosthetic control (Fraser et al. 2009). Threshold crossing has therefore become a popular method for collecting data, where all incoming data that cross a certain threshold (usually an RMS multiplier) are counted as neural activity. The main practical advantage of using threshold crossings is that researchers do not have to sort through neurons at the beginning of every experimental session. If a researcher is fortunate enough to have a prolific array of neurons, sorting could be time-consuming, and

would detract time from the actual experiment. A more scientific advantage of threshold crossing over spike-sorting is that the latter method discards extra signals that are in fact useful for decoding (Todorova et al. 2014)

Ultimately, the decision to sort neurons may depend on the scientific or engineering question at the heart of the experiment. In the experiments described in this thesis, I used both methods. In Chapter 3, I sorted cells because I was initially interested in evaluating the activity of single neurons and their relationship to the different experimental tasks. On the other hand, I used threshold crossings for my decoder-use study in Chapter 4. This is because I was less interested in the specific characteristics of individual neurons, and more interested in general decoder performance using a population of neural activity.

Activating muscles for FES

Muscle stimulation

EMG electrodes for both recording and stimulation can be accomplished using surface, epimysial, or intramuscular electrodes (Navarro et al. 2017). Surface electrodes, true to their name, sit on the surface of the skin. These types of electrodes are the least invasive, but also provide the least reliable and reproducible results, as they require daily placement and recalibration. Epimysial muscles, by contrast, sit on the surface of the actual muscle. Their signal has better signal-to-noise than surface electrodes, but their implantation requires an invasive surgery. The electrodes do not penetrate the muscle but are sutured or otherwise anchored to the surrounding epimysium. Intramuscular electrodes, on the other hand, are placed within the muscle belly. These electrodes can be inserted percutaneously, where a needle is used to drive a hooked wire into the muscle without surgery. The remainder of the wire remains outside of the body. For a more permanent setup, these electrodes can also be implanted intraoperatively. In this case, the exposed end of the wire is threaded into the muscle belly, while the rest of the wire is tunneled under the skin until it reaches a connector, which is usually percutaneous. For the experiments included in this dissertation, we uniquely used intramuscular electrodes to record EMGs, shown in **Figure 1-3**. These same electrodes were also used for cortically-controlled FES experiments (see Appendix).

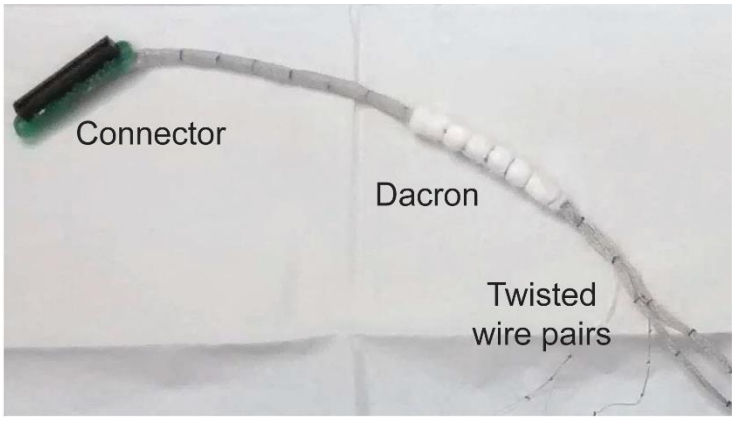

Figure 1-3. Intramuscular EMG wires and connector. In a long surgical procedure, we implant around 20 twisted wire pairs into the muscle belly of forearm and hand muscles. The wires are tunneled under the skin over the shoulder and to the back. They then exit out of the back, where they attach to a percutaneous connector (Samtec, Inc., New Albany, Indiana) like the one shown here.

Nerve cuff stimulation

In the second chapter of this dissertation, I evaluate the ability of nerve cuffs to elicit selective muscle activation. In particular, I evaluate the Flat Interface Nerve Electrode (FINE) cuff, which was developed at Case Western University in Cleveland, Ohio (Tyler and Durand 2002). The advantages of nerve cuffs over individual muscle electrodes are multifold. First of all, the surgery to implant a cuff requires a single implant site, rather than the many implant sites that may be involved when implanting individual muscles in the upper arm, forearm, and hand. This reduces both the length and complexity of the surgery. Second, nerve stimulation may offer the ability to better stimulate intrinsic muscles, which are difficult to implant with intramuscular electrodes, and challenging to individually stimulate without current spillover. Yet another advantage to nerve stimulation is that its current amplitudes requirements are less than intramuscular amplitudes by an order of magnitude.

There are various types of electrodes for nerve stimulation. Extraneural cuff electrodes, such as the FINE cuff, wrap around the nerve and do not penetrate fascicles. Cuff electrodes are not generally intended to manipulate nerve shape, although the FINE is specifically designed to gently reshape the nerve so the electrode contacts are closer to the fascicles. Intrafascicular electrodes, in contrast to the extraneural cuffs, do penetrate the fascicles. These types of electrodes include the Utah Slant-Electrode Array (USEA), which consists of electrodes of various lengths that are inserted into the nerve (Ledbetter et al. 2013).

Another type of intrafascicular electrode is the longitudinal intrafascicular electrode (LIFE) (Yoshida 1993), which involves implanting electrodes in individual fascicles, parallel to the axons. The transverse intrafascicular multi-electrode (TIME) (Boretius et al. 2010) is also a type of intrafascicular electrode, which is implanted perpendicular to the axons and penetrates a number of fascicles along the diameter of the nerve. While cuff electrodes may only stimulate superficial nerve fascicles, LIFEs excite a single fascicle, while TIMEs excite several different fascicles along the diameter of the nerve.

These various types of cuffs offer tradeoffs between invasiveness, ease of stimulation, and selectivity. For example, while nerve cuffs are the least invasive, they have also been shown to require higher stimulation thresholds than the TIME and LIFE. However, they were more also more selective than the LIFE in an experiment that compared the use of the three electrodes to stimulate the rat sciatic nerve (Cutrone et al. 2011). Future studies should continue to evaluate the relative benefits of each type of cuff.

Nerve block to simulate paralysis

While various methods for nerve blocks have been developed, here I describe the methods primarily used by our lab, which involve drug delivery to the major nerves of the arm.

Short-term block with lidocaine

For our current FES experiments in the Miller Limb Lab, we temporarily paralyze the monkey's working arm with a local nerve block. These methods, described in detail in (Pohlmeyer, Jordon, et al. 2009), allow us to selectively block the radial, ulnar, and median nerves in the upper arm. In a surgical procedure, we implant subdermal injection ports (Access Technologies, Skokie, Illinois) under the skin in the upper arm, which route to silicone tubes that lead to a silicone sheet wrapped around the nerve (**Figure 1-4**.) This implant allows us to inject a nerve block agent into the port to block the nerve for experiments. We typically deliver 0.8-1mL of lidocaine mixed with epinephrine (1:100,000) per nerve to induce a nerve block that can last around 1-2 hours.

Long-term nerve block with infusion pump

The next major project in our lab is to conduct continuous wireless FES experiments in the monkey's home cage. This will require a long-term nerve block, lasting as long as days or weeks. While our standard paradigm is to deliver lidocaine to the nerve, as described above, prolonged lidocaine use is neurotoxic, and can therefore injure the nerve (Johnson 2004). As part of my PhD, I led the development of a new protocol for a long-term nerve block using low doses of tetrodotoxin (TTX), a sodium channel blocker. During experiments, we can now route TTX to the nerve using a fully implanted infusion pump, which can be programmed to perform drug delivery at rates as slow as 2uL/hour (iPRECIO, Tokyo, Japan). The pump routes to a catheter, which then connects to a silicone sheet sutured around the nerve. To test the viability of this block, we conducted TTX experiments in rats and monkeys. In the rat, we were able to block the nerve for at least a month, and see a full recovery after replacing the pump's reservoir with a saline flush. In the monkey, the longest block we attempted was a week long, after which the monkey fully recovered. The list of flow rates and concentrations we tested is listed in Table 1-1, and a photograph demonstrating the successful block of the radial nerve in a monkey is shown in **Figure 1-5**.

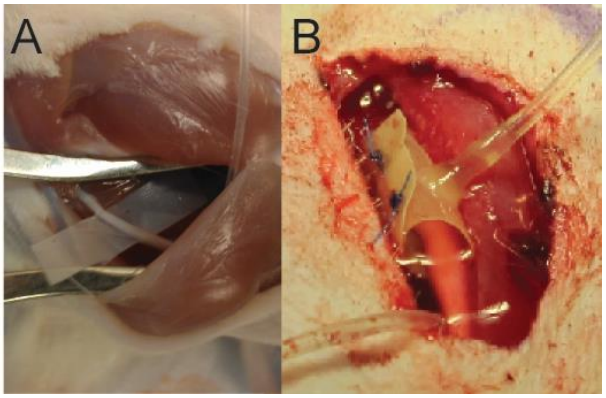

Figure 1-4. Nerve cuffs in the rat and monkey. (A) Nerve cuff ready for placement around a rat sciatic nerve. (B) Nerve cuff sutured around a monkey nerve.

Table 1-1. Parameters for a TTX nerve block.

Flow Rate (uL/hr)	Concentration (ug/mL)	Effect
2	50	None
4	50	None
2	100	None
4	100	None
6	100	Paralysis
2	250	Paralysis

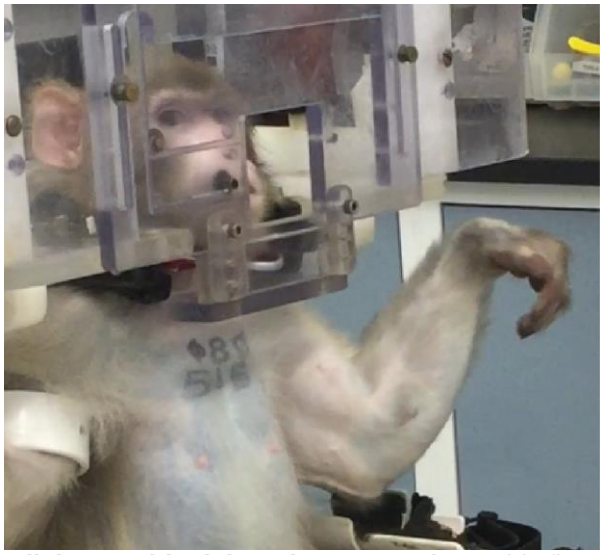

Figure 1-5. A successful radial nerve block in a rhesus monkey. This figure demonstrates the result of a successful radial nerve block using TTX. The radial nerve innervates wrist and finger extensors, and the monkey's flexed hand posture here demonstrates his inability to activate his extensors.

1.7 Summary

The overarching theme of this dissertation is the refinement of control strategies for cortically-controlled FES. The two control strategies I explore involve understanding how to more efficiently and selectively activate muscles, and how to better understand the relationship between M1 and EMG in order to build better neural decoders.

In Chapter 2, I evaluate the ability to selectively activate muscles in the forearm using nerve cuffs. Specifically, I evaluate the performance of the Flat Interface Nerve Electrode (FINE), which was developed at Case Western Reserve University (CWRU) (Tyler and Durand 2003). This chapter was the result of a collaboration between Lee Miller's lab at Northwestern University, and Dustin Tyler's lab at CWRU. The goal of the study was to evaluate the ability of FINE cuff stimulation to produce selective muscle activation. The results reported here are relevant to all general FES for grasp applications, and not just cortically-controlled systems.

In Chapters 3 and 4, I evaluate the robustness of the relationship between M1 and EMG. These studies serve both to add to the neural control of movement knowledge base, and to inform future neural decoder development. In Chapter 3, I evaluate whether a single linear M1-EMG decoder can span three dynamically different wrist tasks: an isometric task, an unloaded movement task, and a spring-loaded movement task. I also compare the performance of the linear decoder to a nonlinear recurrent neural network (RNN). In Chapter 4, I evaluate the ability of monkeys to learn to use two different types of decoders: one that preserves the natural patterns of muscle activation, and one that does not. This study addresses the ability of M1 neurons to readily dissociate from natural muscle biomechanics to successfully learn to control a BMI.

2 Evaluation of high-density, multi-contact nerve cuffs for activation of grasp muscles in monkeys

N Brill[1]*, SN Naufel[2]*, K Polasek[4], C Ethier[3], J Cheesborough[5], S Agnew[6], LE Miller[2,7,8,9], DJ Tyler[10,11] §

Affiliations

[1] Current address: Boston Scientific, 25155 Rye Canyon Loop, Valencia CA 91355
[2] Department of Biomedical Engineering, Northwestern University, 2145 Sheridan Road, Evanston, IL 60208, USA
[3] Centre de recherche de l'Institut universitaire en santé mentale de Québec, Department of Psychiatry and Neuroscience, Université Laval, Quebec City, QC, Canada
[4] Department of Engineering, Hope College, 27 Graves Pl. Holland MI, 49423
[5] Clinical Instructor, Surgery, Plastic & Reconstructive Surgery, Stanford University
[6] Assistant Professor, Division of Plastic Surgery and Department of Orthopaedic Surgery, Loyola University Medical Center
[7] Department of Physiology, Feinberg School of Medicine, Northwestern University, 303 E. Chicago Avenue, Chicago, IL 60611, USA
[8] Sensory Motor Performance Program (SMPP), Shirley Ryan Ability Lab, 355 Erie Street, Suite 1406, Chicago, IL 60611, USA
[9] Department of Physical Medicine and Rehabilitation, Northwestern University, Chicago, IL, USA
[10] Biomedical Engineering Department, Case Western Reserve University, Cleveland, OH, USA
[11] Louis Stokes Veterans Affairs Medical Center, Cleveland, OH, USA

* These authors contributed equally to the preparation and content of this paper.

2.1 Introduction

Paralysis resulting from spinal cord injury (SCI) is devastating, dramatically reducing the independence of affected individuals. In addition to the direct effects, a number of secondary complications emerge as a result of disuse, such as muscle atrophy, contractures and pressure sores (Ragnarsson 2008; Baldi et al. 1998). However, if the motor neurons remain intact after injury, muscles can be made to contract through functional electrical stimulation (FES) (Peckham and Knutson 2005). FES has been used to assist or restore gait (Daly et al. 2011; Granat et al. 1993; Thrasher, Flett, and Popovic 2006), the ability to grasp objects (Alon and McBride 2003; Peckham and Knutson 2005; Peckham et al. 2001; Peckham, Marsolais, and Mortimer 1980; Popovic, Popovic, and Keller 2002) and to augment bowel and bladder function (Gaunt and Prochazka 2005).

While some hand grasp systems use transcutaneous muscle stimulation (Ijzerman et al. 1996; Prochazka et al. 1997) (e.g., Bioness, Myndtech, Belgrade Gasping System), FES often requires an invasive procedure where surgeons must identify and implant electrodes in every muscle of interest. In this case, the intrinsic muscles of the hand present a particular challenge. In addition to being difficult to implant, their small size often results in current spillover to adjacent muscles (Kilgore et al. 1990), rendering selective activation difficult to achieve. In the case of larger, extrinsic muscles with spatially distributed motor units, it is difficult to recruit the fibers of the entire muscle, resulting in partial and ineffective recruitment (Fisher et al. 2008).

Nerve trunk stimulation is an alternative that may address these challenges, and a variety of multi-contact nerve-based electrodes exist (Polasek, Schiefer, et al. 2007; Polasek, Hoyen, et al. 2007; Boretius et al. 2010; Ledbetter et al. 2013; Tyler and Durand 2002; Yoshida 1993; Lago et al. 2007; Lawrence, Dhillon, and Horch 2003). These electrodes vary in how they interface with the nerve, but are similar in that a single implant site can potentially access all the muscles innervated by that nerve. This more efficient access to muscles means a less extensive and shorter surgery, potentially improving outcomes and reducing risks. There is also about a 10-fold decrease in the required stimulation intensity for nerve cuffs compared to intramuscular stimulation, thereby simplifying stimulator design, increasing battery life, and reducing stimulation artifact in cases when concurrently recorded biosignals are used for control.

In this study, we evaluate a particular type of electrode, the Flat Interface Nerve Electrode (FINE), for use in upper extremity hand grasp systems. The FINE is an extraneural electrode designed to gently reshape the nerve and thereby increase access to nerve fascicles (Tyler and Durand 2002). It offers the potential to activate muscles strongly and selectively and has been shown to be stable over several years for restoring sensation in humans (D. W. Tan et al. 2014; D. Tan et al. 2013; Schiefer et al. 2016). It is therefore an attractive candidate for use in motor recruitment for FES. In the experiments presented here, we collected recruitment curves from FINEs implanted in six monkey arms. We evaluated the ability to generate selective activation of several functionally synergistic muscle groups as well as certain individual muscles. Our ultimate goal is to use this technology in tandem with intramuscular stimulation in the development of FES systems, including a cortically-controlled FES system that uses signals in motor cortex to control the time-varying stimulation of multiple muscles (Moritz, Perlmutter, and Fetz 2008; Pohlmeyer et al. 2012).

2.2 Methods

We implanted and tested 12 and 16-channel FINE cuffs on the median, radial, and ulnar nerves of six monkeys: four rhesus macaques (*Macacca mulatta,* Monkeys 1, 2, 3, and 4) and two long-tailed macaques (*Macaca fascicularis,* Monkeys 5 and 6) (Table 1). We collected recruitment curves by varying either pulse amplitude or pulse width of single, biphasic, charge-balanced stimulus pulses and recorded the evoked EMG twitch response of all implanted muscles (Polasek, Schiefer, et al. 2007). Four experiments, monkeys 1-4, were 36-hour non-recovery procedures. Two experiments, monkeys 5 and 6, were chronic experiments to evaluate the performance of chronically implanted FINE cuffs. Measurements were collected under sedation. Monkey 5 was implanted for 6 months, and was involved in 12 stimulation experiments. The study in Monkey 6 spanned 15 weeks, and involved weekly, standardized, eight-hour recording sessions to collect a series of recruitment curves. All methods were fully consistent with the *Guide for the Care and Use of Laboratory Animals* and conducted in accordance with a protocol approved by the Northwestern University Institutional Animal Care and Use Committee.

Table 2-1. Nerves implanted with FINEs in each monkey. This table shows the number of contacts for all the cuffs included in the current paper's analysis. The number of contacts for each cuff ranged from 12 to 16. In Monkey 6, we implanted clinical-grade CFINE nerve cuffs. All radial cuffs were implanted proximal to the elbow. The difference between the proximal and distal median cuffs is relative to the nerve branch to the pronator teres muscles. The distal ulnar cuffs were just proximal to the wrist, while the proximal cuffs were closer to the elbow.

	Median Proximal	Median Distal	Ulnar distal	Ulnar Proximal	Radial
Monkey 1 Left	16	--	--	16	--
Monkey 1 Right	16	--	--	16	--
Monkey 2	16	--	--	16	--
Monkey 3	12	--	--	12	--
Monkey 4	--	12	--	12	--
Monkey 5	--	12	12	--	--
Monkey 6	--	16	16	--	16

2.2.1 Electrode Design and Fabrication.

We designed the FINE electrodes with specific dimensions so they would appropriately fit around the nerves (**Figure 2-1Figure 1-2** (a-c)). We used previously acquired histology of the monkey nerve cross-section to design the nerve cuff opening height (**Figure 2-1** (c)) to fall between the diameter of the second and third largest fascicles. The opening width provided the cuff lumen a cross-sectional area of 1.4 times the expected cross-sectional area of the nerve. Nerve cuffs constructed at Case Western Reserve University (Monkeys 1-5) had opening heights of 1.5 mm (radial implant), 0.7 mm (ulnar distal implant), and 1.4 mm (median elbow and proximal implants). The contact dimensions were 0.25 x 0. 25 mm with an edge-to-edge value modified to equally space the contacts across each cuff width. For Monkey 6, we implanted clinical-grade Composite Flat Nerve Interface Electrodes, made with a high performance poly-ether-ether-ketone (PEEK) polymer to minimize bulk (CFINE) (Ardiem Medical, Indiana, Pennsylvania). Each CFINE cuff housed 16 contacts, eight on each side. All cuffs were wired to a connector with 7-strand 316L VM stainless-steel, PFA-coated wires (Fort Wayne Metals, Fort Wayne, Indiana). The dimensions of the individual contacts of the CFINE were 0.35 mm (width) x 1.5 mm (height) with an edge-to-edge contact spacing of 0.25 mm.

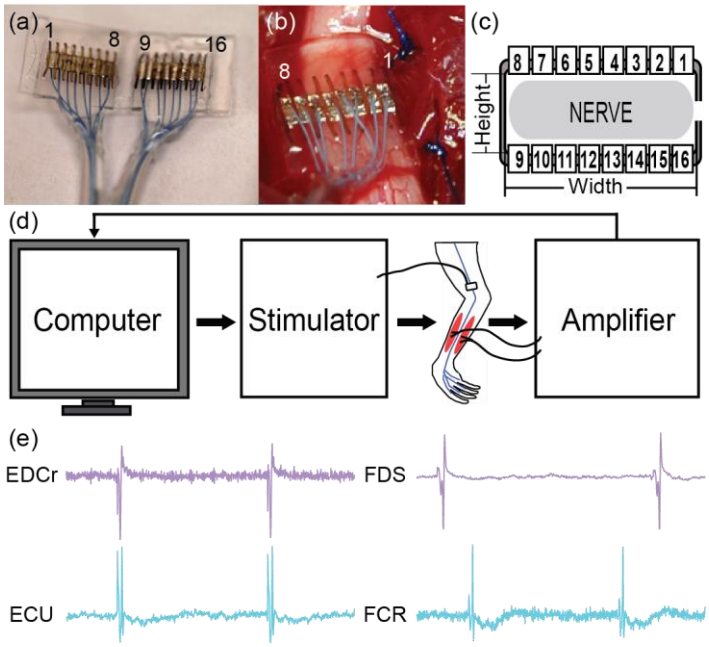

Figure 2-1. Experiment Setup. (a) CFINE cuff made out of poly-ether-ether-ketone (PEEK) with 16 contacts. (b) Placement of the cuff around the radial nerve of a macaque. (c) Schematic illustrating the arrangement of contacts around the nerve. (d) Schematic illustrating the flow of experiment. The computer sent commands to the stimulator, which stimulated the appropriate contact on the FINE cuff. This produced a muscle twitch, which was amplified and sent back to the computer to be saved. (e) Examples of muscle twitches elicited by nerve stimulation on a single contact.

FINE cuff implantation

We implanted up to four FINE cuffs in each arm of the acute study monkeys, on the median and ulnar nerves (

Table 2-1). During surgery, we dissected a 2 cm length of nerve free from surrounding tissue, placed the cuff around the nerve and secured the ends with a suture (**Figure 2-1** (a) and 1(b)). Contacts near the cuff hinge, especially contacts 8 and 9, did not always touch the nerve (**Figure 2-1**(a-c)).

2.2.2 EMG electrode implantation

We implanted pairs of multi-stranded, Teflon coated stainless steel wires (Cooner 632) in each muscle after stripping 2 to 3 mm of insulation from the end of each wire and separating the deinsulated tips by approximately 1 cm (**Table 2-2**). In surgery, we exposed and identified each muscle based on its response to electrical stimulation. For the acute experiments, we either sutured the wires to the muscle

surface (epimysial) or inserted them into the muscle belly using hypodermic needles (intramuscular). We placed two needles in the shoulder to serve as the stimulation return (anode) and the EMG reference. For the chronic experiments, we also implanted a reference wire near the elbow, along with a return electrode on the upper arm. All electrodes were intramuscular, and routed together with the FINE leads to a percutaneous implant on the monkey's back that included three connectors (Samtec Inc., New Albany, Indiana) on a printed circuit board.

Table 2-2. Muscles implanted with electrodes for each monkey. The list of muscles for each monkey includes flexor digitorum profundus (FDP), flexor digitorum superficialis (FDS), opponens pollicis (OP), palmaris longus (PL), pronator teres (PT), abductor pollicis longus (APL), brachioradialis (Brad), extensor carpi radialis brevis (ECRb), extensor carpri radialis longus (ECRl), extensor digitorum communis (EDCr and EDCu to dictate the relative location of electrode pairs), extensor carpi ulnaris (ECU), abductor digiti minimi (ADM), adductor pollicis (AdP), flexor carpi ulnaris (FCU), first dorsal interosseous (FDI), flexor pollicis brevis (FPB), flexor digiti minimi brevis (FDMb), and first lumbrical (Lum1),. Hypothenar and thenar refer to electrodes implanted in the hypothenar and thenar eminence, but that were not more specifically identified.

	Median						Radial							Ulnar								
	FDP	FDS	FCR	OP	PL	PT	APL	Brad	ECRb	ECRl	EDCr	EDCu	ECU	ADM	AdP	Hypothenar	FCU	FDI	FPB	FDMb	Lum1	Thenar
Monkey 1 Left	•	•	•			•											•	•				•
Monkey 1 Right	•	•	•			•										•	•	•				•
Monkey 2	•	•	•			•										•	•	•				•
Monkey 3	•	•	•			•											•					•
Monkey 4	•	•	•		•	•									•		•	•	•			
Monkey 5	•	•	•											•	•		•	•	•			
Monkey 6	•	•	•	•	•	•	•	•	•	•	•	•	•	•		•	•	•		•	•	•

2.2.3 Data Collection

During the acute experiments (Monkeys 1-4), we used two battery-powered, computer-controlled stimulators (custom devices by Crishtronics, Cleveland, OH) to deliver charge-balanced, biphasic, rectangular pulses. We acquired EMG at 2.4kHz, amplified, AC coupled (2^{nd} order, 10 Hz HPF cutoff) and low-pass filtered (2^{nd} order, 1 kHz).

For the chronic experiments with Monkey 6, we conducted experiments every 1-2 weeks for 15 weeks. We induced sedation with either Telazol or a ketamine-midazolam cocktail IM, and maintained an experimental level of sedation with IV propofol. A MATLAB user interface controlling a 16-channel stimulator (Tucker-Davis Technologies, Alachua, FL) sent stimulus pulses to the cuffs and collected EMG signals. The EMG data were sampled at 3kHz, amplified, AC coupled (2^{nd} order, 10 Hz HPF cutoff), low-pass filtered at 1 kHz.

For both acute and chronic trials, we used a binary search routine to generate pulse-width and pulse-amplitude modulated recruitment curves. For each curve, we held one parameter (amplitude or width) constant and varied the other. For each session with Monkey 6, we collected up to four sets of recruitment curves per nerve: two sets with pulse amplitude values of either 0.10 mA or 0.25 mA and varied pulse width, and two sets with pulse width of either 10μs or 20μs with varied pulse amplitude. We used a stimulation frequency of 4 Hz to minimize the experimental time without fusing muscle twitches (Polasek, Hoyen, et al. 2007). At the beginning of each session, we determined the maximum activation for each muscle by stimulating all contacts in the nerve cuff with a pulse width of 100 μs and pulse amplitude of 0.20 mA (Recorded Max Value).

2.2.4 Data Analysis

We analyzed the recruitment curves to determine the stimulation thresholds and selectivity of each contact. We used peak-to-peak EMG amplitude to quantify the magnitude of muscle contraction and normalized to the peak-to-peak of the Recorded Max Value described above. We defined the selectivity of individual muscles as the percent activation of a given muscle before any other muscle reached 20% of the Recorded Max Value (**Figure 2-2**).

To evaluate muscle selectivity over time, we used two different types of analysis. In the “Fixed Contact” analysis, we chose the contact that yielded the highest selectivity across all weeks, and computed its selectivity in each session. In the “Best Contact” analysis, we computed selectivity for each session using the most selective contact for that session.

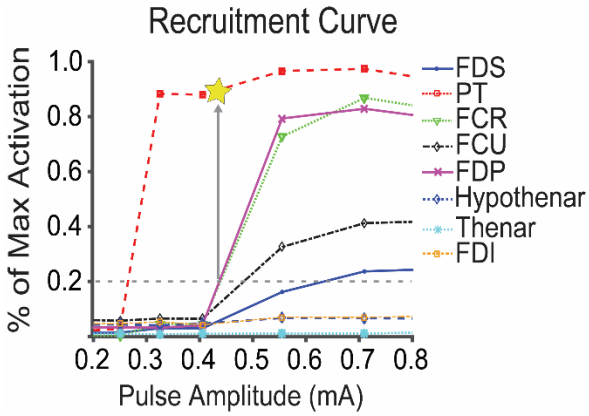

Figure 2-2. Median Nerve Recruitment Curve. These recruitment values are for the right arm of Monkey 1, who had a FINE cuff implanted around the median nerve proximal to the elbow. The dotted line at 20% shows the threshold for determining selectivity. In this example, the first muscle to reach 20% is the Pronator (PT), and it remains the only muscle above this line until it reaches 90% activation, which is when the next muscle, FDP, reaches 20%. The selectivity value for the Pronator in this example is therefore 0.90.

2.3 Results

2.3.1 Activation Thresholds

For all monkeys, we evaluated activation thresholds for all contacts in the median nerve cuffs. As the cuffs were somewhat larger than the nerves, contacts at either end were typically the farthest from the fascicles (**Figure 2-1** (a-c)), and had somewhat higher thresholds. The highest thresholds were for contacts 8 and 9, located at the hinge of the cuff, and often not in direct contact with the nerve (**Figure 2-1**(c)). The thresholds across all muscles, regardless of monkey and nerve, were mirrored for the top and bottom of the cuff, such that opposing pairs of contacts had comparable thresholds (**Figure 2-3**). The intraoperative thresholds were initially high for Monkey 5, but decreased at five weeks and at further at six months during the terminal experiment. **Figure 2-4** shows thresholds for Monkey 6 in more detail for each nerve. For the radial nerve, the thresholds for contacts 1 and 16 were low, a result of being in close proximity with the nerve in this particular case (**Figure 2-1** (b)).

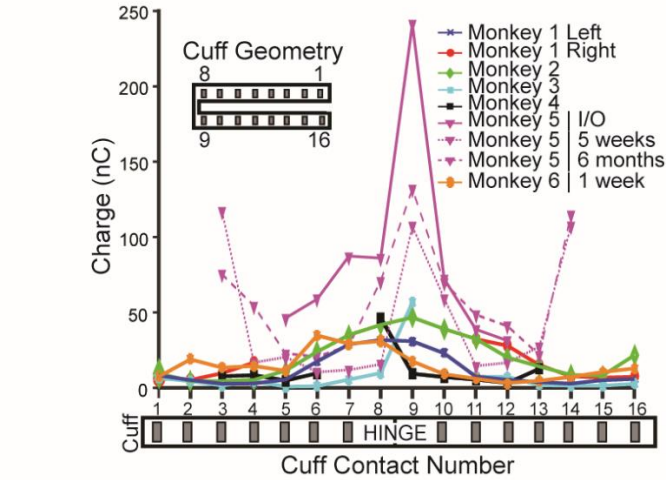

Figure 2-3. Stimulation thresholds for all monkeys for the median nerve cuff. The data from each monkey are centered around the hinge at contact 8 and 9 because not all cuffs had 16 channels. Missing data points indicate that the contact could not activate muscle, or that the data were not collected.

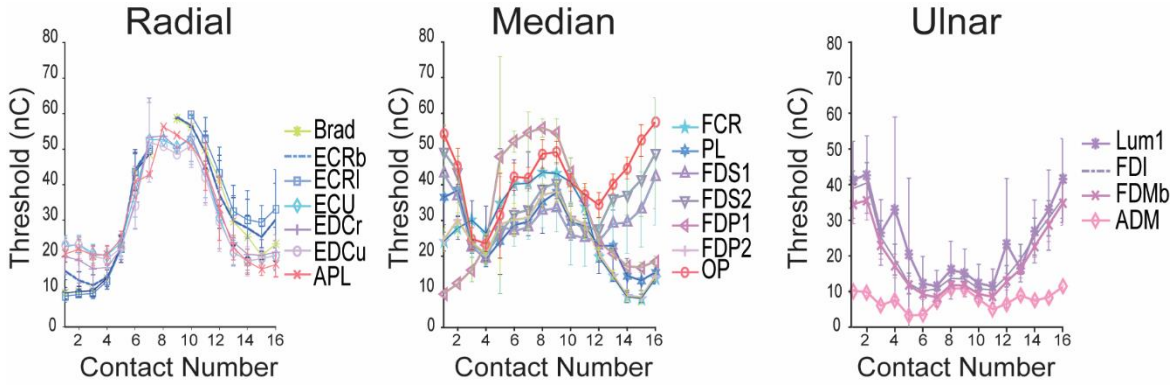

Figure 2-4. Thresholds. These plots show the mean charge at threshold (0.2 EMG value) of each muscle at each contact across all three nerves in trials collected after 2 months post implant in Monkey 6.

2.3.2 Selective recruitment of muscles with FINES

We were able to achieve at least partially selective activation of muscles in all monkeys (**Figure 2-5**). In all cases where the median nerve cuff was implanted just proximal to the pronator teres (PT) branch,

we could recruit that muscle with a selectivity value of 0.62 to 0.90 (**Figure 2-5**(a)). The best results for the proximal implant were in Monkey 1 (Left arm) with selective activation of four muscles: PT (Selectivity=0.9), FDP (0.8), FCR (0.7), and FDS (0.3). For Monkey 3, the selectivity of activation of intrinsic thumb muscles in the thenar eminence was 0.45.

To avoid dominance of PT recruitment in Monkeys 4-6, we placed the median nerve cuffs distal to its nerve branch. This enabled selective activation of finger and wrist flexors for these three monkeys. For Monkeys 4 and 6, FDP and FDS were active selectively, which demonstrates an ability to control finger flexors. In Monkey 6, four muscles were selectively activated, including both finger: FDP (0.6), FDS (0.4) and wrist flexors: PL (0.35), FCR (0.25), at 6 days post-surgery.

The ulnar nerve cuffs in Monkeys 1-4 were implanted proximal to the elbow and activated flexor carpi ulnaris (FCU), the first muscle to branch distal to the cuff, with selectivity ranging from 54% to 100%. In Monkeys 5 and 6, the ulnar cuff was implanted just proximal to the wrist, well past the nerve branch to FCU. Using these cuffs, we recruited FDI and ADM at 55% and 34% selectivity, respectively.

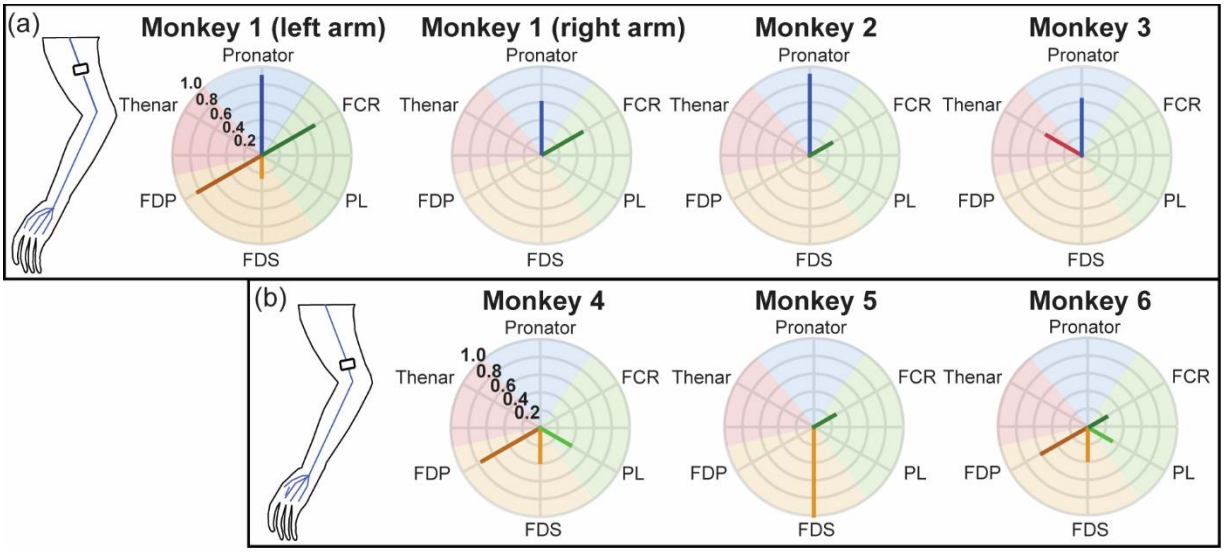

Figure 2-5. Summary of selective muscle activation for the median nerve. Each plot represents the highest selectivity value for each muscle across the range of pulse amplitudes and widths tested. Selectivity for each muscle was therefore achieved using different stimulation parameters. All data were collected intraoperatively except the data for Monkey 6, which were collected 6 days post-implantation. The background shading of each polar plot separates the muscles into functional groups, showing the ability to get functional selectivity in addition to muscle selectivity.

2.3.3 Recruitment Order

Order of recruitment of multiple muscles, especially functionally synergistic muscles, affects the functional result of stimulation. Recruitment order two months post-implant in Monkey 6 shows multiple different recruitment orders from single contact stimulation (**Figure 2-6**). For example, contact 6 on the radial nerve (**Figure 2-6**(a)) first activated the finger extensors EDCr and EDCu, then the wrist extensor, ECU, and finally thumb abductor, APL. In contrast, contact 5 first activates wrist extensors, ECRb and ECRi, then finger extensors EDCr and EDCu. For the radial nerve, there were 11 unique recruitment orders for 16 contacts. For the median nerve (**Figure 2-6**(b)), there were 10 unique recruitment orders for 16 contacts.

Four of the five muscles of the radial nerve (APL, Brad, EDC, ECR, and ECU) were activated first by at least one of the electrodes. Only the brachioradialis was not activated first by any contact. Each of the four muscles innervated by the median nerve (FDS, FDP, ECR, and ECU) were recruited first by at least two contacts. Of the four muscles in the ulnar nerve (ADM, FDMb, FDI, and First Lumbrical) all contacts always activated the muscles in the same order of ADM, FDMb, FDI, and First Lumbrical (not shown in figure). Only contact 13 reversed the order of the FDI and First Lumbrical activation.

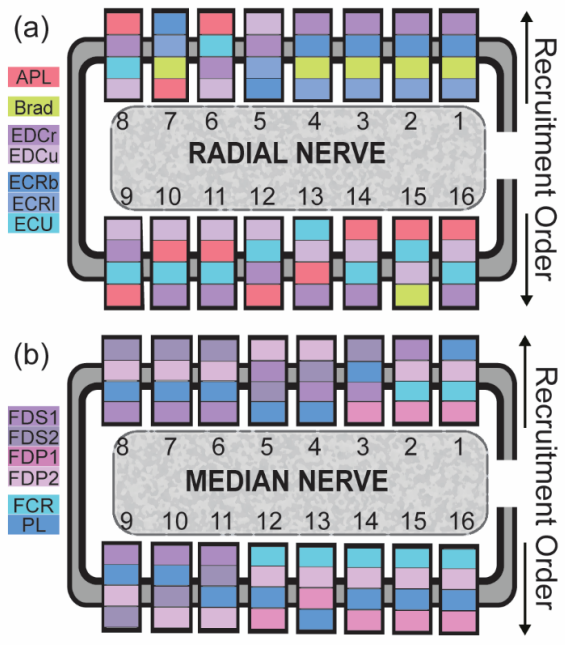

Figure 2-6. Recruitment order. The order for muscle recruitment for each contact in Monkey 6 at 2 months post implant. Muscles depicted closest to the nerve were recruited first. The muscles are grouped according to functional synergy.

2.3.4 Stability of muscle selectivity for chronically implanted cuffs.

To evaluate the stability of muscle recruitment over time for Monkey 6, we obtained recruitment curves for the most selective muscle recruited by each cuff, and averaged the recruitment curves for experimental sessions 9 through 14 (**Figure 2-7**). For these recruitment curves, pulse width was held static at 10 or 20 μs while pulse amplitude varied. Ulnar nerve stimulation selectively recruited ADM, an intrinsic hypothenar muscle, with selectivity values of 0.69 ± 0.06. For the radial nerve, the muscle with the highest selectivity value was APL, (0.51 ± 0.05 at 20 μs). For the median nerve, FDP was most selective (0.83 ± 0.05). These three muscles not only had the highest selectivity, but were also recruited with the highest stability across weeks, indicated by their low standard deviations. Conversely, the muscles that were activated with the least stability across sessions, FCR and PL, were only selective for 3 sessions (selectivity means of 0.29 and 0.30, respectively). Due to external factors, FCR and PL were only tested in 5 of 6 sessions.

2.3.5 Achieving selectivity with more than one contact

In many cases the same muscles were selectively activated by more than one contact, and we therefore evaluated selective muscle activation across sessions using two different analyses (**Figure 2-8**). The Fixed Contact analysis (**Figure 2-8**a)) shows selectivity of a single contact across all sessions for Monkey 6, while the Best Contact analysis (**Figure 2-8(**b)) shows results for the contact that produces the greatest selectivity in a given session. The largest difference in selectivity between the Fixed and Best contact results is seen in the wrist flexor functional group, where selectivity using the Best contact was better by more than 15% for weeks 3, 8, and 11 (**Figure 2-8**(a) and (b), Median Nerve). The difference in selectivity between the Fixed and Best contact for the finger flexors was more than 10% for weeks 5, 13, and 14 (**Figure 2-8**(a) and (b), Median Nerve). In another example, the wrist extensor functional group, selectivity using the Best contact was better by more than 15% at week 2. (**Figure 2-8**(a) and (b), Radial Nerve). These examples demonstrate the ability to improve selectivity by switching to another contact.

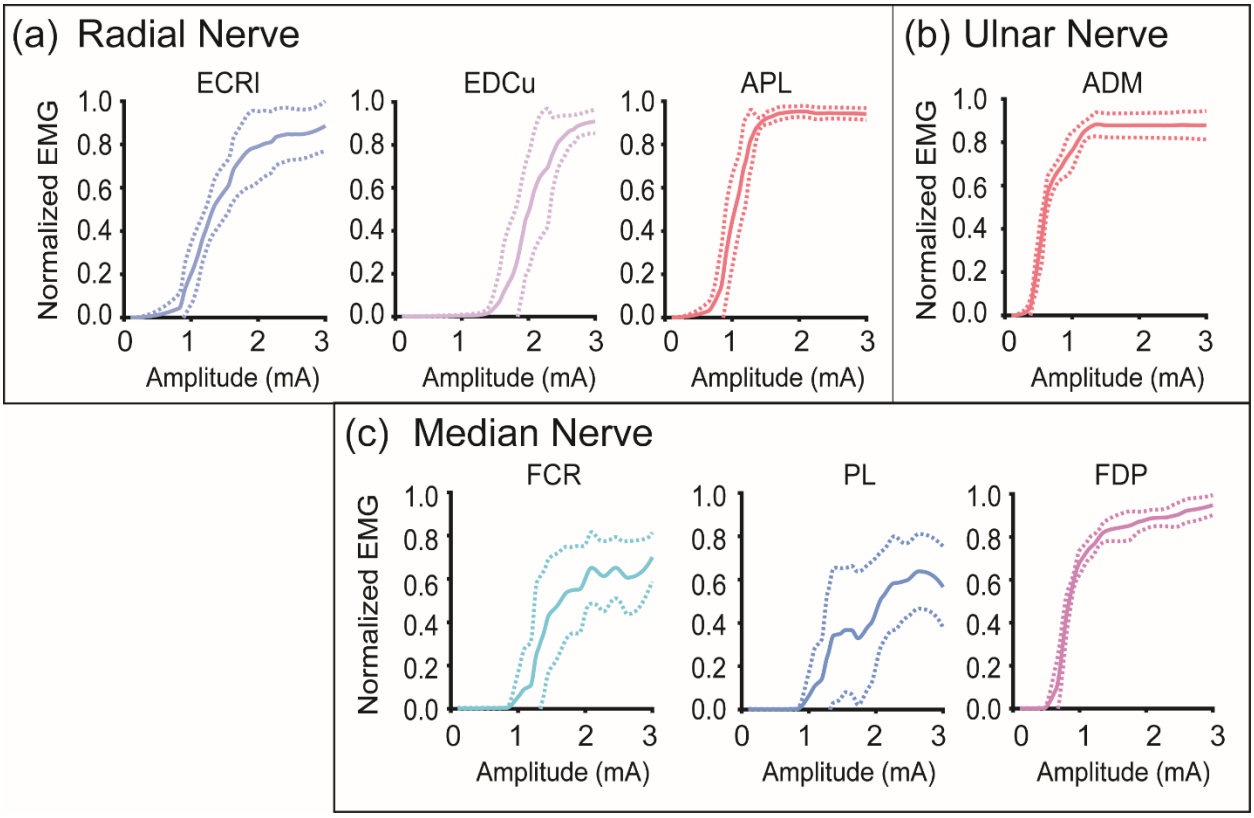

Figure 2-7. Mean recruitment curves of selective muscles. These curves average data from trials collected after 1.5 months post-implant in Monkey 6. The dotted line indicates one standard deviation from the mean (solid line). The mean is calculated across all recruitment curves for the contact and pulse width that produced the most selective recruitment.

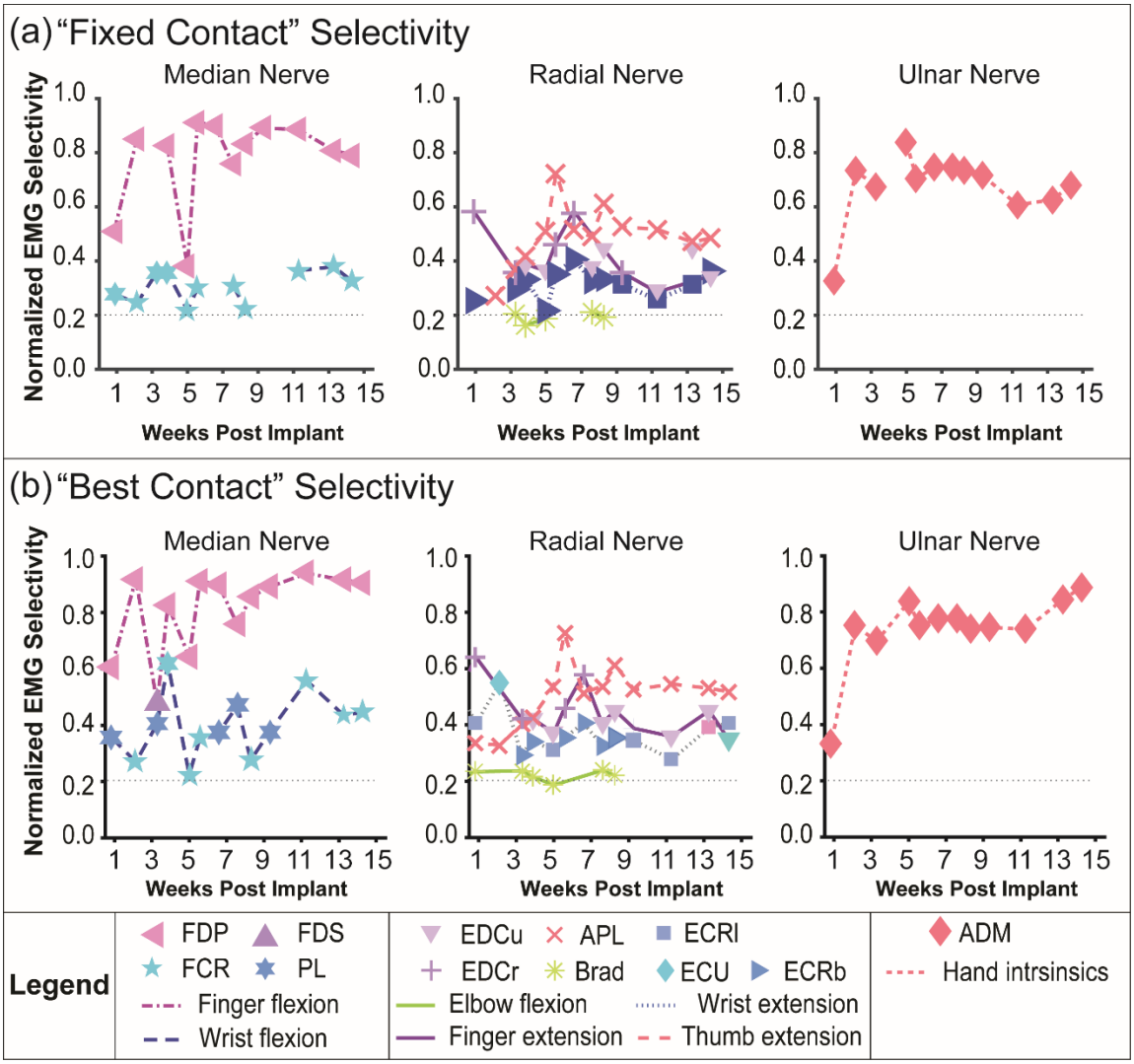

Figure 2-8. Selectivity over time. (a) Selectivity, as calculated by the Fixed Contact Analysis, for the three nerves in Monkey 6. (b) Selectivity, as calculated by the Best Contact Analysis.

2.3.6 Multiple-contact stimulation

In a brief experiment in Monkey 6, we used the FINEs to activate muscles using multiple contacts from the median and radial cuffs simultaneously. Based on recruitment curve information, we identified contacts that drove the hand from a posture with the fingers extended to a posture with the fingers closed in a fist (Supplementary Video A). In another trial, we caused the fingers to spread, an action mediated largely by the dorsal interossei (Supplementary Video B). By stimulating on multiple contacts, we were able to achieve

strong wrist extension in tandem with finger flexion. In both videos, the monkey's wrist extends, and remains extended while all fingers flex. This type of activation is crucial for restoring effective grasp.

2.4 Discussion

In the current study, we demonstrate the feasibility of using extraneural FINE cuffs for evoking muscle activity, a promising avenue for improving FES. FINEs offer an advantage over individual muscle stimulation in part because their implantation requires much less extensive surgery. Implanting a cuff requires surgery at a single site rather the multiple sites required for all the muscles innervated by that nerve. In particular, FINEs also improve access to the small, intrinsic muscles, the size and location of which make them particularly difficult to implant with individual intramuscular electrodes. Furthermore, the small distance between intrinsic hand muscles makes them prone to current spillover, even at relatively low intensity stimulation. Another limitation of intramuscular electrodes is the limited force that may be produced through partial activation of the muscle. In particular, activation of finger flexors during a power grasp, also causes wrist flexion torque which can overpower the torque produced by intramuscular activation of the much weaker wrist extensors. We found this not to be in the case in our multiple-contact stimulation experiment (Supplemental Videos A and B). In both videos, the monkey's wrist extends, and remains extended while all fingers flex. This type of activation is crucial for restoring effective grasp.

2.4.1 Selective activation of muscles and functional muscle groups

While recent studies have demonstrated the successful chronic use of 8-channel FINEs in humans for evoking sensory percepts [25-26], here we focus on the viability of 12, 14, and 16-channel designs for motor applications. The more closely spaced electrodes may explain why adjacent contacts often activated muscles in a similar sequence. In many cases, we could achieve similar selective activation of a given muscle or functional group using multiple contacts. This meant that for sessions where we could not achieve great selective activation using a particular contact, we could often instead use a neighboring contact. The high-density design provides a redundancy that allows more contact options to choose from, which is helpful

for maximizing selective activation of muscles and functional groups, and could also contribute to long-term stability of selective activation.

2.4.2 Monkey as a model for evaluating nerve stimulation

In the current study, the monkey proved to be a valuable model to evaluate and improve stimulation algorithms more readily than would be possible with human subjects. While the experiments described here are important for exploring ways to improve stimulation techniques, they are time consuming and therefore not ideal for human experiments. Our chronic experiments spanned as much as eight hours, while the acute ones spanned as much as thirty-six hours. These long sessions permitted a comprehensive evaluation of the feasibility of the FINE cuffs, allowing us to test muscle responses to stimulation using a wide range of pulse widths and amplitudes. As reported elsewhere (Natalie Brill 2015), we also developed a genetic algorithm (GA) to optimize parameters for multiple-contact stimulation, and our 8-hour experiments allowed us to run several GAs. Use of a monkey model further afforded us the ability to investigate other practical issues, including the posture dependence of the stimulation, which proved to be minimal, and the ability to form functional grasps using multi-contact stimulation.

However, anatomical differences between the monkey and human should be taken into account when considering how our results will translate to the clinic. Monkeys have considerably fewer fascicles than the human, a difference that is important, given that selectivity improves with increasing number of fascicles (Brill et al. 2009). It is likely then, that selectivity in humans will be better than what we report here in monkeys.

2.4.3 The use of FINES for FES

Although FINEs offer advantages over intramuscular electrodes, challenges to implementing real-time control with them remain. Implementing FINEs in an FES system will also require developing methods to map FINE cuff stimulation parameters to desired EMG output. For muscles that cannot be selectively activated with FINEs, it may also be necessary to supplement nerve stimulation with intramuscular stimulation.

2.5 Conclusions

Here we present results from several acute and chronic experiments conducted under sedation with six monkeys. We were able to achieve selective activation of individual muscles, or distinct functional groups of muscles. The high-density cuff design led to overlap in the sets of muscles activated by different contacts, allowing the ability to choose contacts that provided the most selective activation. Overall, the monkey model allowed us to test a wide range of stimulation parameters, and will continue to be a valuable model for exploring FINE capabilities.

3 Evidence of a downstream gain mechanism in the production of EMG

Stephanie N. Naufel[1], Joshua Glaser[2,3], Chad Purnell[4], Konrad P. Kording[3], Lee E. Miller[1,2]

[1]Department of Biomedical Engineering
[2]Department of Physical Medicine and Rehabilitation, Northwestern University, Chicago, IL, USA
[3]Rehabilitation Institute of Chicago, Chicago, IL, USA
[4] Northwestern Memorial Hospital, Department of Surgery, Division of Plastic and Reconstructive Surgery, Chicago, IL

3.1 Introduction

It is easy to take for granted the range of forces and dynamical conditions over which we can make accurate, stable movements. Whether for turning the page of a book, or carrying heavy loads, the motor system can accommodate a tremendous range of dynamic conditions and load forces. Understanding the control of these wide-ranging motor behaviors by neurons in the primary motor cortex (M1) has been an on-going challenge, even before Evarts first made recordings in M1 from behaving monkeys over a half century ago (Evarts 1968). Motor cortical activity leads directly to muscle activity and force generation, but this relationship appears to be context-dependent. Some corticomotoneurons are more active during precision grip than power grasp, despite much lower EMG occurring in their target muscle (Buys et al. 1986; Muir and Lemon 1983). In another study, the relation between M1 neurons and precision grip force depended on the anticipated range of required forces in any given block of trials (Hepp-Reymond et al. 1999). Likewise, during supination / pronation movements, MI activity appeared to be especially important in controlling precise, fine movements at low forces (Evarts et al. 1983).

Brain-machine interfaces (BMIs) are a promising technology, and may allow the restoration of movement for patients with spinal cord injury or other forms of paralysis. BMIs typically translate neural signals from the brain into kinematic control signals that can be used to move computer cursors or robotic arms (Taylor and Tillery, 2002; Serruya et al. 2002; Carmena et al. 2003; Hochberg et al. 2006; Velliste et al. 2008). However, beyond the kinematics of movement, an ideal BMI might allow a user to reproduce the wide range of movement dynamics that normally occur as a person moves at different speeds and interacts with objects of different mass and compliance. Although it is well known that the primary motor cortex (M1) contains a great deal of information about forces and movement dynamics (Evarts 1968; Humphrey, Schmidt, and Thompson 1970; Hepp-Reymond et al. 1999; Cheney and Fetz 1980) this information is ignored by kinematic decoders. Instead, movement dynamics are handled by the controller rather than the user.

Arguably the earliest BMI study made predictions of both force and kinematic variables using as many as five neurons. While force was predicted the most accurately of the movement-related signals, it required that the decoder gains be scaled across tasks with different ranges of applied force (Humphrey, Schmidt,

and Thompson 1970), consistent with several of the single-neuron studies reviewed above. More recently, a few groups have attempted to control reaching with BMIs that combined kinematic and torque decoders (Chhatbar and Francis 2013; A. Suminski et al. 2011) or incorporated musculoskeletal models into their decoders (H. K. Kim et al. 2007; Héliot et al. 2010). Perhaps the most direct control of movement dynamics has been achieved by predicting the intended activity of paralyzed muscles and using those predictions to control electrical stimulation that causes them to contract (Moritz, Perlmutter, and Fetz 2008; Pohlmeyer, Oby, et al. 2009; C Ethier et al. 2012; Bouton et al. 2016; Ajiboye et al. 2017). Functional Electrical Stimulation (FES) is already in broad use clinically, typically controlled only by the patient's residual movements (Venugopalan et al. 2015; Snoek et al. 2000; AM et al. 2005). With a BMI-controlled FES prosthesis, a user might control limb impedance directly through muscle co-contraction, as well as compensate for external interaction forces. Given the increasingly successful development of wireless BMI technology (Yin et al. 2014; Borton et al., 2013), one can imagine the use of BMI-controlled FES for normal activities of daily living in completely unconstrained environments.

The varied evidence of context dependence in the relation between M1 and motor output suggests that a gain control function may be implemented downstream of M1. In this case, a single linear M1-to-EMG decoder may be inadequate for the broad range of movement dynamics we envision. When EMG decoders have been tested across different postures or in the presence of different loads, they tended to generalize more successfully than did predictions of kinematic decoders (Cherian, Krucoff, and Miller 2011; Morrow, Jordan, and Miller 2007; Oby, Ethier, and Miller 2013) (Cherian, Krucoff, and Miller 2011; Morrow, Jordan, and Miller 2007). However, even for this relatively limited range of movement dynamics, the generalization was considerably less than complete.

Here we examine the ability of decoders to predict wrist EMG across three highly varied dynamical conditions: isometric force production, unloaded movements, and movements against an elastic load. Neither linear Wiener filters nor nonlinear recurrent neural networks (RNNs) extrapolated well to tasks beyond those they was trained on. Only the RNN works well when trained on all three tasks. To allow the Wiener filter to also perform well across tasks, we needed to incorporate a task specific gain. Furthermore, most of this gain effect can be attributed to mechanisms downstream of cortex.

3.2 Materials and Methods

3.2.1 Behavioral tasks

We trained two male rhesus monkeys (*Macaca mulatta*: Monkey J, 10.5kg, and Monkey K, 11.4 kg) to sit in a chair with the forearm restrained, and to grasp a wrist-operated joystick. The monkeys either applied flexion/extension forces (Isometric task), or made flexion/extension movements against no load (Movement task), or against an elastic load (Spring task). For the Movement and Spring tasks, endpoint position of the hand was represented by a computer cursor displayed on a computer screen placed at eye-level. For the Isometric task, the cursor position instead displayed force. A trial began when the monkey moved the cursor to a central target, which for all three tasks meant that the wrist was in a neutral position with the forearm and hand aligned. After a hold time of 500ms, a second target appeared, chosen randomly from three extension and three flexion targets of different magnitude. To complete a trial successfully and receive a liquid reward the monkey had to reach this target within five seconds and hold it for 500ms. We recorded 15 minutes of data per task during each experimental session. All methods were approved by Northwestern University's IACUC committee and were done in accordance with the *Guide for the Care and Use of Laboratory Animals.*

3.2.2 Surgical Procedures

After training both animals to perform all three tasks, we implanted a 96-channel microelectrode array (Blackrock Microsystems, Salt Lake City, Utah) into the hand area of primary motor cortex (M1). During the surgery, we identified the hand area through sulcal landmarks and by stimulating the surface of motor cortex to elicit twitches of the wrist and hand muscles. In a separate procedure, we implanted 24 pairs of intramuscular electrodes into wrist and hand muscles. The muscles most relevant to the tasks we focus on in this paper were the wrist flexors and extensors: flexor carpi ulnaris (FCU), flexor carpi radialis (FCR), extensor carpi ulnaris (ECU), and extensor carpi radialis (ECR).

3.2.3 Data collection

We recorded neural activity, EMG and force using a 128-channel Cerebus data acquisition system (Blackrock Microsystems, Salt Lake City). Data collected during the Spring task are shown in **Figure 3-1**. We discriminated action potential waveforms and their corresponding time-stamps using

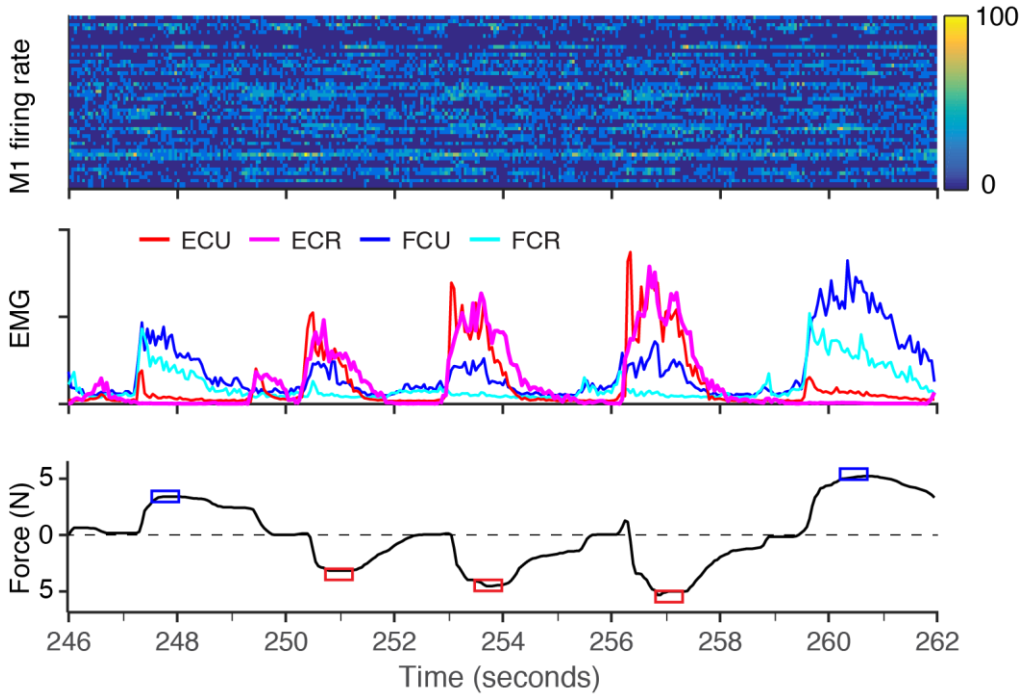

Figure 3-1. Spring task data. Neural activity, EMG activity, and applied force during the Spring task.

Offline Sorter (Plexon Inc, Dallas, Texas), and subsequently binned firing rates of single neurons into 50ms bins. We collected both flexion/extension and radial/ulnar force data at a sampling rate of 2000 Hz. EMG was amplified (500x), band-pass filtered (80-500Hz) and sampled at 2000 Hz. The EMG signals were then rectified, low-pass filtered at 10Hz, and down-sampled to 20Hz to correspond to the bin size of the neurons. We evaluated EMG quality by examining the power spectral density of the raw signals, and omitted any from a session that were corrupted by noise. Before computing decoders, we normalized the EMG data across tasks to the 99th percentile of EMG in each session. For some of the data from Monkey J, we also identified and removed brief artifacts. Examples of EMG data from all three tasks are shown in **Figure 3-2**.

3.2.4 M1-to-EMG decoder development

For each experimental session, we computed separate M1-to-EMG decoders for each muscle for each task. For each task, we used 10 minutes of data for training the decoder, and the remaining five minutes for testing. We refer to *Within* decoders for cases where we trained and tested a decoder on data

from the same task. *Across* decoders were trained on a single task, and tested on data from another task. We computed both linear and nonlinear versions of each decoder using a linear Wiener filter and a recurrent neural network (RNN), respectively. All decoders used 10 lags, resulting in a total filter length of 500ms.

The nonlinear decoder we used was a long short term memory (LSTM) network, a type of RNN. The inputs and outputs were z-scored, and the inputs fed into a single recurrent layer with 200 or 400 units, depending on whether three or four muscles were being predicted, respectively. The recurrent units were densely connected to the output units. We used a dropout rate of 25% to avoid overfitting (Agarwal, Negahban, and Wainwright 2012). The model was implemented using the Keras package and the LSTM weights were fit to minimize the mean squared error using the RMSprop algorithm.

We also trained linear and nonlinear *Hybrid* decoders using training sets consisting of ten minutes of data from each task. To avoid biasing in the linear decoders toward the data with the greatest variance, we used weighted least mean squares regression to calculate our decoders, weighting the squared error of each data point according to the variance of EMG relative to Isometric EMG. For the nonlinear decoders, we also altered the objective function to weight the squared error of each data point inversely to the task's EMG variance relative to Isometric EMG.

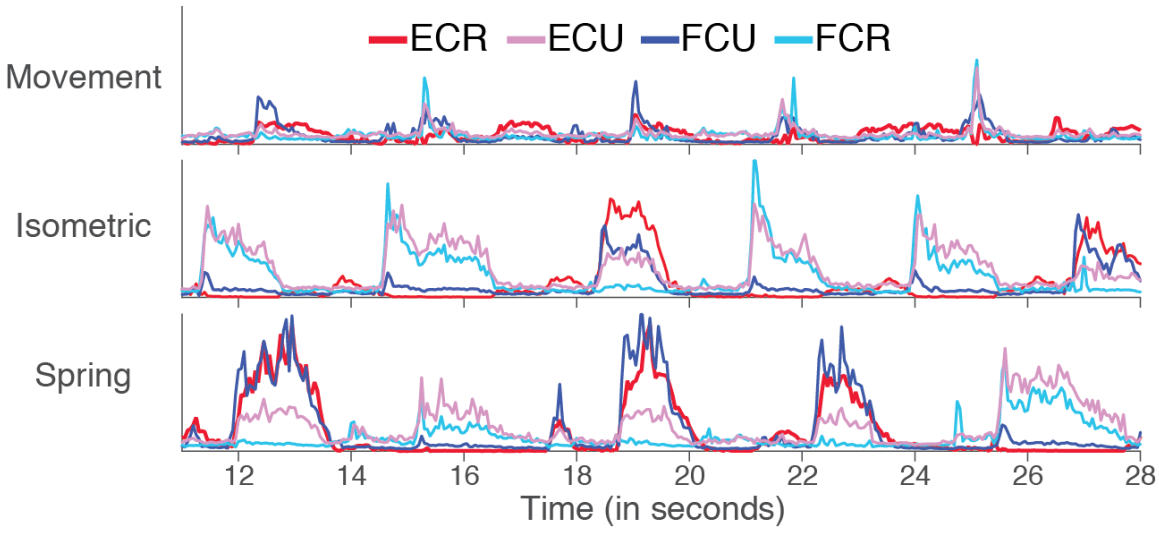

Figure 3-2. Differences in EMGs across tasks. The movement task required the lowest muscle activation, while the Isometric and Spring tasks required similar levels of muscle activation.

3.2.5 Modified Hybrid Decoders

To understand why a single linear M1-to-EMG decoder did not work across all tasks, we tested whether a downstream gain and/or threshold that was independent for each task could explain the differences in mappings across tasks. To do so, we computed additional parametric decoders that cascaded task-specific gain and/or thresholds after a Wiener filter that was shared for all tasks. The Hybrid-GT decoder had independent gain and threshold parameters for each task. The Hybrid-G decoder had the same threshold for all tasks followed by an independent gain for each task. The Hybrid-T decoder had an independent threshold parameter for each task.

The original *Within* and *Hybrid* decoders did not have any threshold, while the gain and threshold models did. In order to be able to facilitate a fair comparison to the gain and threshold models, we therefore created 1) a modified *Within* decoder that included a threshold unique to each task; and 2) a modified *Hybrid* decoder that included a threshold shared by all tasks. A summary of the features of each decoder is summarized in Table 3-1.

Table 3-1. Modified decoder parameter summary. This table describes which parameters were shared across tasks and which were independent.

Decoder	Wiener Filter	Gain	Threshold
Modified Within	Independent	Independent	Independent
Modified Hybrid	Shared	Shared	Shared
Hybrid-GT	Shared	Independent	Independent
Hybrid-G	Shared	Independent	Shared
Hybrid-T	Shared	Shared	Independent

We used the Keras package to implement these models, fitting all parameters simultaneously. For example, for the Hybrid-G model, the Wiener filter parameters and gain parameters were fit simultaneously, rather than sequentially fitting a Wiener filter and then gain parameters. Thresholds were implemented as a bias term followed by a rectified linear unit to set all negative values to zero. All parameters were optimized using the Adam algorithm (Kingma and Ba 2015).

To evaluate whether cortical or downstream gain changes led to changes in EMG, we analyzed the fit parameters of the Hybrid-G model. We defined cortical contribution as the 95th percentile of the output of the Wiener filter portion of the model. The downstream gain was simply the value of the gain parameter. In this Hybrid-G model, the cortical contribution multiplied by the downstream gain is what resulted in the 95th percentile of predicted EMG. However, the actual values of the cortical contribution and downstream gain were meaningless by themselves. This is because there was an extra degree of freedom when fitting the models – it is possible to multiply the gain by a constant, *K*, and divide the cortical contribution by *K* to get an identical model fit. We estimated this constant to more meaningfully compare the two parameters, and to analyze how these parameters changed between small to large EMGs.

To demonstrate the difference between cortical contribution and downstream gain, we evaluated these parameters versus the 95th percentile of EMG. We estimated the constant K for each model fit, which was fit separately for each muscle and session. To estimate *K*, we assumed that, at the minimal EMG of 0.03, there was a gain of 1 and a cortical contribution of 0.03. For each model fit, we first fit a line to the cortical contributions in each task. For example, if the value of the line at EMG=0.03 was C_0, we found *K* so that $C_0 * K = 0.03$. In other words, we simply scaled the line so that it met our assumption. We multiplied all cortical contributions by *K* and divided all the gain parameters by *K.* Finally, to plot the results, we scaled the cortical contributions so that the line of best fit had a y-intercept at 1, in order to more easily interpret the rate of growth. It is important to note that the specific assumption that there is a gain of 1 and cortical contribution of 0.03 at EMG=0.03 is irrelevant for looking at the increase of gain and cortical contribution over increasing EMG. For instance, assuming a gain of 2 and cortical contribution of 0.015 would give equivalent results, because we are simply scaling all values by a constant. The important measure here was the ratio between the cortical contribution and gain at the minimum and maximum EMG values, and not the exact values of the points.

3.2.6 System analysis

For each day, we input white noise into the three types of single-task decoders (Isometric, Movement, Spring). We computed the mean power of the output between 0 and 1 Hz, which is in the

frequency range of normal hand movement. We then plotted the mean power of each output between 0 and 1 Hz versus the mean power between 0 and 1Hz of the actual EMG.

3.2.7 Evaluation of decoder performance

In order to evaluate the quality of fit between actual and predicted signals, we computed the variance accounted for (VAF) using the following equation:

$$VAF = 1 - \frac{\sum_{i=1}^{N}(\hat{s}_i - s)^2}{\sum_{i=1}^{N}(s_i - \bar{s})^2} \quad \text{(Eq. 1)}$$

where N is the number of data samples, s_i is an actual signal sample, $\hat{s}_i$ is a predicted signal sample, and $\bar{s}$ is the mean of the actual signal. VAF is similar to the coefficient of determination, but requires a match between the two signals rather than just a correlation, making it a more appropriate metric for evaluating a control signal. As a consequence, if the variance of the prediction is larger than that of the actual signal, VAF can be negative (Nemati et al. 2007).

To summarize prediction quality across muscles, we computed a multivariate mVAF, a slight modification of Eq. 1:

$$mVAF = 1 - \frac{\sum_{m=1}^{M}\sum_{i=1}^{N}(\hat{s}_{i,m} - s_i)^2}{\sum_{m=1}^{M}\sum_{i=1}^{N}(s_{i,m} - \bar{s})^2} \quad \text{(Eq. 2)}$$

where M is the number of muscles. This equation can also be written as

$$mVAF = 1 - \frac{\sum_{m=1}^{M} SS_{res,m}}{\sum_{m=1}^{M} SS_{tot,m}} \quad \text{(Eq. 3)}$$

where SS_{res} is the residual sum of squares and SS_{tot} is the total sum of squares, both computed across all muscles. We also computed the ratio between the sum of squared errors of each *Across* or *Hybrid* decoder over the sum of squared errors (SSE) of the *Within* decoder:

$$SSE_{ratio} = \frac{\mathrm{SSE}_{\mathrm{Across/Hybrid}}}{\mathrm{SSE}_{\mathrm{Within}}} \quad \text{(Eq. 4)}$$

This metric summarizes the performance of each *Across* or *Hybrid* decoder relative to the *Within* performance for each task. We chose this metric instead of a ratio of VAFs to avoid the complications that arise from negative VAF. To evaluate differences between the mVAFs or SSE_{ratio} for each decoder across days, we used one-sided Wilcoxon signed-rank tests.

3.3 Results

Our goal here was to evaluate the extent to which several different types of decoders could make accurate EMG predictions across three dynamically different tasks, and to investigate the mechanisms that make this multi-task decoding a challenge. We recorded data from two rhesus monkeys during performance of isometric, spring-loaded, and free movement wrist tasks. We computed both linear and nonlinear decoders, trained with data from various combinations of these tasks, and tested the accuracy of the predictions on each task.

3.3.1 Single task linear prediction performance

To evaluate decoder performance, we computed *Within* task and *Across* task predictions for all combinations of training and testing data. *Within* predictions for the Isometric and Spring data (made using training and testing data from the same task) typically were generally more accurate than for the Movement task, perhaps due to the small magnitude of those EMGs, or their dynamically more complex structure. For the examples shown in Figure 3-3, the variance accounted for (VAF) computed between actual and predicted EMG was 0.74, 0.46, and 0.70 for the Isometric, Movement, and Spring *Within* predictions, respectively.

In contrast, *Across* prediction accuracy was significantly poorer. Predictions of Isometric data using decoders trained with Spring data tended to overshoot (in this example in Figure 3-3A, the VAF between the predicted and actual signals was 0.38), while the corresponding predictions using Movement-trained decoders dramatically undershot the actual EMG (VAF = -0.12). *Across* prediction performance of Movement data was even worse. In a representative example (Figure 3-3B), the Isometric and Spring decoders both produced predictions which overshot the signal, with negative VAF (-0.47 and -0.88, respectively). For Spring data (Figure 3-3C), the Isometric and Movement decoders also undershot (VAF=0.40 and -0.18).

3.3.2 Accurate predictions spanning all tasks require a nonlinear decoder

Given the failure of the single-task decoders to generalize across tasks, we tested the accuracy of decoders when trained with data from all three tasks, which we refer to as *Hybrid* decoders (see Materials and Methods). Importantly, to prevent the *Hybrid* decoder from being dominated by the task with the

greatest signal power, we weighted the squared error of each data point according to the variance of EMG relative to Isometric EMG. While the *Hybrid* decoder predictions were significantly more accurate than the *Across* predictions (Figure 3-5) they remained poorer than the *Within* decoders. In these examples, the *Hybrid* predictions of both Isometric (**Figure 3-4**A; VAF=0.53) and Spring EMG (**Figure 3-4**C; VAF=0.46), tended to undershoot. The Movement data were also fit relatively poorly, (VAF = 0.30), but with no obvious gain error (**Figure 3-4**B).

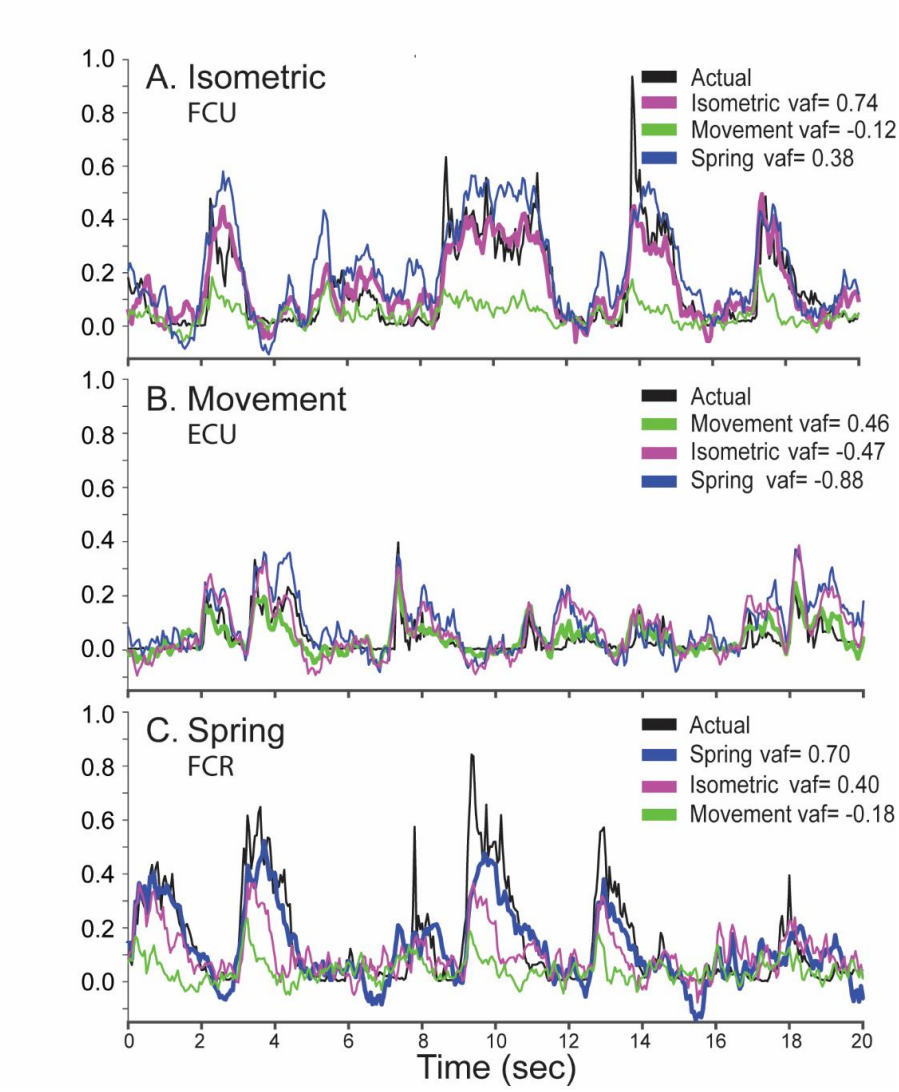

Figure 3-3. Across Predictions for the Three Tasks. Each panel in this figure shows the actual normalized EMG trace for each task in black. The other traces show predictions made using the Isometric decoder (pink), the Movement decoder (green), and the Spring decoder (blue).

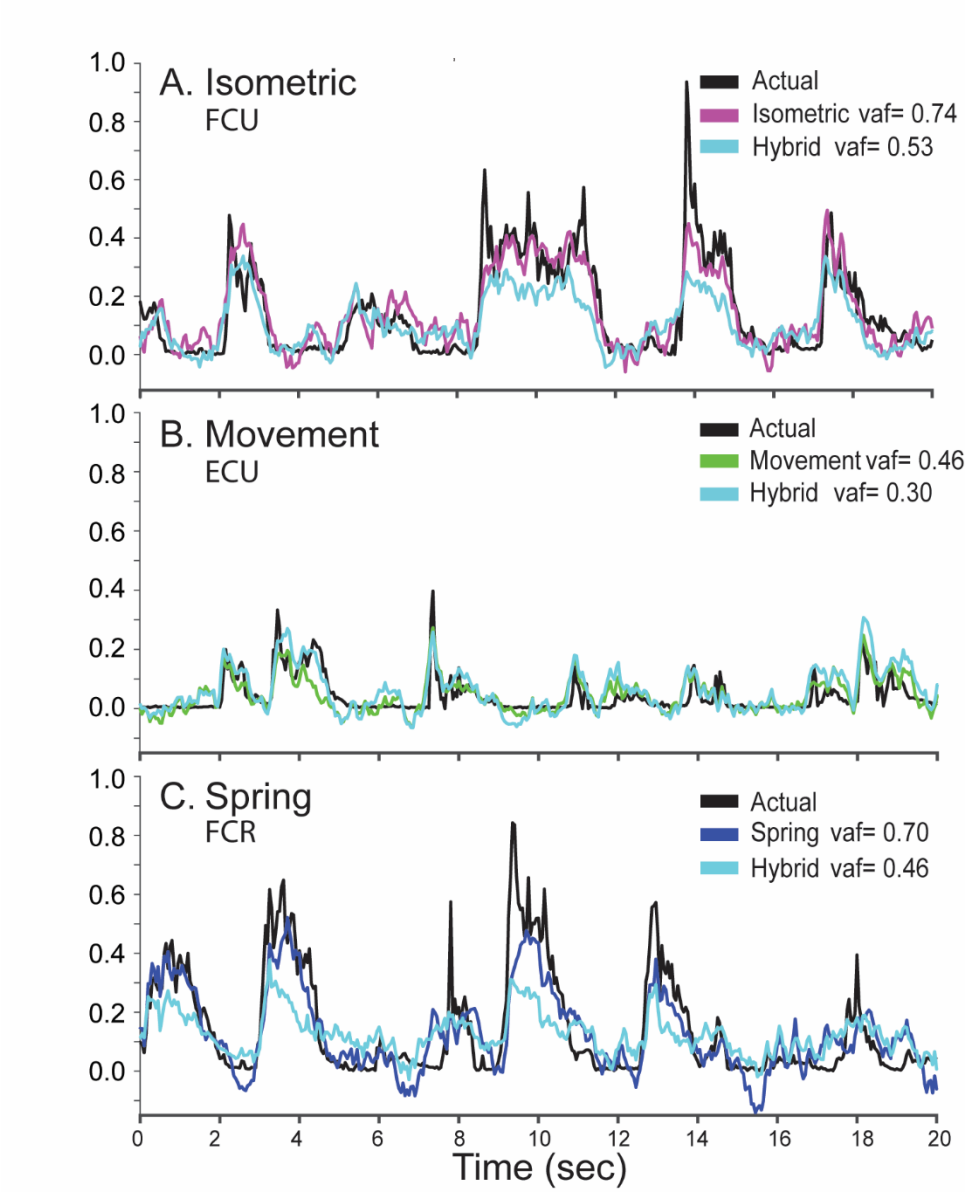

Figure 3-4. Hybrid Linear predictions. The black trace in each panel shows an example the actual normalized EMG trace for each of the three tasks. The cyan traces show predictions made from the Hybrid decoder, while the third trace in each panel shows the respective *Within* predictions.

Consistent with the examples, the *Across* decoders performed significantly worse than *Within* on all experimental days for both monkeys (Figure 3-6, top panels). To summarize prediction quality, we developed a multivariate VAF (mVAF) metric that allows us to report goodness of fit across all muscles, discounting muscles that were not well activated in any given task (see Materials and Methods). As shown

in the mVAFs in **Figure 3-5**, all *Across* decoders were significantly less accurate than the *Within* decoders (one-sided Wilcoxon signed rank tests, largest p value p=0.02). The linear *Hybrid* decoder results fell between those of the *Within* and *Across* decoders. This can be seen most clearly in terms of the SSE ratio comparing each decoder's performance to the corresponding *Within* decoder (**Figure 3-5**, bottom panels). The SSE ratio for the *Hybrid* decoder ranged from 0.53-0.79 for Monkey J and 0.70 and 0.85 for Monkey K, all significantly better than the *Across* decoders (largest p=0.049 for Monkey J, largest p=0.03 for Monkey K) , but consistently poorer than the *Within* performance (largest p=0.02 for Monkey J, largest p=0.03 for Monkey K).

To further understand the modest multi-task performance of the *Hybrid* decoder, we also explored nonlinear methods, repeating our analyses using an RNN (see Materials and Methods). Across-task predictions with the RNN did not generalize, similar to linear decoder results (Supplementary **Figure 3-11**), but a *Hybrid* RNN generally outperformed the linear *Hybrid* for all three tasks, as demonstrated in the examples in **Figure 3-6**. In these examples, the *Hybrid* RNN captured the Isometric EMG trace very well, while the linear *Hybrid* failed to capture the full magnitude of actual signal (Figure 3-6A; VAF=0.82 for RNN *Hybrid*, VAF=0.53 for Wiener *Hybrid* example). During movement (Figure 3-6B), the RNN *Hybrid* followed the Actual trace well, yielding a VAF of 0.71 compared to the analogous linear result of 0.30. Although the RNN *Hybrid* did not capture all peaks of the Spring data (Figure 3-6C), it nonetheless performed remarkably well, with a VAF of 0.80. The linear *Hybrid* trace modulated but failed to capture either baseline or peaks of Spring muscle activity (VAF=0.45).

Overall, the nonlinear decoders outperformed their linear counterparts (**Figure 3-7**, largest p=0.02 and p=0.03 for Monkey J and K, respectively). SSE ratios of each Hybrid decoder compared to its respective linear or nonlinear *Within* values are shown in the bottom panel of **Figure 3-7**. The SSE ratios for the nonlinear *Hybrid* predictions ranged from 0.85 to 0.98 in Monkey J, and from 0.87 to 1.05 in Monkey K. Overall, these ratios demonstrate the nonlinear *Hybrid* decoder's improved performance over the linear *Hybrid*.

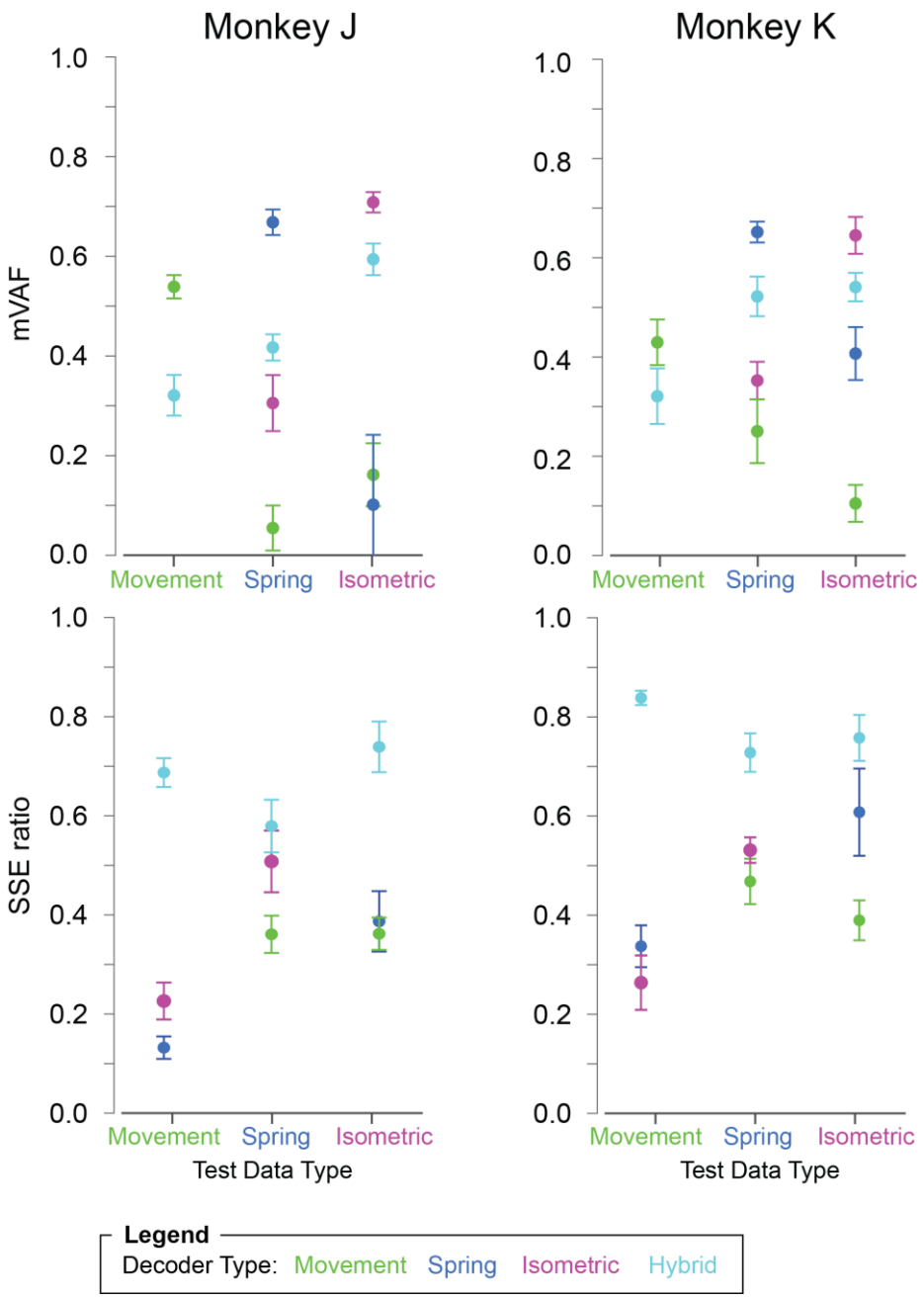

Figure 3-5. Summary for all linear decoders. The top panel shows the mVAF for all the muscle predictions averaged across all experiment days for Monkeys J and K. The bottom panel shows the SSE ratio of each decoder's predictions relative to the *Within* decoder.

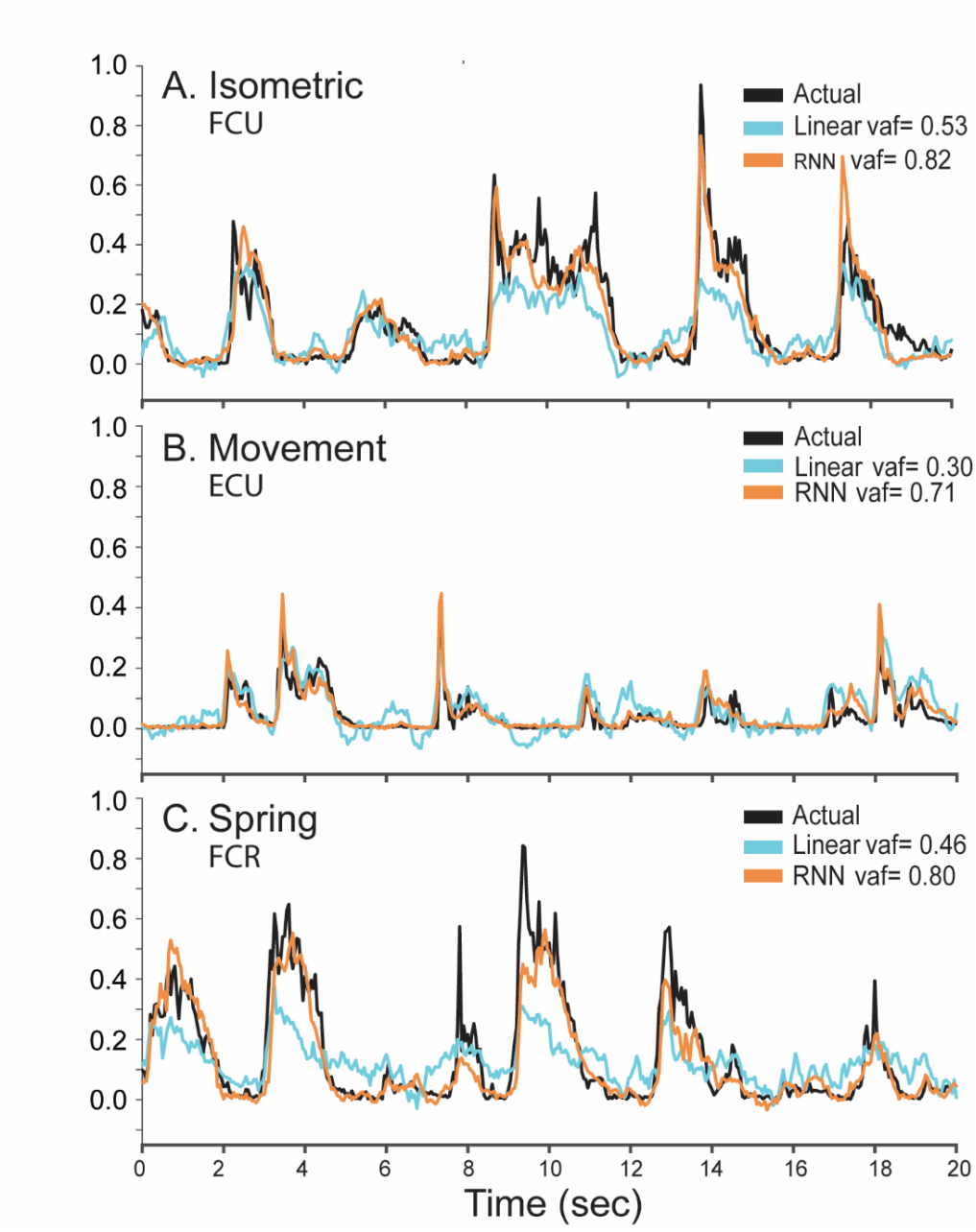

Figure 3-6. Examples of linear and nonlinear predictions. For all three tasks, the Hybrid RNN decoder outperformed the Hybrid linear decoder, as shown for the example predictions shown here.

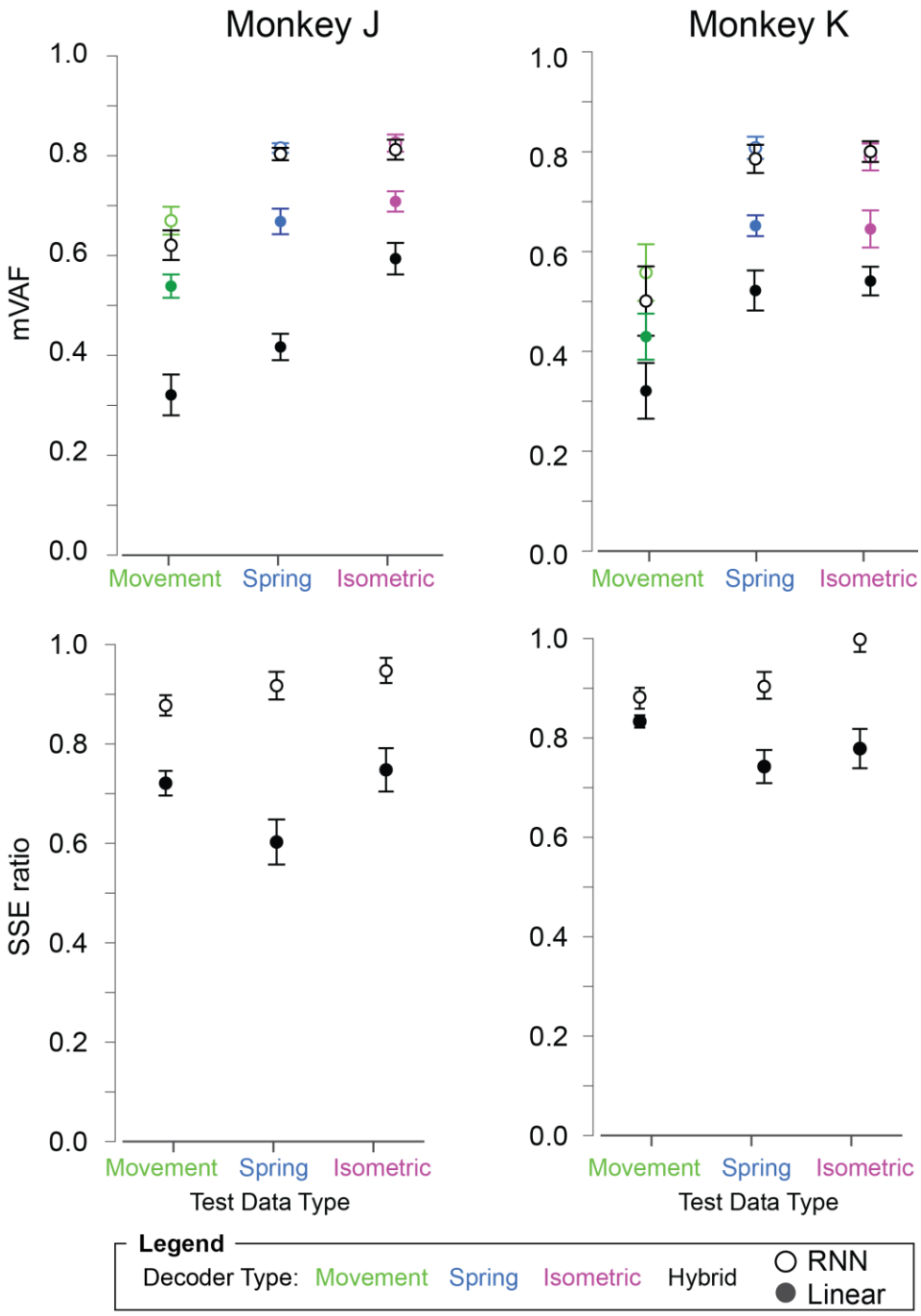

Figure 3-7. Linear versus Hybrid RNN Summary. The top panels of this figure show the absolute mVAF across muscles for predicting EMG in the three tasks. The *Hybrid* decoders are shown in black, while the *Within* decoders are shown in the color corresponding to each task. The bottom panels show the SSE ratio between the SSE of *Hybrid* decoder relative to the SSE of the *Within* decoder predictions.

3.3.3 Mechanisms downstream of cortex

If the nonlinearity captured by the RNN decoders were simple task-dependent gain or filter characteristic, it might be apparent in the output of the linear decoders. To test this hypothesis, we input white noise into each decoder and examined the output. We plotted the power of the predicted output from 0-1Hz against the power of the actual EMG at 0-1Hz, as shown in Figure 3-8. Surprisingly, there was a generally linear relationship between predicted and actual EMG power, related not simply to the task, but rather the EMG power. This is demonstrated in the figure, where ratio between predicted and actual EMG increased with increasing EMG power independently of the task, and even across muscles. These results suggests that mechanisms downstream of our recordings in M1, unaccounted for by the linear decoders, substantially transformed the signals.

The linear relationship in **Figure 3-8Figure 1-1** could be explained by either a signal-dependent gain, or a fixed threshold, gradually exceeded by an increasing proportion of the descending signal. Both functions have been proposed to exist with spinal circuitry (Humphrey, Schmidt, and Thompson 1970; Wei et al. 2014). We therefore explored this question by including explicit gain and threshold parameters separately, and in combination, following the linear dynamic component of the *Hybrid* decoder (see Materials and Methods). A Hybrid decoder that included both parameters was able to capture 82-88% of the nonlinear Hybrid RNN for Monkey J, and 86-93% of the Hybrid RNN for Monkey K, as demonstrated by the means in **Figure 3-9**.

The order of the gain and threshold functions made no difference. Including only the gain parameter yielded performance almost as good as the gain+threshold decoder, and significantly better than threshold-only decoder (significant for Spring and Movement tasks across both monkeys, $p=0.0009$ and 0.0001, respectively). Overall, these results suggest that the spinal cord may play mostly an autogain role that reduces the required dynamic range of cortical activity. If there is also a spinal threshold function, it would appear to play a more minor role.

Lastly, we evaluated the relative magnitude of the postulated downstream gain effect relative to the "cortical contribution" – the output of the Wiener filter portion of the model – by computing their respective contributions as a function of actual EMG (refer to *Materials and Methods*) (Figure 3-10). For Monkey J, the

gain component increased by a factor of 15 over the range of normalized EMG (from 0.03 to 0.6), while cortical gain increased by a factor of only 1.3. For monkey K, downstream gain increased eight-fold, and cortical gain by 2.5. These results suggest that a downstream gain mechanism plays a very large and important role as cortical output spans its full dynamic range.

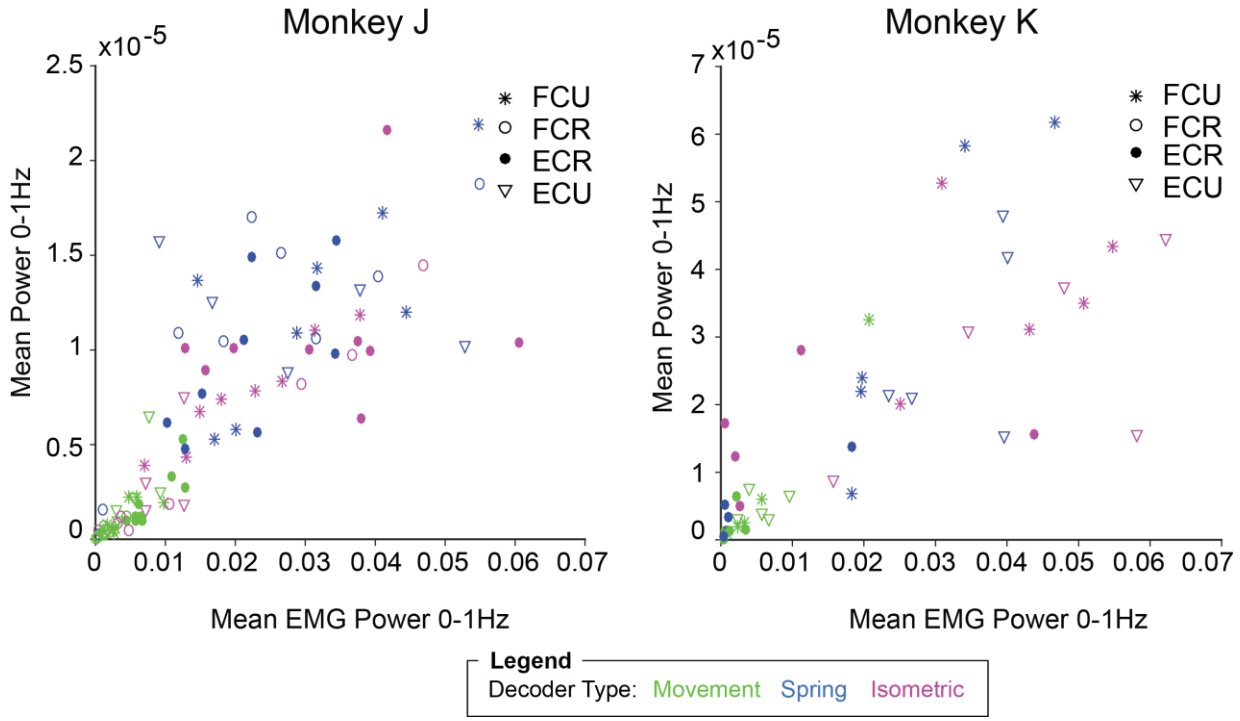

Figure 3-8. System gain. For each muscle, we show the relationship between the power of the output of the signal when white noise is input into each decoder, versus the power of the actual EMG signal. Power is computed as the mean from 0 to 1Hz, which is in the range of natural movement.

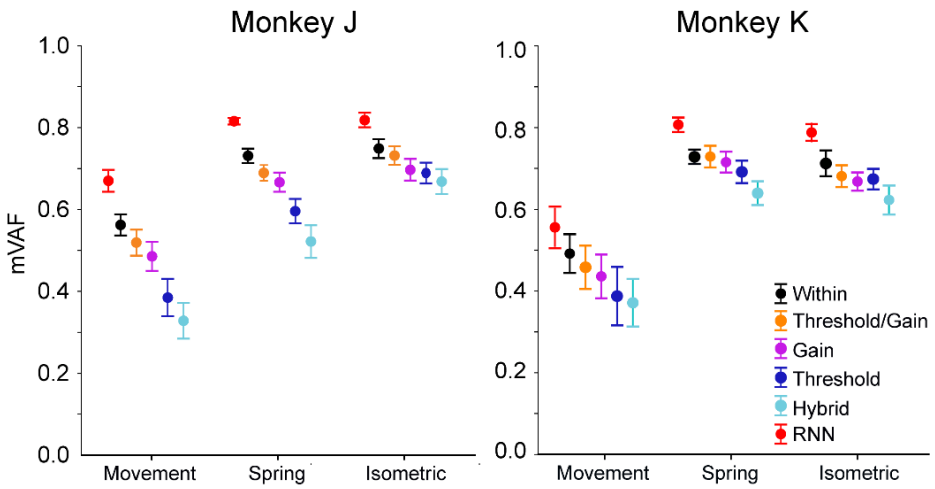

Figure 3-9. Modified hybrid decoder predictions. Summary mVAF values for the modified *Hybrid* decoders, which either included a gain parameter, a threshold parameter, of both. The *Hybrid* RNN mVAFs are shown here (red) for reference.

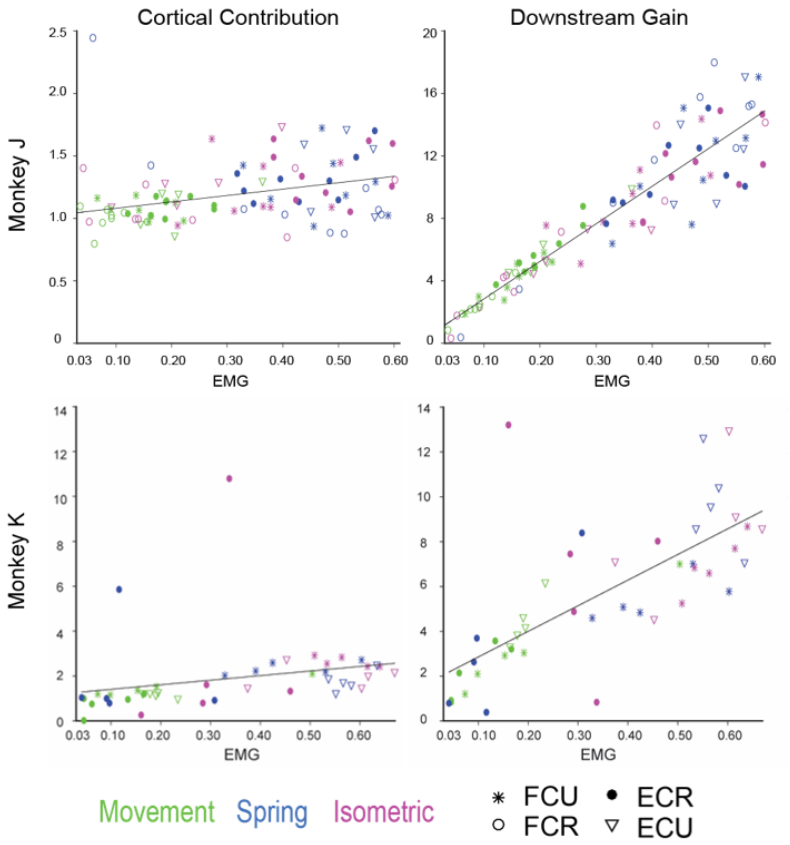

Figure 3-10. Cortical contribution and downstream gain. These subplots show the cortical contribution and downstream gain parameters from the Hybrid-G model versus the 95th percentile of EMG.

3.4 Discussion

3.4.1 Summary

We have studied the role of M1 in controlling tasks that have widely varied dynamics: one involving isometric torques about the wrist, another unloaded wrist movements, and a third requiring elastically-loaded movements. These tasks also spanned a broad range of muscle activity. We used the quantitative methods of BMI technology to compute M1 to EMG "decoders" that predicted EMG from multi-electrode M1 signals. We showed that decoders trained with data from one or even two tasks failed to generalize accurately across tasks, whether the decoder was a simple linear map or nonlinear recurrent neural network. Furthermore, only a nonlinear "Hybrid" decoder, trained with data from all three tasks, could make accurate predictions for all three. We could account for much of this apparent nonlinearity between M1 and EMG by explicitly modeling a signal-dependent gain following a linear decoder. Our analysis also revealed that a surprisingly large proportion of muscle activity at high levels of contraction is due to downstream mechanisms. These results have important implications for our understanding of the descending control of normal limb movements, and also in the design of more robust BMIs.

3.4.2 A context-dependence between M1 and EMG that is driven by the magnitude of cortical output

A number of studies have suggested that the relationship between M1 and movement may be context-dependent. In his seminal 1970 paper, Don Humphrey described the ability to decode force, dF/dt, position, and velocity using a small handful of simultaneously recorded M1 neurons (Humphrey, Schmidt, and Thompson 1970). As in the earlier single-neuron experiments of Evarts (Evarts 1968), force was generally the best-predicted variable. However, Humphrey discovered that when the mass against which the monkey moved was changed, although predictions remained well correlated with actual force, it was necessary to scale the regression coefficients between M1 and force. In later experiments, Evarts found what might be a similar nonlinearity among pyramidal tract neurons during a supination-pronation task. Well over half of the neurons were disproportionately active (relative to EMG) during small, corrective movements compared to rapid, ballistic ones (Fromm and Evarts 1977). The net effect was that M1 modulation was disproportionately large for small force ranges. Similar observations have been made for

wrist movements (Werner, Bauswein, and Fromm 1991). Finally, in a precision grip task that required a sequence of force levels, Hepp-Reymond and colleagues found that firing rates depended on the anticipated range of forces. Among 85 neurons displaying similar finger-related discharge across all trial types and showing significant force modulation, 15 (18%) appeared to remap their range of firing rates depending on the expected range of required force (Hepp-Reymond et al. 1999). Notably, this effect disappeared when the subjects when the force range cue was removed from each trial.

Other types of context-dependence have also been reported, including in pyramidal tract neurons (PTNs), which are motor neurons that originate in cortex and terminate in the spinal cord or brainstem. These PTNs have been shown to vary their relation to muscle activity between rake use, picking up treats, and precision grip (Muir and Lemon 1983; Quallo, Kraskov, and Lemon 2012). More recently, Rasmussen and colleagues demonstrated a kinematic context-dependent firing of M1 position predictions between a 2D and a 3D task (Rasmussen, Schwartz, and Chase 2017). While the motor control system may be subject to different kinds of context dependence, here we specifically demonstrate an EMG-dependence, similar to the results of Humphrey, Evarts and colleagues, and Hepp-Reymond and colleagues. Like Humphrey (Humphrey, Schmidt, and Thompson 1970), we were able to improve predictions across a broad range of muscle activity by implementing a gain parameter. While some of this gain could be attributed to differences in cortical firing, we also found that much of this gain was implemented downstream of cortex.

3.4.3 The downstream gain mechanism may be due to the regulation of persistent inward currents

Persistent inward currents (PICs), present in spinal motoneurons, are one possible explanation for the downstream gain adjustments we observe here. PICs are generated by voltage-sensitive sodium and calcium currents that are slow to inactivate, and are therefore capable of prolonging depolarization. In motoneurons, PICs are mostly concentrated in the dendrites, and are dependent on descending drive from monoamines such as serotonin and norepinephrine. Serotonin production is signaled by neurons in the raphe nucleus, where conduction velocities for two different groups of raphe-spinal neurons are between 0.7-1.0m/s and 3.1-6.0m/s (Wessendorf, Proudfit, and Anderson 1981). This means that serotonin can reach the spinal cord of primates on the order of about a second or less. Once in the spinal cord, serotonin

and norepinephrine in turn influence the initiation of PICs, which have an onset time constant of about 50ms. PICs can have a remarkably strong effect on motoneuron firing, potentially amplifying the effect of synaptic input five-fold or more (Heckman et al. 2009; Lee and Heckman 2000). The magnitude of this effect is compatible with the apparent contribution of downstream gain to EMG production that we have observed (Figure 3-10). The timing of descending neuromodulatory drive and PIC effect also generally aligns with our task, where monkeys typically acquired targets between 0.8 to 4 seconds after target presentation, a time frame during which PICs can potentially influence motoneuron excitability on a trial-by-trial basis.

The large effect of PICs on synaptic input has been demonstrated in decerebrate and pentobarbital-anesthetized cats, where synaptic input scaled with increasing neuromodulatory drive (Lee and Heckman 2000). By monitoring their effect on the spinal stretch reflex, Wei and colleagues showed that serotonin reuptake inhibitors and agonists can modify the gain of descending signal transmission in humans (Wei et al. 2014). Voluntary activation of one muscle group caused widespread effects that dissipated about two seconds after the contraction ended. The downstream effect of these mechanisms has also been observed in the behavior of spinal-projecting serotonergic neurons. In their 2002 study, Jacobs and Fornal reported that these neurons, recorded from the caudal raphe nuclei of cats, vary their tonic firing rates in proportion to the speed of locomotion. The tonic relation of these neurons to overall speed, rather than each phase of locomotion, suggests that these cells set the overall state of the spinal locomotor apparatus (Jacobs, Martín-Cora, and Fornal 2002). Similarly, these cells may increase neuromodulatory input for tasks requiring increases in muscle activation. In light of these studies, our results suggest that when the motor system expects to produce more output, it increases the presence of neuromodulators in the spinal cord, which amplifies the excitability of motor neurons.

3.4.4 Other mechanisms beyond gain that may explain the inability to predict across tasks

In addition to a downstream gain-regulatory function potentially mediated by PICs, other factors may also have affected our ability to predict muscle activity across tasks with a linear decoder. For instance, despite requiring similar magnitudes of muscle activation, predictions of Isometric data using a Spring

decoder, and vice-versa, did not generalize completely. Differences in firing across-tasks might therefore be due to the M1 encoding of muscle properties, such as the force-velocity and length-tension relationship, which differed among tasks. In one example, Fromm demonstrates that M1 activity reflects the length-tension relationship of muscles (Fromm 1983). In a single-unit study, he showed differences in M1 firing between an isometric and an isotonic, load-bearing task, similar to the Spring task here. M1 firing varied as a function of muscle length even during a constant load.

Differences in afferent feedback from muscle spindles and Golgi tendon organs about muscle length and tension are especially important considering that proprioceptive signals reach motor cortex (P L Strick and Preston 1982; Zarzecki and Asanuma 1979), and evidence that output from M1 may be modified by differences in proprioceptive feedback (Gandolla et al. 2014). This latter point was demonstrated in a study where nerve stimulation was used to alter proprioceptive information, resulting in a greater facilitatory effect of M1 on S1.

Another explanation for difficulties in across-task decoding is that there may exist different control systems for movement and posture (Brown, Rosenbaum, and Sainburg 2017; Scheidt and Ghez 2017; Humphrey and Reed 1982). Evidence for this comes partially from the activity of neurons with load-related activity that differs during posture and movement tasks (Kurtzer, Herter, and Scott 2005). This may be the reason that a dual-state movement / posture decoder led to better BMI performance than a simple linear decoder (Sachs et al. 2016).

3.4.5 Few BMIs currently give the user control of dynamics

There have been impressive demonstrations of BMI use in recent years (Hochberg et al., 2006, 2012a; Velliste, Perel, Spalding, Whitford, & Schwartz, 2008), including a tetraplegic human user who learned to control a robotic limb using seven and later ten degrees of freedom (Collinger et al. 2013; Wodlinger et al. 2015). In all of these experiments, however, the user modulated neural activity to control only kinematics, such as speed or endpoint position of a robotic arm, while the robotic controller took care of dynamics (Vogel et al. 2015). By design, these kinematic decoders leave the control of dynamics to be handled by an external controller. There has therefore been rather little investigation into how well neural

decoders might take advantage of the rich force and movement-dynamics-related information in M1 (Evarts 1968; Humphrey, Schmidt, and Thompson 1970; Cheney and Fetz 1980; Evarts et al. 1983). If these variables were also decoded from M1 activity, the user might be able to control movement in a more nearly natural manner that allows for the modulation of impedance and for dealing with interaction forces.

A small number of studies have evaluated BMI use across dynamically-different conditions, though most of these have included only offline predictions, as in the current study (Suminski et al. 2011; Chhatbar and Francis 2013). In one example, a BMI was designed to estimate both kinematic variable and joint stiffness, using EMG-like inputs to a musculoskeletal model of the arm (Héliot et al. 2010). In another study, Cherian and colleagues evaluated the accuracy of proximal arm EMG, hand position, and velocity predictions for reaching movements made in two different workspaces, and with and without added forces (Cherian, Krucoff, and Miller 2011). EMG predictions made across these force-field and normal conditions had R^2 values that were approximately 50-70% of those for within-task conditions. The generalization in that study was substantially greater than ours, though the relative force differences they studied were smaller. Furthermore, that study focused on the proximal arm, which is dynamically more complex than the hand.

3.4.6 Future development of multi-task BMI decoders

Clinically-viable BMIs should execute all types of movements with user effort that feels natural, whether for simply making a rapid pointing movement, or for interacting with objects of varied weight. We show here that it may be possible to give a BMI user full control of movement dynamics by accounting for downstream gain differences across dynamic tasks. Letting the user, rather than a controller, handle dynamics also increases user autonomy. Furthermore, using a BMI to control muscle activity allows for natural impedance control, as the user can appropriately contract the muscles to change arm stiffness as he or she deals with different loads and interaction forces. This natural impedance control will allow the user to successfully operate their BMI during a variety of daily activities that vary dynamically, such as lightly turning the page of a book or lifting a full thermos of coffee. Decoders that work for all the

unconstrained activities of daily living will become more important as fully implantable, continuously available wireless prostheses become feasible (Yin et al. 2014; Borton et al. 2013; Schwarz et al. 2014).

Importantly, another major challenge to real-life multi-task decoding remains that human SCI patients do not have muscle activity with which to compute M1-to-EMG decoders. Current decoders in human clinical trials are computed using observation-based methods (Collinger et al., 2013; Hochberg et al., 2006, 2012; Wodlinger et al., 2015). In human BMI-FES trials, neural activity is correlated to the activation levels of muscle stimulation patterns as the subjects imagine producing coordinated grasp (Ajiboye et al. 2017; Bouton et al. 2016). For practical multi-task decoding, these systems will also need to incorporate a gain parameter into their calibration. Iterative decoder recalibration, as is employed in many BMI studies, will also help to fine-tune gain parameters as the subject undergoes initial trial and error with their system.

Future animal experiments, where EMG is available for decoder-building, will further evaluate the potential of robustly designed Hybrid decoders. While we have shown here that a nonlinear Hybrid decoder trained on multiple tasks can make accurate predictions for those tasks, we have not demonstrated the viability of the Hybrid decoder for extrapolating to new activities. It is unclear how the Hybrid decoder will perform on the continuum of behavior confronted in an unconstrained environment. Another question will be how to appropriately train new Hybrid decoders with data from various unconstrained tasks. Changes in EMG magnitude will be more nuanced as unconstrained BMI users progress from grooming, to grasp, to free movement, and other activities. Unlike the current experiment, where we could weigh the objective function according to signal size in the three discrete tasks, this weighting will be less clear with more rapid changes in EMG magnitudes. A first pass may require training a multi-task decoder on a number of unconstrained activities without any weighting, and evaluating performance.

3.5 Supplementary Material

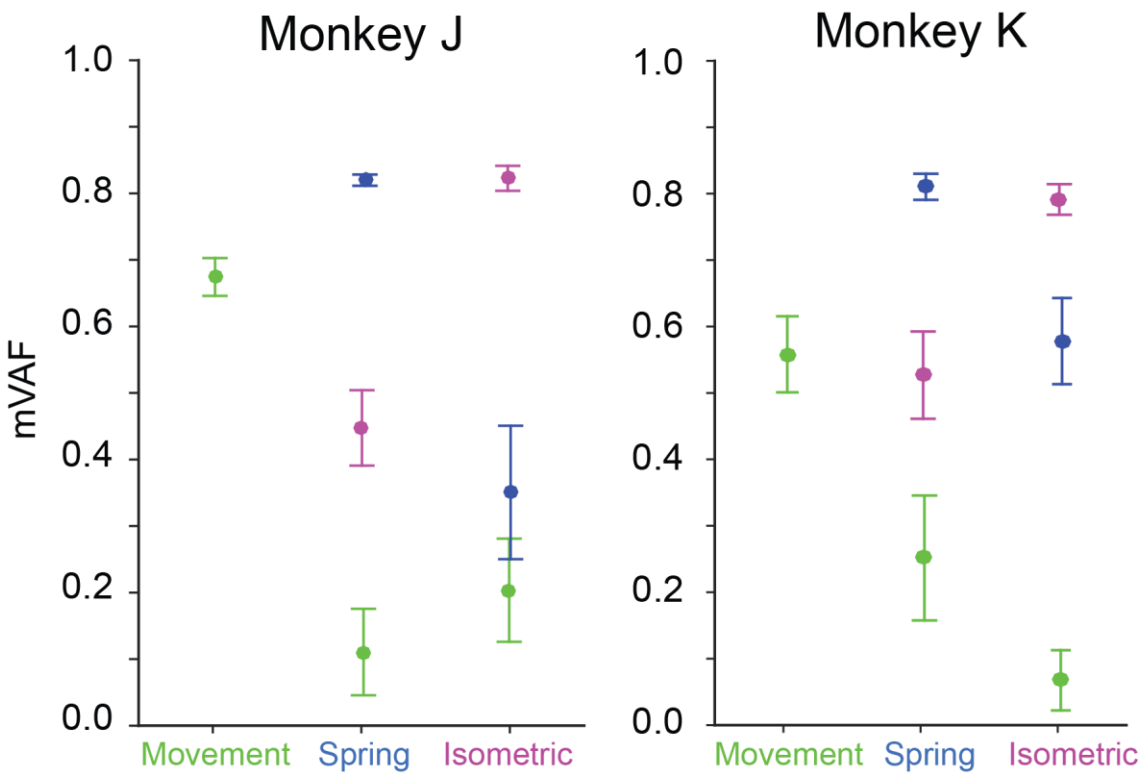

Figure 3-11. Across-task RNN predictions. These plots show the performance of the RNN for within and across-task predictions of actual EMG for the three different tasks, where color reflects the type of task used to train the decoder. Values below zero are not shown.

4 Superior performance using BMI decoders that preserve natural muscle activation patterns

4.1 Introduction

We are constantly faced with the need to learn new motor tasks, from handling a new tool to the undertaking of a new hobby, be it tennis, skiing, or dancing. Many psychophysical studies have quantified this ability to learn new tasks by imposing perturbations on the movement, including visuomotor rotations (Krakauer et al. 2017), prisms that shift the visual field (Martin et al. 1996), and force fields that displace the hand (Shadmehr and Mussa-Ivaldi 1994; Lackner and Dizio 1994). The cerebellum is involved in motor learning (Ito 2000; Llinás and Welsh 1993), as is motor cortex. For example, preferred directions in M1 change during adaptation to a force field task (Li, Padoa-Schioppa, and Bizzi 2001). Understanding the involvement of M1 in learning may be important for the development of brain-machine interfaces (BMI), a remarkable new technology, capable of restoring movement to amputees and patients with spinal-cord injury, stroke, and other movement disorders.

Motor BMIs typically translate neural signals from primary motor cortex (M1) into kinematic control signals for computer cursors or robotic arms (Taylor, Helms Tillery, and Schwartz 2002; Serruya et al. 2002; Hochberg et al. 2006; Hochberg et al. 2012; Velliste et al. 2008; Wodlinger et al. 2015; Collinger et al. 2013). In a few cases, BMIs have been used to predict muscle activity, and in turn stimulate the muscles to restore movement (Pohlmeyer et al. 2009; Ethier et al. 2012; Bouton et al. 2016; Ajiboye et al. 2017). Despite these impressive capabilities, BMI decoders are realistically less than perfect for numerous reasons, including the differences in feedback between brain control and normal conditions, as well as the altered dynamics of the plant being controlled (i.e. cursor control versus hand control). Decoders therefore require user adaptation. Understanding the limits of a user's ability to adapt to these imperfect decoders is important to developing useful BMIs for patient populations.

BMI studies have already shown that users can adapt to a variety of kinematic decoders. This includes adaptation to decoders that are nonbiomimetic, where the decoder weights for individual neurons have been shuffled (Ganguly and Carmena 2009), or in cases where the relationship between M1 and kinematics for a subset of BMI-control neurons has been rotated (Jarosiewicz et al. 2008). However, some decoders are easier to adapt to than others. For example, Sadtler et al. recently demonstrated that kinematic decoders that require M1 neurons to change their covariance structure are more difficult for

monkeys learn than those that do not (Sadtler et al. 2014). A conceptually similar study by Berger et al. described differences in the learning rates between two kinds of muscle-to-force decoders (Berger et al. 2013). Decoders that preserved muscle synergies were easier to learn than those that disrupted synergies. To our knowledge, no study has extended this finding to neural decoders that predict muscle activity, which would probe ability of M1 to adapt to muscle-based decoder perturbations.

Here we trained rhesus macaques to complete a center-out isometric task using both hand and brain control. We used a BMI to evaluate the initial and adapted performance when using two types of altered decoders: one that preserved the natural patterns of muscle activation, and one that did not. Ultimately the monkeys were able to use the decoders that preserved the natural patterns of muscle activation more successfully than those that disrupted this relationship.

4.2 Materials and Methods

4.2.1 Experimental task and design

We trained two rhesus macaques (*Macaca mulatta*, Monkey J, 11kg, and Monkey K, 9kg) to perform a center-out isometric wrist task. During the task, the forearm was held in the mid-prone position by a sled that supported the forearm, elbow, and upper arm, to encourage the monkeys to only use torques about the wrist to complete the task. The monkey's working hand was placed in a padded box, and a force-torque sensor measured force applied about the wrist. The monkeys sat in a chair facing a computer screen, which delivered visual feedback about the task, including target and cursor positions. Feedback about X and Y force was displayed by the cursor, which the monkey had to direct into the different targets. To begin a trial, the monkeys held the cursor in a center target for between 0.2 and 0.5 seconds. After the center-hold time, a second target appeared on the screen. The appearance of the target served as a Go Cue, indicating that the monkeys were free to move to the target. If they acquired and held the cursor in the target within the specified reach time (4 seconds for Monkey J, 8 and 10 seconds for Monkey K during short and long perturbation sessions, respectively), they received a water reward.

We recorded neural activity from primary motor cortex (M1), muscle activity (EMG) from the wrist muscles, and force data while the monkeys completed the hand control (HC) version of the task (**Figure**

4-1). These data were used to compute a two-step M1-EMG-Force decoder. We gave the monkey normal and altered versions of this decoder (see *Decoders*) and evaluated performance during Brain Control (BC). All surgical and experimental procedures adhered to the standards listed in the National Institutes of Health *Guide for the Care and Use of Laboratory Animals*, and were approved by Northwestern University's Institutional Animal Care and Use Committee.

4.2.2 Surgeries

After training both monkeys to complete the isometric task under hand control, we implanted a 96-channel microelectrode array (Blackrock Microsystems, Salt Lake City, Utah) into hand area of M1. We identified hand area intraoperatively by stimulating the surface of cortex and identifying where stimulation produced hand twitches. In a separate surgery, we implanted 24 pairs of bipolar wire electrodes (Cooner 632) into the arm and hand muscles. Here we focus only on the four major wrist muscles: extensor carpi radialis (ECR), extensor carpi ulnaris (ECU), flexor carpi radialis (FCR), and flexor carpi ulnaris (FCU).

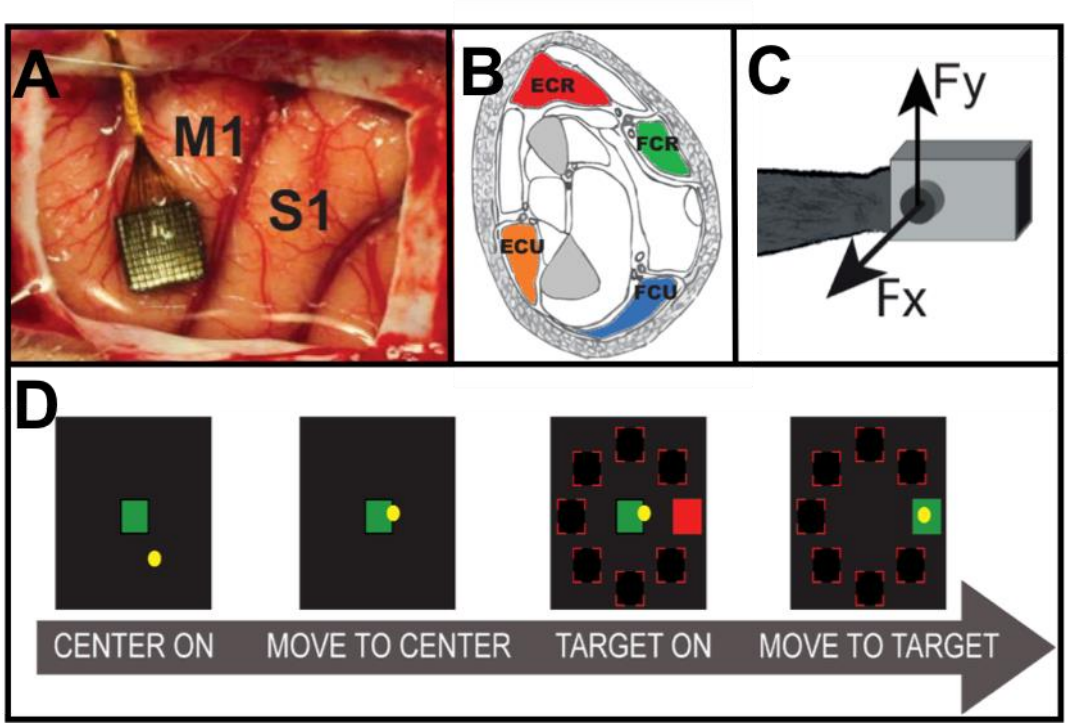

Figure 4-1. Experiment setup. (A) Utah array implanted in hand area of motor cortex. (B) Cross-section of the forearm depicting the four implanted muscles. Both monkeys did the task with their left hand, which meant that flexion targets were on displayed on the right half of the computer display, while extension targets were displayed on the left half. (C) Cartoon depicting the isometric hand task, where X and Y force were applied about the wrist to control a computer cursor. (D) Center-out task timeline.

4.2.3 Data Collection

We simultaneously acquired neural, EMG, and force data using a 128-channel Cerebus system (Blackrock Microsystems, Salt Lake City, Utah). We collected multi-unit neural activity from M1 using threshold crossings (-6xRMS) on every channel of the electrode array. We recorded X and Y force data and EMG from each muscle at 2000 Hz. The EMG signals were amplified (500x), band-passed filtered (80-500Hz), and then rectified and low-pass filtered at 10Hz. Both neural signals and EMG were then down-sampled to 20 Hz to compute neural decoders.

4.2.4 Decoders

We computed a two-step decoder made of two multiple-input, linear filters: one to decode EMG from neural activity, and a second to decode force from EMG. The filter length for the M1-to-EMG decoder was 500ms, while the EMG-to-Force decoder was 250ms. We determined these lengths by comparing offline decoder performance for a variety of lengths. While we computed a new M1-to-EMG decoder on every experimental day, we did not do the same for the EMG-to-force decoder, as this relationship was assumed to be stable.

In addition to the Normal decoder, we designed two additional “perturbation” decoders in order to study adaptation. The first was a synergy-preserving, *Rotated* decoder that used an EMG-to-force decoder that was trained using data from sessions where the monkey performed the task with the forearm rotated 90 degrees to the pronated position. We also designed a *Radial-Swap* decoder, in which the EMG-to-force weights for ECR and FCR were swapped, reflecting their lines of action across their insertions at the wrist, and simulating an anatomically impossible configuration. The differences in decoder design are delineated in **Figure 4-2**.

4.2.5 Block design

For each experimental day, the monkeys first performed the isometric task using hand control. These data were used to train the M1-EMG part of the decoder. The EMG-Force part of the decoder was assumed to be stable, and was retrained only weekly. For initial experiments with Monkey K, we alternated 15-minute blocks of the Normal decoder with one of the perturbation decoders, for a total of six blocks. In later experiments with monkey K and in all experiments with monkey J, we tested a single perturbation

decoder per session, preceded and followed by the Normal decoder. On any given day, we only tested one perturbation decoder, chosen at random.

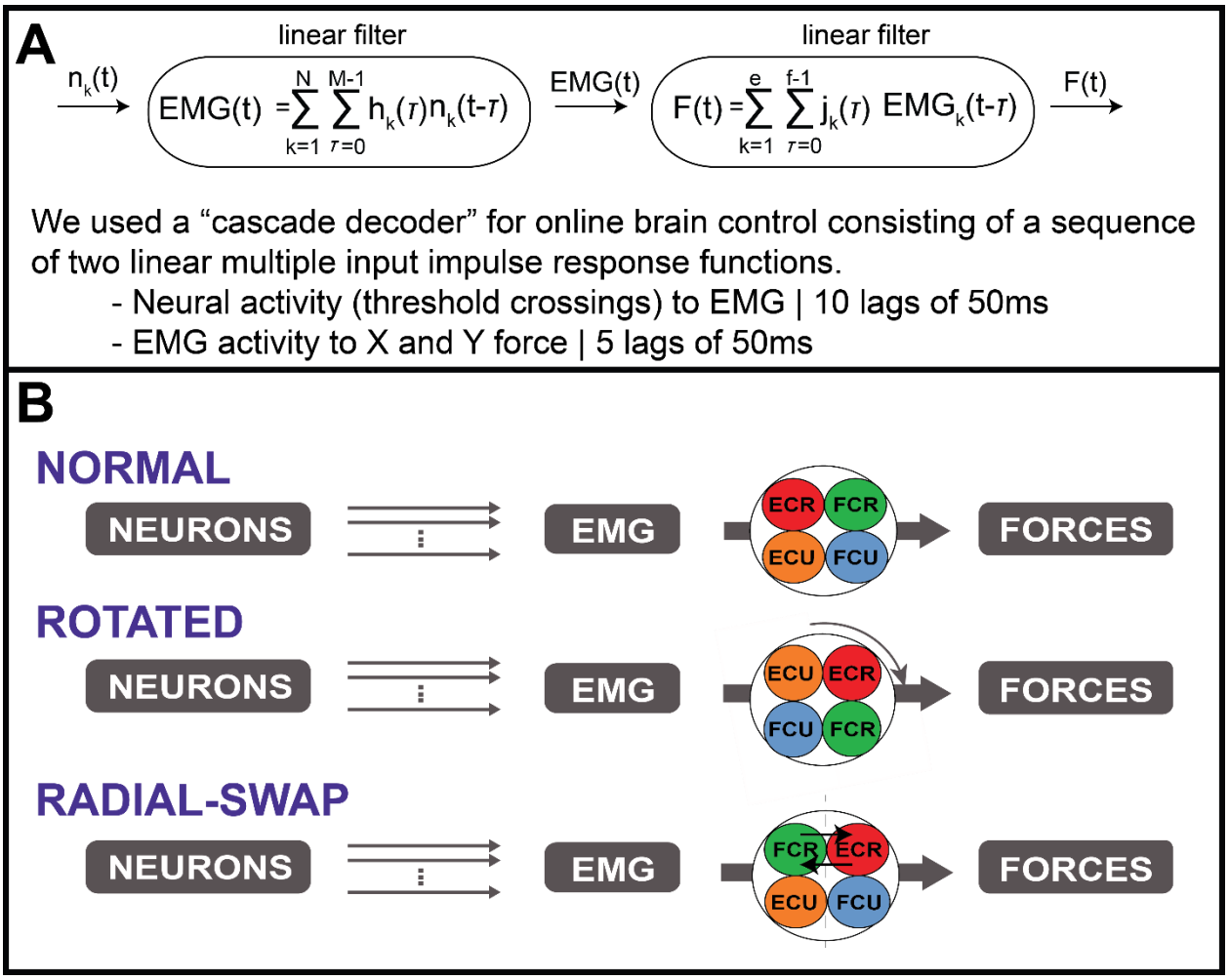

Figure 4-2. Decoder design. (A) Equations describing the cascade of two linear decoders we computed in order to make predictions from M1 to EMG to X and Y Force. (B) Cartoon depicting the different decoder configurations.

4.2.6 Data Analysis

To evaluate the monkeys' performance during brain control, we computed several task metrics, including percent success, initial trajectory error, and normalized path length. Initial trajectory error was defined as the angle between the monkey's initial force trajectory and a vector pointing to the target. We computed the vector for the predicted force trajectory between 200ms and 400ms after the Go Cue. For

the ideal trajectory, we computed a vector from monkey's actual starting point 20ms after Go Cue to the center of the target.

Normalized path length was defined as the ratio of the integrated path length over the distance directly to the target center. The integrated path length was computed by summing the Euclidean distance between the predicted forces at each time step from the time of the Go Cue until the end of each trial. A normalized path length above one meant that the monkey made a trajectory longer than the straight path to the target, and suggested that the monkey was trying to reach the target. If the monkeys did not attempt to acquire the target, the normalized path length would be less than 1. Although Monkey K's allotted reach times were different between the initial (8 seconds), and later experiments (10 seconds), we consistently calculated path length up to 8 seconds for all Monkey K sessions.

4.2.7 Statistics

To examine across-session performance for a given decoder for path length and trajectory error, we evaluated differences for the first 10 trials per target between the first and last two sessions using a one-way repeated measures ANOVA, where time was the independent variable, and the related dependent groups were targets. We used Tukey's test for post-hoc multiple comparison. We used a similar approach for within-session learning, using a one-way repeated measures ANOVA to compare the first and last 10 trials per target in a single session. Percent success, unlike the other metrics, is binary for individual trials, and required a different approach. Instead, we evaluated both within and across-session learning using a chi-squared test for the same sets of trials described above.

4.3 Results

We compared brain control performance using two different types of decoders: a muscle synergy-preserving Rotated decoder, and a Radial-Swap decoder that disrupted natural muscle synergies. The monkeys were ultimately more successful with the Rotated decoder, which they were able to use to acquire all eight task targets. However, they were never able to acquire more than four out of eight targets using the Radial-Swap decoder, and were unable to acquire targets that required adaptation. While both

monkeys improved their normalized path length across both types of perturbation sessions, the improvement was greater for Rotated sessions.

4.3.1 Influence of Decoder Remapping on Initial Target Acquisition Difficulty

We first evaluated the effect of the EMG-to-force remapping by passing neural activity recorded during normal hand control through each of the perturbation decoders. We plotted the resulting force and evaluated the initial trajectories to each target, as shown in **Figure 4-3**. The mean percent of target acquisition across sessions using these unadapted force trajectories are shown for each target. The Radial-Swap decoder allowed the acquisition of a few targets without adaptive changes because it only swapped the action of ECR and FCR, while the action of ulnar-deviation muscles, FCU and ECU, remained unaltered. Both monkeys could still acquire Targets 6 and 7, which primarily involved the ulnar deviators. Both monkeys were also able to acquire Target 3, which required equal activation of FCR and ECR. However, because the action of these two muscles were swapped, if the monkeys made an error going to this target, they would have needed to account for the new mechanics when correcting their path.

4.3.2 Percent Success

To evaluate both monkeys' ability to adapt and successfully acquire targets using the two decoders, we evaluated percent success for each target across experiment days. These results for both the Rotated and Radial-Swap decoders are shown in Figure 4-4. Both monkeys were able to adapt to acquire all targets in the Rotated case, but not in the Reflected case. Furthermore, monkey J and monkey K significantly improved performance across Rotated sessions for 6 and 5 targets, respectively (chi-squared test, largest $p=0.002$ for monkey J, and $p=0.035$ for monkey K). For monkey J, this improvement included all but two targets in the radial deviation hemisphere (**Figure 4-4**A, blue markers, Targets 2 and 3, $p=1.00$ and $p=0.490$, respectively) while monkey K, improved for all targets except those in the flexion hemisphere (**Figure 4-4**B, blue markers, Targets 8, 1, and 2, $p=0.311$, 0.527, and 1.00, respectively).

Using the Radial-Swap decoder, the monkeys were able to acquire at most four targets. Of these, monkey J significantly improved percent success targets primarily requiring ulnar deviation (Targets 6 and 8, $p=0.035$ and $p=\sim0$, respectively). There was no significant difference across sessions for Target 3, which he acquired with 100% success throughout ($p=1$). There was also no significant difference for Targets 1, 2,

4, and 5, which he was never able to acquire. Of the 4 targets monkey K could acquire, he only significantly improved his percent success for Target 3 (p=~0).

While across-session improvements in percent success were significant, within session improvements were minimal. At best, monkey J significantly improved his success for two targets in a given Rotated session and one target in a given Radial-Swap session. Monkey K at best improved his success for one target in any given Rotated and Reflected session.

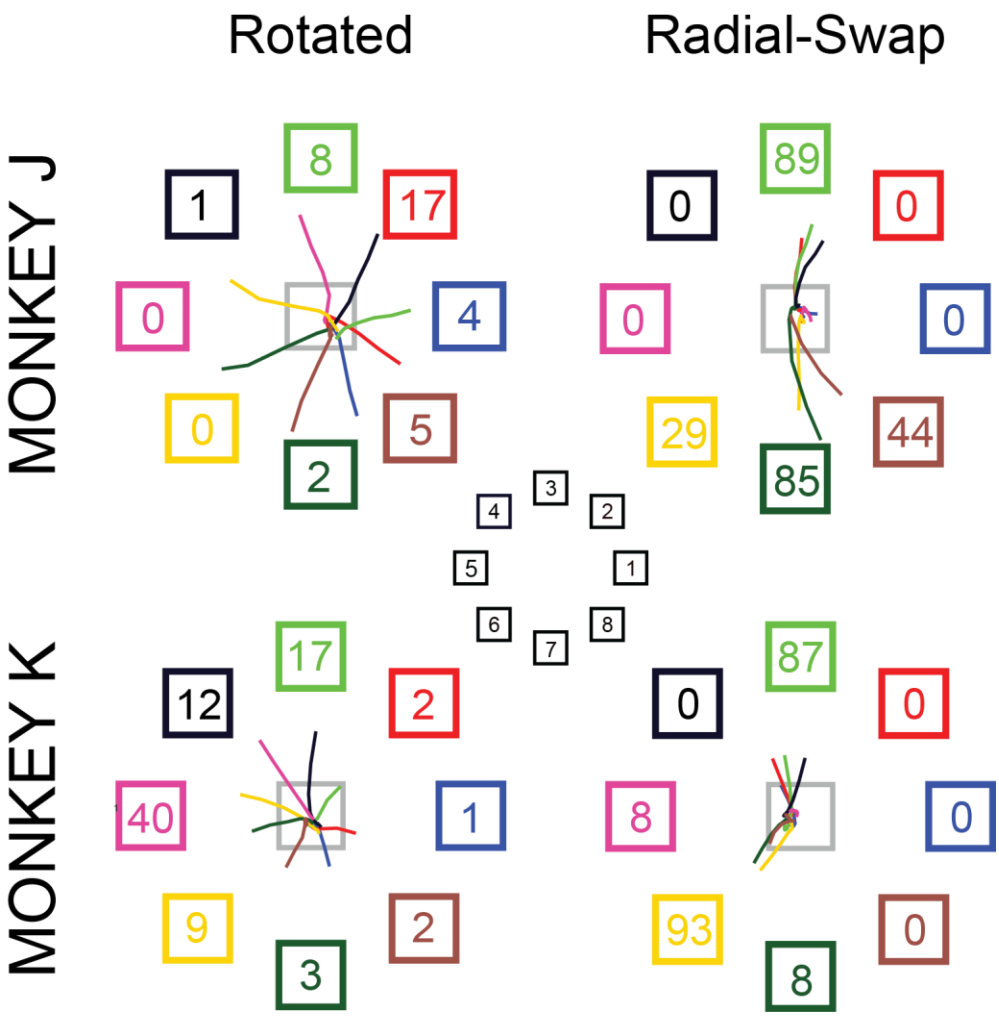

Figure 4-3. Decoder effect. These figures show the initial trajectories from Go to Go+500ms when neural activity during hand control is input into the two types of decoders. The numbers in each target box show the mean percent success across days when using these unadapted force trajectories for a particular target. A legend with target numbers is shown in the center.

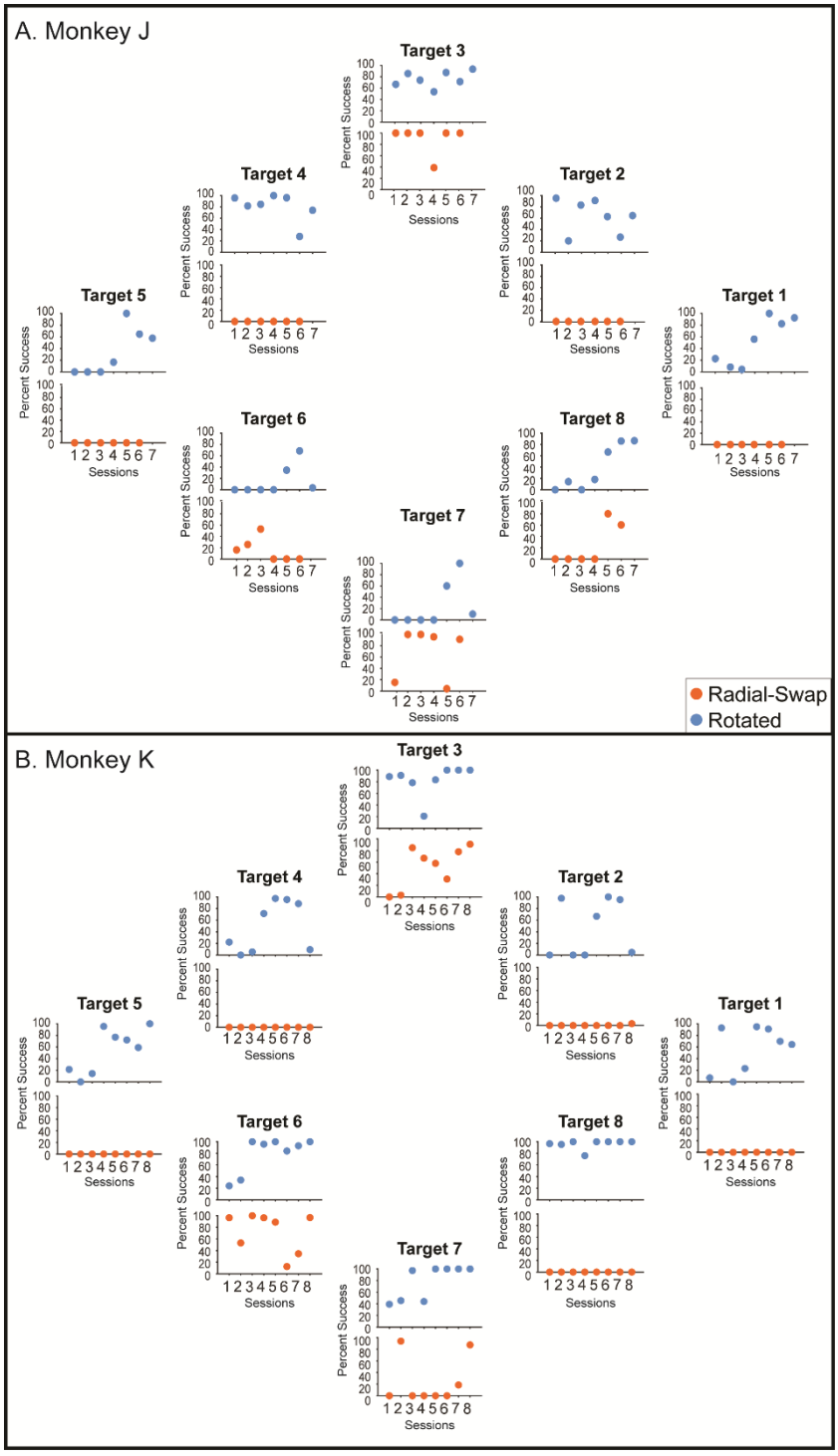

Figure 4-4. Percent success per target. Each subplot shows percent success for an individual Target across experiment sessions. The top subplots show Rotated success, while the bottom Subplots show Radial-Swap success.

4.3.3 Relationship between acquired targets and target difficulty

Using the Rotated decoder, both monkeys were able to adapt in order to acquire all targets. However, using the Reflected decoder, neither monkey adapted over the course of the experiment to acquire the targets that were initially difficult.

A summary of final percent success versus the target difficulty percent success from **Figure 4-3** is shown in **Figure 4-5**. For both monkeys, most of the points for the Rotated decoder (left panels) are close to the y-axis, indicating that percent success without adaptation was close to zero while actual success was greater. On the other hand, when using the Radial-Swap decoder, both monkeys continued to acquire the targets that did not require a change in adaptive strategy, but almost never acquired any other targets (**Figure 4-5**, right panels).

4.3.4 Actual Trajectories and Initial Trajectory Error

To understand how the monkeys were adapting in order to acquire targets, we examined the trajectories to each target during brain control. Successful initial trajectories to each target for early and late perturbation sessions are shown in Figure 4-6. Using the Rotated decoder, monkey J never straightened his initial trajectories to the target, but maintained a strategy of correcting his trajectory later in the trials. Monkey K, on the other hand, did slightly improve his trajectories, though he started with smaller initial errors than did monkey J. Using the Radial-Swap decoder, both monkeys acquired only a subset of targets, and made trajectories that matched the Radial-Swap decoder effect trajectories shown in **Figure 4-3**. These results suggest that the monkeys did not adapt to acquire the harder targets. The occasional success with target 2 on the last Radial-Swap session for monkey K was an exception, but he acquired this target only on this day, with only 3% success.

To quantify improvements in the monkeys' trajectories, we calculated initial trajectory error. This metric compared the monkey's initial vector with a vector pointing directly to the center of the target (see Methods). If the monkeys internalized the perturbation decoder models over time, we would expect to see the trajectory error decrease across sessions. Using the Radial-Swap decoder, this was not the case for either monkey (**Figure 4-7**A, repeated measures ANOVA, $p=0.285$ and $p=0.339$ for monkey J and monkey K respectively). However, using the Rotated decoder, monkey J significantly reduced trajectory error across

sessions (**Figure 4-7**A, top left, p=~0), though monkey K did not (p=0.648). Oddly, while Monkey J significantly improved trajectory error for targets in the ulnar-flexion quadrant (repeated measures ANOVA, Tukey test, Targets 7 and 8, p=~0and p=~0), his trajectory error significantly increased between the early and late sessions for the targets in the radial-deviation quadrant (repeated measures ANOVA, Tukey test, Targets 2, 3, 4, p=0.020, p=~0, p=0.011). With respect to within-session learning, both monkeys showed little evidence of significant initial trajectory error changes. Both monkey J and monkey K significantly modified trajectory error for one Rotated session and two Radial-Swap sessions.

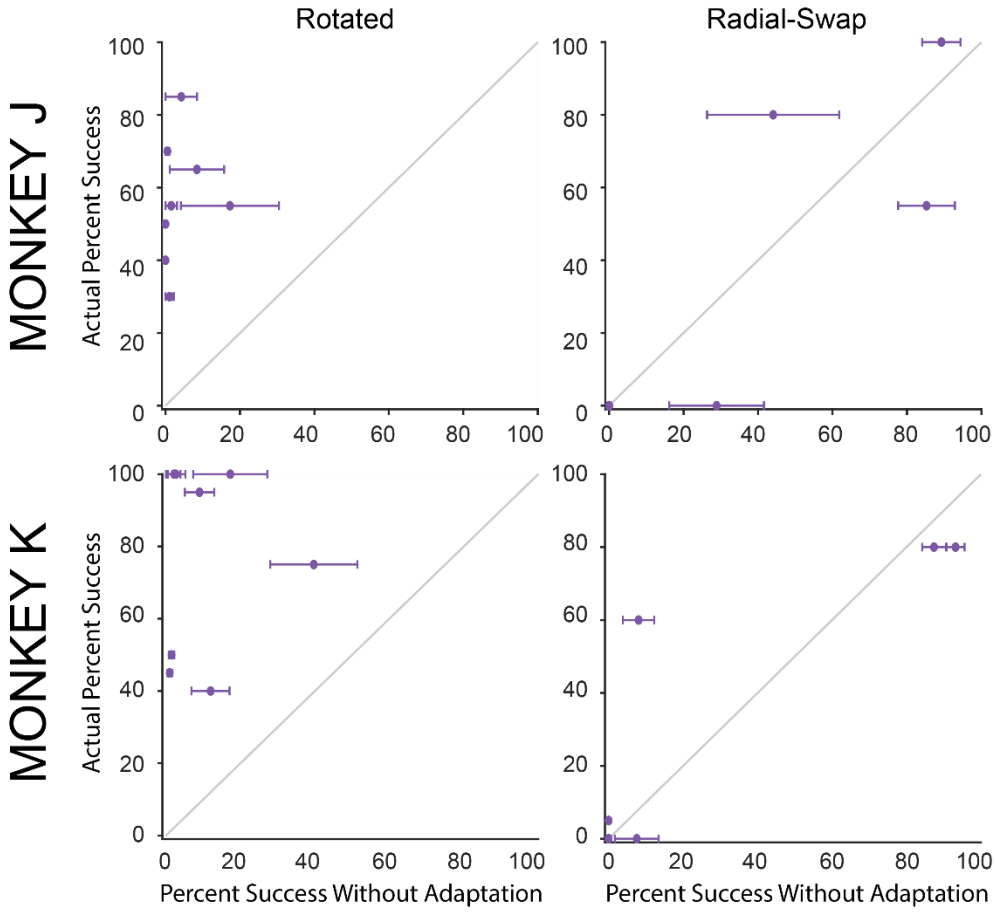

Figure 4-5. Actual success versus percent success without adaptation. Here, the average success for the first 10 trials per target in the last two sessions are plotted against the mean percent success without adaptation across all sessions. Percent success without adaptation is the percent success using the force trajectories that result from putting normal neural activity through each perturbation decoder.

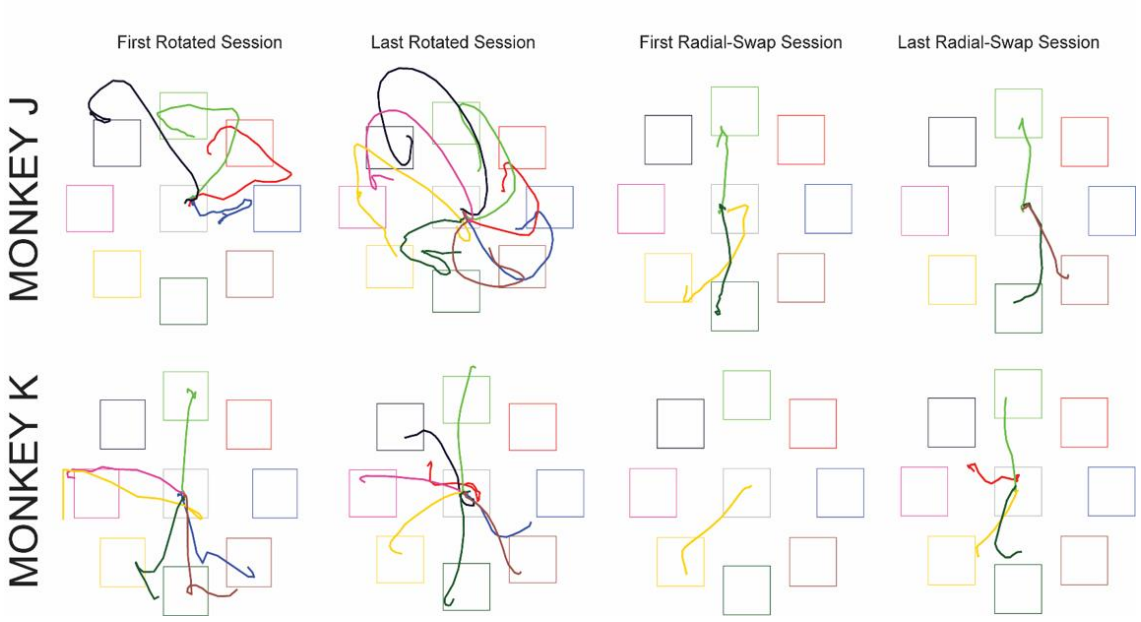

Figure 4-6. Successful target trajectories. Mean initial trajectories from Go Cue to Go Cue + 1200ms for successfully acquired targets.

4.3.5 Normalized path length

Since initial trajectory error could not fully explain the monkeys' ability to learn to acquire targets, we also evaluated the normalized path length to the target. If the monkeys learned to make straighter trajectories to the targets over time, this metric would approach one. For both perturbation conditions, both monkeys significantly changed their normalized path length to targets between the first and last two sessions (repeated measures ANOVA, monkey J p=0.009 Rotated, p=~01 Radial-Swap, monkey K p=~0 Rotated, p=~0). **Figure 4-8** summarizes path length per target for the first two sessions (blue traces) compared to the last two sessions (purple traces). While both monkeys changed their path lengths overall, their performance across targets was not uniform. For example, using the Rotated decoder, monkey J significantly shortened path length for some targets (Targets 5, 6 and 7, largest p=0.002), while the others were unchanged (**Figure 4-8**, top left, smallest p=0.052). Similarly, monkey K significantly improved path length for the ulnar-extension quadrant (Targets 7 and 7, p=~0 and p=~0), but became worse at targets in the radial-flexion quadrant (**Figure 4-8**, top right, Targets 1 and 2, p=0.001 and p=0.004). The

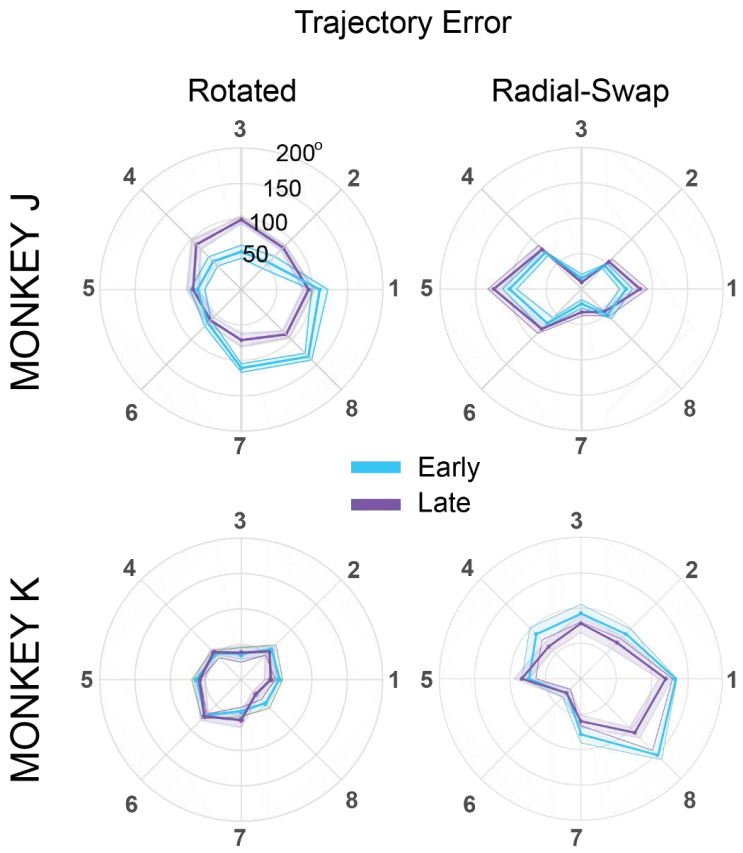

Figure 4-7. Trajectory error across sessions. These plots show the average and standard error of the initial trajectory error for the first 10 trials per target for the first (early) and last (late) two sessions for each type of perturbation decoder.

improvements using the Radial-Swap decoder were also non-uniform across targets, as shown in the **Figure 4-8**, but were generally smaller than with the Rotated decoder.

Figure 4-9 shows examples of normalized path lengths within single sessions for both monkeys and both types of decoders. Monkey J's path length did not change significantly in either the first or the last Rotated session **(**Figure 4-9A, top, repeated measures ANOVA, p=0.124 and p=0.061). Monkey K had large differences in path length to each target during the first Rotated session that didn't change significantly by the end of that single session (Figure 4-9A, bottom, repeated measures ANOVA, p=0.748). However, by the last Rotated session, he had improved his path length for all but three of the difficult targets, and within-session learning for this session was significant (p=~0).

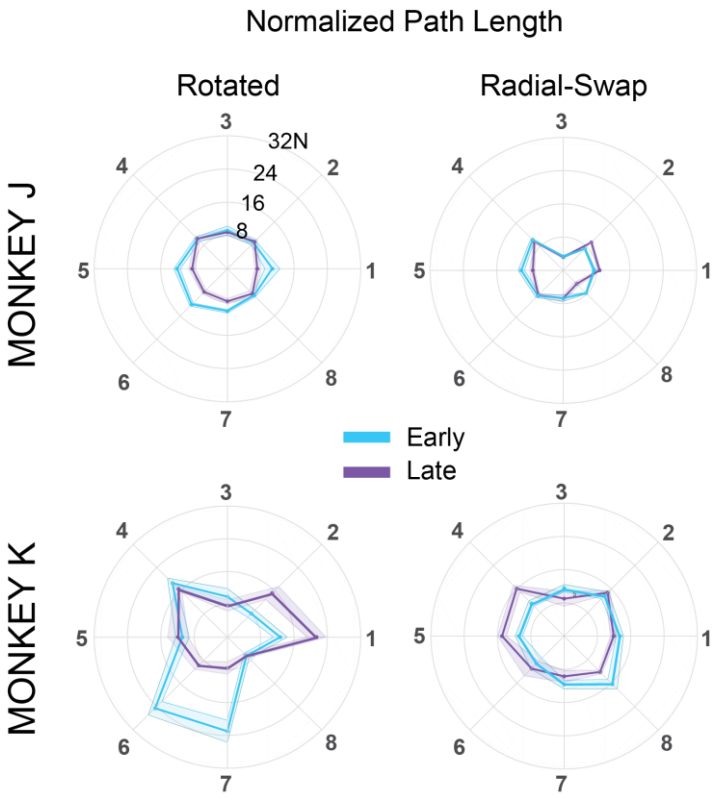

Figure 4-8. Normalized path length across sessions. These plots show the average and standard error of the normalized path length for the first 10 trials per target for the first (early) and last (late) two sessions for each type of perturbation decoder.

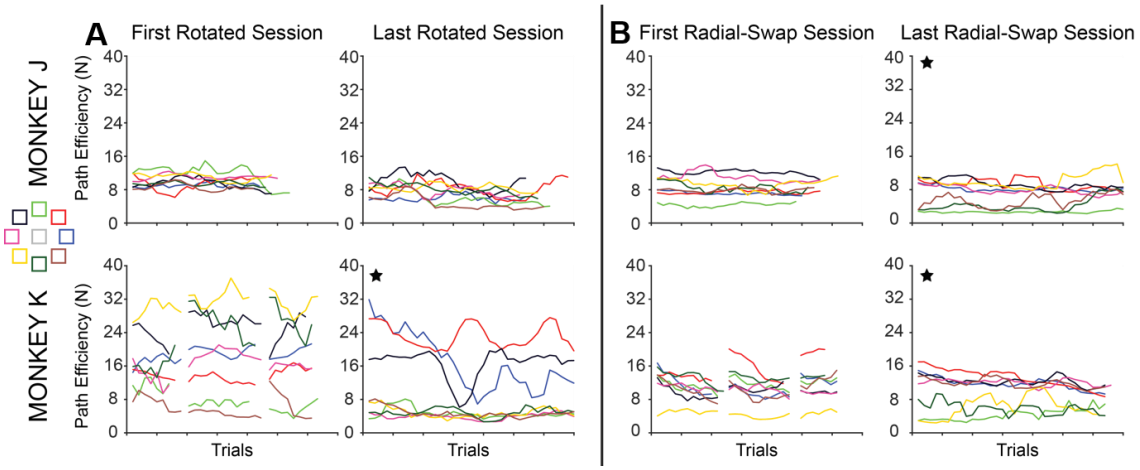

Figure 4-9. Within-day normalized path length. These panels show normalized path length for the first and last session for each perturbation. Each trace is a different target, and the trial traces were smoothed with a moving average filter using five samples.

With the Radial-Swap decoder, monkey J did not significantly modify his path length in the first session (Figure 4-9B). However, during the last session, the only one with a significant change, path length

improved for nearly half the targets. For monkey K, the traces in first Radial-Swap session demonstrate that he was most efficient at Target 6, the only target he could acquire at this point. His overall path length did not change significantly within this session (repeated measures ANOVA, p=0.355). On the other hand, during the last Radial-Swap session, his path length improved for Target 7, which he could successfully acquire, as well as for all the difficult targets that he couldn't acquire (repeated measures ANOVA, Tukey test, p=0.001.) Overall, monkey K, in particular, shortened his path length in four and five out of eight Rotated and Radial-Swap sessions, respectively (repeated measures ANOVA, largest p=0.020 for Rotated, and largest p=0.007 for Radial-Swap). On the other hand, path length for monkey J only improved in one Rotated and one Radial-Swap session (repeated measures ANOVA, p=~0 for Rotated, and p=0.026 for Radial-Swap).

4.3.6 Effort during Radial-Swap decoder use

We also used normalized path length to determine whether the monkeys were actually trying during the difficult Radial-Swap trials for targets that were never acquired. If the monkey did not try, the normalized path length value would be less than one. **Figure 4-10** shows path length for each session for two example targets that were never successfully acquired by either monkey: Targets 1 and 5. In all cases, normalized path lengths greatly exceeded 1, suggesting that the monkey was indeed attempting to move to the target. To ensure that this metric was not influenced by noise in the cursor prediction, which could have resulted in a high value without the monkey's effort to produce force, we also calculated path length during the center target hold period at the beginning of each trial. All these values were well below 1, demonstrating that when the monkey did not try to move the cursor, the normalized path length was low.

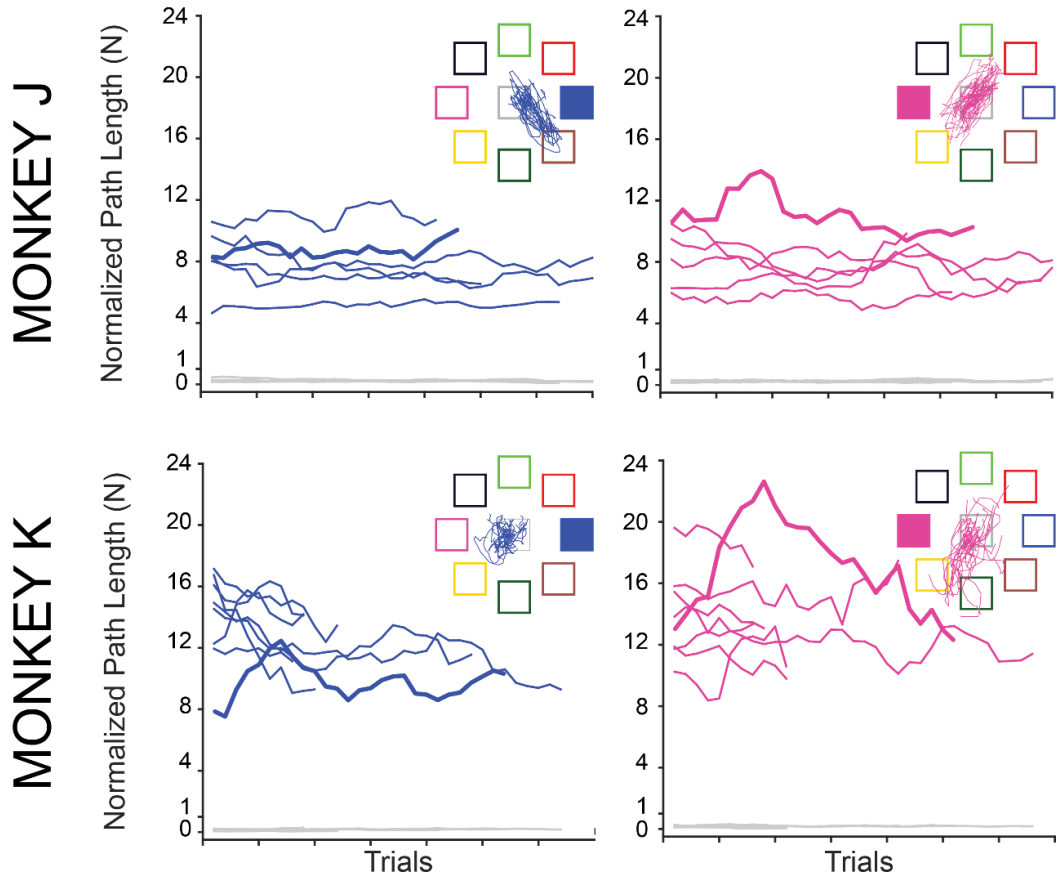

Figure 4-10. Effort during difficult trials. To demonstrate that the monkey was trying to acquire difficult targets, we plotted normalized path length during Radial-Swap sessions for two example targets that were never acquired by either monkey. Each trace represents path length for a different session. The shorter traces for monkey K show normalized path length for the first perturbation block for the sessions where the normal and perturbation decoders were alternated. Trial values were smoothed using a moving average filter using five samples. As a comparison, the gray traces show normalized path length during the hold period, when the monkeys held the cursor in the center target.

4.4 Discussion

After millions of years of evolution, the ability to learn to use novel tools remains largely unique to primates. The advent of the brain-machine interface has introduced an entirely new tool that presents new learning challenges and new opportunities to explore the limits of motor learning. We have pursued this problem by asking monkeys to learn to use two different BMIs, one that resembles a routine postural variation of a normal hand movement (Rotated decoder), and another that represents an anatomical impossibility (Radial-Swap decoder). Although the Rotated decoder caused greater alteration of the mechanics of force production, ultimately, both monkeys learned to use it successfully for all targets, but

achieved at best only four targets using the Radial-Swap decoder. Furthermore, the successful targets using the Radial-Swap decoder were those that required relatively little adaptation.

Importantly, hypotheses to explain the extent of learning in the current study are complicated by the different effect of the Radial-Swap decoder between targets. The ulnar deviation targets, for example, could still be acquired using largely normal muscle activation. Targets that were difficult to acquire, however, required the monkey to produce an unnatural pattern of muscle activation. For example, to acquire the flexion target, the monkey had to activate ECR and FCU without activating FCR and ECU, a combination that does not occur normally. In contrast, the targets in the Rotated case required new patterns of muscle activation, but these patterns corresponded to those needed when the forearm is physically rotated 90 degrees; for all these targets, both monkeys ultimately learned to acquire. The particular inability to acquire the difficult targets in the Radial-Swap case suggests that on a short time-scale, M1 neurons cannot be activated in a way that is necessary to produce unnatural muscle activations.

4.4.1 Neural constraints on learning

The inability to use the Radial-Swap decoder may be related to constraints on the ability to alter the firing patterns of neurons independently, and therefore the neural population cannot readily change its covariance structure. The poor performance using the Radial-Swap decoder may therefore have been because acquisition of the difficult targets required the neural population to change its normal covariance, while the easy targets did not. This explanation is similar to the conclusions of a study by Sadtler and colleagues, who evaluated the ability of monkeys to learn to use altered decoders that either did or did not require changes in neural covariance. The former decoders, which they refer to as “out-of-manifold” decoders, were rarely learned in a single session (Sadtler et al. 2014). However, the Rotated decoder may have been similar to the Sadtler “within-manifold” decoder, which required different patterns of neural firing, but ones that are likely preserved for other normal tasks, such as those where the forearm is rotated.

Other studies support the idea that there exist constraints on the ability to modulate neurons independently in a short time frame, closely related to the idea that a neural population cannot readily change its covariance structure. Hwang and colleagues demonstrated this idea in a BMI learning study in the parietal reach region (PRR), an area that encodes planned target reach locations (Hwang, Bailey, and

Andersen 2013b). They used a subset of their recorded neurons for decoding, and evaluated changes in neural firing between neurons involved and excluded from BMI use, similar to a previous study in M1 (Ganguly et al. 2011). Similar to the M1 result, they report that both groups of neurons alter their firing, even though the activity of the excluded neurons had no relationship to task reward, suggesting that neurons are not adapted individually. Importantly, they also describe the ability of monkeys to learn seemingly arbitrary neural activations, but that these patterns of activations always belonged to a response set for normal reaching movements.

The Hwang et al. observations, to the extent they are relevant for M1, further support the Sadtler result that “out-of-manifold” decoders, which require neurons to change their covariance structure of their mutual activity patterns, are not readily learnable. Similarly, Fetz and Baker operantly conditioned the firing patterns of individual neurons, and found that some adjacent neurons similarly modulated their activity (Fetz and Baker 2017). However, they also found evidence of adjacent units that could indeed be independently controlled, demonstrating that there are exceptions to the ability of neuron groups to change their co-modulation. These exceptions are important to consider, but these studies may also suggest that the difficult Radial-Swap targets were hard to acquire because of actual neural constraints on modifying neural covariance.

4.4.2 Limitations in the extent of neural space exploration

In this experiment, both monkeys improved across sessions, especially when using the Rotated decoder. The greater success with the Rotated decoder may have been because a successful strategy was more readily apparent. To acquire the Rotated targets, the monkeys initially aimed toward the wrong target, but later made seemingly corrective movements to hit the right target. This is similar to the strategy employed by monkeys in a study by Jarosiewicz and colleagues, in which monkeys adapted to a decoder where the relationship to kinematics between some but not all BMI neurons was rotated (Jarosiewicz et al. 2008). In early trials, the monkeys corrected their trajectory at around 400ms into the movement, based on observation of the cursor error. After learning, their initial trajectories went straight for the intended targets. However, in the current experiment, the initial trajectories still had large errors in the final experimental session. This suggests that while the monkeys had adopted an adequate strategy, they had not yet

developed an accurate internal model of the dynamics of the Rotated decoder, which would have resulted in more direct initial trajectories to the targets. On the other hand, using the Radial-Swap decoder, the monkeys almost never acquired the targets that required the most strategic and neural adaptation. Not only were they not able to internalize the new dynamics of the decoder, they were also unable to identify a corrective strategy in order to adjust their trajectories.

Another possible explanation for the monkeys' inability to learn to use the Radial-Swap decoder is that they did not fully explore the space of readily possible neural activations, not requiring covariance changes, during the experiment. In this study, we chose a decoder perturbation type randomly each day, instead of giving the monkeys the same type over a series of days. We also recomputed the M1-to-EMG decoder in every experimental session, with the original intention of evaluating short-term rather than long-term adaptation. We found that the Radial-Swap decoder was more difficult to learn than the Rotated decoder, but within-session learning of both types may have been limited by the short length of each session. Learning across sessions may also have been limited by the interchange of decoder type. As demonstrated by Ganguly and Carmena, using fixed decoders, provided the neural inputs remain stable, facilitates long-term learning (Ganguly and Carmena 2009).

While the limited time to explore more of the neural space may in part explain the inability to use the Radial-Swap decoder, the main explanation may be the need to generate new neural covariance patterns. Providing direct evidence for the latter explanation is not trivial. Because the monkeys were able to use the normal and Rotated decoders, it is possible to compare differences in neural activation during the two tasks. However, because the monkeys never successfully used the Radial-Swap decoder, it is difficult to compute hypothetical neural activations for success. Comparing these hypothetical neural activations to the neural patterns during normal decoder use could reveal whether successful decoder use required abnormal modifications in neural covariance or not. Further work will be required to better address this question.

4.4.3 The influence of afferent feedback on learning

The disruption of normal afferent feedback in the perturbation sessions may also have affected the monkeys' ability to learn, especially because somatosensation is implicated in motor learning. Ablation of somatosensory cortex, for example, has prevented monkeys from learning a new task, though this lesion did not affect the retention of learned motor skills (Pavlides, Miyashita, and Asanuma 1993). Proprioceptive information from the limb also synapses in primary motor cortex (Peter L. Strick and Preston 1978b; Zarzecki and Asanuma 1979), where it may also have an effect on motor learning. Proprioceptive information from the limb is important to consider, especially since afferent conditions often differ between decoder training and testing conditions.

To maintain similar afferent conditions between decoder training and testing conditions, some groups compute "observation-based decoders", where the decoder is trained through visual observation of movement rather than actual movement (Wahnoun, He, and Helms Tillery 2006; Tkach, Reimer, and Hatsopoulos 2007; Hochberg et al. 2006). This method is becoming increasingly common, especially because it is required for human BMI users, who cannot make movements with which to train decoders. In observation-based experiments, the limb is not engaged in the task during either decoder training or use, and therefore afferent feedback from the limb may be similar in both cases. Part of this approach may also include recalibrating decoders during initial brain control to further reduce differences between training and testing conditions, such as is done using the ReFIT decoder algorithm (Gilja et al. 2012). In cases where observation-methods and decoder recalibration are not used, animal subjects make movements during decoder training, but afferent feedback during this condition may not match feedback during brain control, where the limb might not be engaged in the task in the same way. Despite these discrepancies, however, monkeys can still learn the use the decoders (Lebedev et al. 2005; Velliste et al. 2008).

In nearly all monkey BMI studies including ours, animals have intact proprioception during BMI control. In the current study, the monkeys retained proprioception consistent with a mid-prone forearm position. This type of proprioception was incongruent with the virtual muscle configuration imposed by the perturbation decoders. In the Rotated sessions, for instance, real afferent feedback was rotated from the decoder configuration. However, the afferent feedback during Radial-Swap sessions may have been

especially confusing, because of the unnatural muscle configuration. Ultimately, despite incongruities in proprioceptive feedback, the monkeys were able to acquire all targets with the Rotated but not the Radial-Swap decoder. This may be because the monkey's disparate feedback conditions during Rotation were still natural, and therefore the monkey could understand how to account for them.

It is also possible that correct proprioceptive information was not necessary for learning, at least for the Rotated decoder. Contrary to studies that report the importance of accurate afferent feedback for learning and performing tasks, Ingram and colleagues present a slightly different view (Ingram et al. 2000). In a 2000 study, they compared learning in normal subjects versus learning in a subject who had lost the sense of proprioception below the neck. The deafferented subject was able to adapt to a visuomotor perturbation, requiring single-joint arm movements to visual targets. This study suggests that proprioception is not a requirement for adaptation. Jones and colleagues show that proprioceptive feedback is reduced during visuomotor adaptation (Jones, Wessberg, and Vallbo 2001). Spindle firing rates were decreased in 83% of the adaptation trials during a center-out reach task, where feedback about hand position was rotated 45º. They propose that the decrease in sensory signals was a way to reduce the effect of the discrepancy between visual and proprioceptive feedback during visuomotor adaptation. While the Rotated decoder was not a simple visuomotor rotation, the two share some characteristics, such that it may be applicable to the arguments put forth here. The successful use of the Rotated decoder may have been facilitated because the altered proprioception was still natural, but also because proprioceptive feedback may have been somewhat reduced during decoder use. In the Radial-Swap case, the less natural disparity between normal afferent feedback and the imposed mechanics of the decoder may have led to a decrease in proprioceptive signaling, as in the example above, but could also have in part hindered learning. Overall, while proprioceptive signals may not be absolutely necessary for learning, accurate proprioceptive feedback does improve performance (Suminski et al. 2010) .

4.4.4 Implications for future BMI development

BMI adaptation studies are complicated by the fact that current studies are performed in lab settings for only a few hours in a given session. At the end of the session, animal subjects are returned to their

cages, and human subjects go home, where they cannot continue decoder use. However, unconstrained use of a BMI, facilitated by wireless technology, could allow researchers to evaluate decoder use for extended periods of time, and these methods are becoming rapidly available thanks to recent advances in wireless BMI technology (Borton et al. 2013; Yin et al. 2014; Schwarz et al. 2014). Giving the subjects a decoder to learn without interruption may reveal new insights into the time course and extent of learning. More time to fully explore their neural space with extended decoder use could also help determine whether decoders are difficult to learn because of time or actual neural constraints.

BMI adaptation is especially important to understand because decoders will never be perfect for many reasons. For one, BMIs use a very limited number of individually noisy neurons for control, and therefore provide an oversimplified interface for neural control. They also do not directly account for processes downstream of cortex, such as the activity of interneurons, which may modulate descending commands between M1 and movement output in a nonlinear, context-dependent manner (Hepp-Reymond et al. 1999; Humphrey, Schmidt, and Thompson 1970). Other considerations include differences in afferent feedback between decoder training and testing conditions, namely in cases where observation-based decoders are not used, as well as differences in the dynamics of the plant being controlled and those of the user's actual arm. For these reasons, users will have to adapt in order to use their decoders successfully. One main goal for BMI development is to design decoders that require minimal adaptation, in order to facilitate quick and intuitive BMI use.

In the current experiment, the short experimental sessions may have limited the extent of learning. However, the inability to acquire all Radial-Swap targets may also have been due to neural constraints that prevent changes in neural covariance. In light of studies that support this idea (Sadtler et al. 2014; Hwang, Bailey, and Andersen 2013a; Fetz and Baker 2017) and the implications of the current results, the optimal approach to building an intuitive decoder should preserve natural patterns of neural covariance. This will facilitate a more rapid rate of learning, allowing users to more readily manage their BMI in both normal and new tasks, and reduce the cognitive load required to adapt.

Designing decoders that require only normal neural covariance patterns, however, may not always be possible. Fortunately, difficult decoders may still be learnable with proper algorithm design. Researchers

are beginning to show that even out-of-manifold perturbations, such as the ones described by Sadtler and colleagues, can eventually be learned with coaching, with decoder weights gradually modified with learning (Oby et al. 2015). Gradual learning, in fact, has been shown to improve adaptation. For example, in a prism adaptation study, incremental visual rotation resulted in a greater level of adaptation than adaptation to a single rotation, and also had larger negative after-effects (Michel et al. 2007). In summary, while coaching may eventually improve decoder learning, BMI users would obviously prefer not to undergo extensive training to use a decoder for real-world tasks if it were not necessary. Decoder design for rapid and intuitive use should therefore require natural patterns of neural activation, and avoid the need to modify the neural covariance structure to the extent possible.

5 Discussion

5.1 The refinement of control strategies for cortically-controlled FES

In this dissertation, I have presented three research studies, each focusing on a different approach to improving control strategies for FES, such as stimulation techniques, and decoder design. First, in Chapter 2, I evaluated the ability to use a nerve cuff, the FINE, to activate muscles selectively. My results showed that FINEs can indeed be used to activate a subset of muscles for grasp, and that selectivity is relatively stable across time. We further showed the ability to use multi-contact stimulation to produce different types of grasp. These results are useful for both standard and BMI-FES systems. Furthermore, FINE stimulation in future human clinical trials are likely to produce better selective muscle activation than what we report in the monkey, because of the much higher fascicle count in humans. Fascicle count is important because fascicles are thought to facilitate selective muscle activation due to their insulating perineurium (Brill et al. 2009). Still, while the monkey may not be the perfect model, it is useful for the continued evaluation of FINE stimulation routines.

In Chapters 3 and 4, my focus was on the relationship between M1 and EMG, both in an attempt to better understand the neural control of movement, and with an eye for developing more useful decoders for cortically-controlled FES. My results in Chapter 3 revealed strong evidence for a gain-mechanism operating downstream of motor cortex, which amplifies the relationship between M1 neurons and EMG depending on the magnitude of required EMG. Including gain parameters when computing neural decoders may therefore be useful for FES systems for tasks that require different dynamics and magnitudes of muscle activation. In Chapter 4, I evaluate the ability to use and adapt to two different types of FES decoders: one that preserves natural patterns of muscle activation and one that does not. I report that neither of the two monkey subjects was able to acquire all the targets using the less natural decoder. This suggests that M1 cannot readily change its firing patterns to control force when the decoder relationship between muscle activation and force is unnatural, at least in the short term. Decoders that are easy to use should therefore be designed in a manner that preserves the biomechanical structure of the motor system.

5.2 Designing decoders that reflect the structure of the motor control system

BMIs are remarkable in that they can make use of a very small population of neurons to accurately predict a variety of movement variables. Their performance is especially impressive considering that BMI decoders inevitably provide an oversimplified interface for control, especially as they do not perfectly capture the complexity of the neural control of movement, such as the nonlinear downstream modulations of movement signals that may vary across behaviors. In many cases, there are discrepancies in afferent feedback between BMI training and testing conditions, as well as differences in the dynamics between the natural arm and the plant being controlled. With this in mind, in this dissertation I address the major question of how accurate a decoder needs to be for effective BMI use. Specifically, I evaluate the ability to use a single linear decoder for making accurate predictions across dynamically-different tasks, and how biomimetic a decoder needs to be to facilitate learning and intuitive use.

The results I report in this dissertation suggest that for the continued successful development of BMIs, it is important to build structure into the BMI that reflects the natural motor control system. I first discuss this in Chapter 3, where I evaluate the ability of a single linear decoder to span three dynamically different tasks: an isometric task, an unloaded movement task, and a spring-loaded task. These tasks also spanned a broad range of muscle activations. I ultimately demonstrate that a nonlinear relationship spans the three tasks more than a linear relationship does, but that the decoder has to be robustly trained with data from all three tasks. I also show that much of this nonlinearity is due to a gain mechanism downstream of cortex that is dependent on the magnitude of EMG output.

My results from Chapter 3 add to the knowledge base of how the motor system naturally controls movement, and specifically expand upon the ideas of context-dependence and gain that have been considered by researchers in the past (Hepp-Reymond et al. 1999; Humphrey, Schmidt, and Thompson 1970). Understanding the nature of downstream gain mechanisms also improves BMI design. My results demonstrate the increased value of accounting for gain with a nonlinear decoder, by showing that predictions across tasks with this nonlinear decoder are significantly better than linear predictions, provided both decoders are robustly trained.

Accounting for EMG-dependent gains will be particularly important for the future development of cortically-controlled FES systems, which require the prediction of individual muscle activity. Real-life BMIs should work for a variety of tasks requiring different dynamics and interactions with various kinds of loads. To make accurate predictions across these conditions, one should therefore incorporate knowledge about the nonlinear structure of the motor control system into a decoder, and include gain parameters that are specific to levels of EMG production.

The results here may also broadly apply to BMI experiments that use kinematic decoders, which currently use a controller to alter the dynamics of a robotic arms (Collinger et al. 2013; Wodlinger et al. 2015; Velliste et al. 2008; Hochberg et al. 2012). As information on how the motor system controls dynamics increases, group that only use neural data for predicting kinematic variables may ultimately incorporate these insights to allow BMI users to control dynamics themselves with cortical activity. This could mean an increased use of musculoskeletal models, or other methods that would allow the user to employ neural activity to control the stiffness of their robotic prosthesis. This type of control would allow for natural dynamic movements that are completely under the volition of the user, giving them full control over their prosthetic device.

******

While it may seem like an obvious conclusion that decoder design should reflect the structure of the motor system, this conclusion is not entirely essential in light of the brain's ability to adapt to various types of BMIs. In fact, monkeys have demonstrated the ability adapt even to nonbiomimetic BMI decoders, as in cases where the decoder weights were shuffled across neurons (Ganguly and Carmena 2009), and during a task that rotated the relationship between a subset of BMI neurons and cursor velocity (Jarosiewicz et al. 2008). There are also the many circumstances under which the activity of cortical neurons can become dissociated from movement, such as during mental imagery and visuomotor dissociation, where visual feedback does not match limb position (Schieber 2011). This phenomenon is especially helpful for BMI control, where the brain seems to recognize that a "native limb no longer is being controlled" and neurons can therefore alter their firing rates to complete seemingly unnatural tasks, such as the use of the nonbiomimetic decoders described above.

Despite the ability to adapt, there do exist neural constraints on the ability to learn to use BMI, and one challenge for the BMI field is to identify the extent of these limitations. In Chapter 4, I explore limitations on BMI use by evaluating the ability of monkeys to learn to use two altered decoders: one that preserved the natural patterns of muscle activation, and one that did not. The design for my learning study was influenced by recent findings from Sadtler and colleagues (Sadtler et al. 2014) as well as a study by Berger and colleagues (Berger et al. 2013). Sadtler et al. evaluated the ability of monkeys to learn two different types of altered decoders. To do so, they first computed what they call an "internal manifold" using factor analysis to reduce the dimensionality of their neural space to 10 factors. They gave the monkey two different types of decoders, ones that altered the relationship between neural activity and these ten factors (outside-manifold), and ones that altered the relationship between these factors and cursor kinematics (within-manifold). Ultimately, the monkeys were able to learn to use decoders with within-manifold perturbations much better than ones with outside-manifold perturbations, the latter of which required a change in neuron covariance structure. In the second study, Berger and colleagues designed a learning experiment that evaluated the ability of human subjects to learn to use two types of muscle-to-force decoders. They identified synergies from EMG patterns, and then asked the human subjects to use decoders that altered these synergies in ways that were either compatible or incompatible. Ultimately, the subjects were better able to use the compatible decoders, and could never acquire certain targets using incompatible decoders.

My experiment was intended to combine the ideas of constraints on learning from both the Berger and Sadtler studies by evaluating a muscle-based analog of the Sadtler BMI experiment. I found that the monkeys were unable to learn the Radial-Swap decoder, which required unnatural activation patterns. In Chapter 4, I conjecture that this result may be because the monkeys did not have enough experimental time to fully explore the possible neural space not requiring changes in covariance structure. However, another hypothesis could be that the decoder did require the neural population to change its covariance structure, similar to the limitation described in the Sadtler et al study. The overall implications here for cortically-controlled FES are that future decoders should preserve as much of the natural structure of the motor system as possible, including the biomechanics of how muscles produce force. At least in the short term, M1 firing cannot dissociate from these limb mechanics to differentially control muscles in a way that

is not natural. More broadly, these results suggest that both kinetic and kinematic BMI decoders for rapid and intuitive use should require natural patterns of neural activation, and avoid the need to modify the neural covariance structure to the extent possible.

5.3 The importance of afferent feedback

One main consideration, critical to the future development of motor BMIs, is the importance of afferent feedback. In the absence of sensory feedback, even the most robust motor system fails. For example, in rare conditions where motor capabilities are retained but proprioception is lost, individual experience enormous difficulty in producing movement. Such was the case for Ian Waterman, an individual who lost proprioception below the neck (Cole 1995). Unlike other individuals with similar conditions, however, he was able with great difficulty to learn to move again, relying on vision to focus on the individual steps required to move. Cutaneous feedback, in addition to proprioception, is also important to normal motor control. Without it, as shown by experiments where the digits of the hand are numbed with anesthesia, the ability to appropriately adapt grip force when lifting objects deteriorates, and objects are more readily dropped as slip cannot be easily detected (Augurelle 2002; Nowak et al. 2002; Schenker et al. 2006).

In BMI experiments, the afferent feedback available during decoder use is often different from the conditions under which the decoder was trained. For instance, as discussed in Chapter 4, in some experiments, the decoder is trained using data collected while monkeys complete a reaching task or move a manipulandum. In these experiments, the monkeys are moving their arms and receiving natural feedback relevant to the task. However, during brain control, the monkeys arms might be restrained, or they might move their arm less on their own volition after discovering that movement is not needed for decoder use (in example: Carmena et al. 2003; Velliste et al. 2008). In these cases, information about limb state is quite different between decoder training and testing. While the monkeys can still learn to use decoders even with incongruent feedback compared to training conditions, this performance may be less optimal than if the feedback in the two conditions matched. Relatedly, in an experiment by Suminski and colleagues, monkeys

were able to use a BMI where visual and proprioceptive feedback aligned, while performance decreased when visual and proprioceptive feedback of arm position did not match (Suminski et al. 2010).

The difference in afferent conditions between decoder training and testing may have influenced the results I present in this dissertation. In Chapter 3, for example, I demonstrate an inability to make across-task predictions among an isometric, unloaded movement, and spring-loaded movement task. While I attribute these results mostly to an EMG-dependent gain mechanism between M1 and EMG, I also discuss the differences in afferent feedback between the three tasks. The three cases span the dynamic range of movement, and there are therefore differences in the ways the muscles change length and produce force between tasks. This would mean that sensory receptors, such as muscle spindles and Golgi tendon organs, are signaling information about muscle length and force differently in the three tasks. This information may in turn have an influence on M1 firing, especially considering the anatomical connections from sensory receptors in the limb to motor cortex (Strick and Preston 1978; Zarzecki and Asanuma 1979)

In Chapter 4, I also describe differences in afferent feedback as a possible explanation for why the monkeys struggled to use the Radial-Swap decoder. We did not employ a nerve block during this experiment, and therefore the monkeys retained proprioception during brain control that was congruent with the mid-prone position of the limb. This feedback was especially incongruent when compared to the unnatural limb configuration imposed by the Radial-Swap decoder, and the mismatch in feedback may have been a factor in hindering performance. While there was also a mismatch in afferent feedback between training and testing of the Rotated decoder, the rotated decoder still corresponded to a natural limb configuration, and therefore the feedback mismatch may not have been as important.

All of these considerations relate to cortically-controlled FES, where BMI users may also experience a loss of both sensation and movement. However, afferent feedback may also not always be an issue. For example, in cases of incomplete SCI, individuals may retain somatosensation while movement capabilities are lost. Similarly, victims of stroke may also experience movement but not sensory deficits. It is possible – given what we know about the importance of somatosensation – that BMI users with proprioception may be more proficient at control than deafferented individuals because of their intact afferent feedback. If true, this further highlights the importance of sensory feedback for a BMI. To evaluate

this, it is possible to design an experiment that could more directly evaluate the influence of afferent feedback simply by comparing BMI performance with and without proprioceptive and cutaneous feedback. Our well-established nerve block protocol puts us in a unique position to address this question. My first experiment in the lab, in fact, attempted this, and I piloted an experiment to evaluate differences in BMI performance under normal afferent conditions and during a nerve block. My preliminary results did not indicate a significant difference in behavior between the two conditions, as indicated by task metrics, such as Time to Target and Path Length. While this was an interesting result, the nerve cuffs implanted in the monkey subject were several years old and the monkey unfortunately had to be explanted not long after these preliminary experiments. The study was never revisited. However, it could provide valuable insights into the influence of afferent feedback on BMI use, and is a project worth pursuing again in the future.

5.3.1 Methods for providing sensory feedback

Researchers are developing methods in both the central and peripheral nervous systems that may one day restore sensation to individuals. One method for providing sensory feedback is by directly stimulating somatosensory cortex (S1) using intracortical microstimulation (ICMS). However, understanding how to provide sensory feedback has long been a challenge for a variety of reasons. One main issue is researchers cannot know how many neurons are being affected by intracortical microstimulation (ICMS), though researchers have attempted to better understand the effects of ICMS through computational modeling (Overstreet, Klein, and Helms Tillery 2013). Another obstacle to understanding how to provide sensory feedback up until recently has been the fact that most sensory studies are performed in animals, who obviously cannot verbally inform the experimenter about the sensations they are feeling. To learn about the effects of sensation, scientists must therefore train animals on cleverly designed tasks that allow them to report what they are feeling. For example, in our lab, we were able to instruct monkeys to move to targets in order to report their ability to distinguish different types of microstimulation (London et al. 2008). In recent years, however, somatosensory studies have begun in human subjects, which has allowed for explicit descriptions of the sensory percepts that are evoked with stimulation. In these experiments, subjects can simply report what they feel, such as pressure and perceptions of intensity changes, without the need for

complicated task design (Flesher et al. 2017). The continuation of these types of studies may rapidly expand the knowledge base of what is possible with ICMS.

Sensory feedback can also be provided at the level of the periphery. In fact, researchers have recently demonstrated the viability of FINEs, which I discuss in Chapter 2, for restoring sensation. The ability of the FINE to provide sensory feedback has recently been established in human clinical trials, where it has been used to elicit sensation corresponding to different locations on the phantom limbs of upper-limb amputees (Tan et al. 2014; Schiefer et al. 2016). The amputees further cite many of the receptive fields of sensation as being relatively small, which demonstrates that feedback of cutaneous sensation can be delivered to patients with a high degree of precision. The ability of FINEs to both activate muscles and provide sensory feedback is an exciting prospect for FES systems. However, because sensory and motor axons are mixed together in the nerve, a future challenge will be to separate out stimulation of paralyzed limbs with the restoration of feedback.

5.4 Future experiments

Future FINE experiments

The FINE experiments described in Chapter 2 primarily consisted of stimulating single electrodes and recording recruitment curves to characterize the effect of stimulation. While we did try to elicit functional grasp in one brief session using multi-contact stimulation, we did not pursue this further. Future experiments will need to further examine how to combine the abilities of multiple contacts in order to produce useful muscle activation patterns. While we can conduct these experiments in anesthetized monkeys, the next challenge will then be to add FINEs to the cortically-controlled FES system with a behaving monkey. This may not be a trivial task, as it is yet unclear how to appropriately control stimulation of the FINES. Future studies will require finding a way to translate recruitment curve information into pulse-width stimulation trains in order to stimulate a set of muscles.

Future decoder experiments

Despite progress in decoding techniques and general BMI sophistication, the majority of motor BMI experiments have been constrained to short-term laboratory settings. During experiments, subjects use the

BMI for at most a few hours, and then return home without the device. This setup is likely to experience widespread change in the next few years, as groups are actively working to develop wireless devices that will allow for continuous and unconstrained BMI use (Borton et al. 2013; Yin et al. 2014; Schwarz et al. 2014). Doing so will allow researchers to more effectively address questions regarding long-term and generalizable decoder use, as well as adaptation, which can more efficiently be studied in a continuous-use paradigm.

In our lab, we have begun implementing a wireless system for long-term, unconstrained, cortically-controlled FES (see Appendix). This setup will greatly facilitate generalizability and adaptation studies, which will allow for follow-up experiments to the ones I have described in this dissertation. With respect to multi-task decoding, one major challenge to successful FES in the cage will be developing a decoder that will make accurate muscle predictions for the unconstrained tasks that the monkeys will attempt. In Chapter 3, I provide strong evidence that facilitating multi-task decoding will not be trivial. One of my conclusions from that study is that multi-task decoding requires robust training with different types of tasks ("Hybrid" decoders). To develop my "Hybrid" decoders, I also had to explicitly weight the error when computing my decoders, according the differences in variance between the three tasks (see Chapter 3, Materials and Methods). This may be more difficult to implement in a cage setting, where there will be a gradient of muscle activations in the training set rather than distinct tasks.

Future experiments to further address the issue of multi-task decoding will include building decoders from unconstrained data acquired from the monkey's cage. Already in the lab, we have begun to record multi-hour neural and EMG data while monkey subjects are in their cage (Appendix Figure 8-4**).** During this time, the monkey ambulates about the cage, interacts with an experimenter to accept treats, and completes a bimanual grasp task in order to receive a liquid reward. Going forward, these types of datasets will be valuable for examining the ability of decoders to make accurate predictions for a variety of unconstrained tasks. We will be able to ask questions about the number of tasks that should be included in a multi-task decoder dataset, as well as the nature of these tasks (high force production, free reaching, et cetera).

Additionally, beyond addressing questions about multi-task decoding, the cage setup will also facilitate follow-up adaptation experiments to the one I present in Chapter 4. In that chapter, the data I present

suggest that decoders for cortically-controlled FES should preserve the natural activation patterns of muscles for ready easy-of-use. However, my experiment did not evaluate long-term decoder use. In each individual session, I did not give the monkeys a lot of time to adapt. Furthermore, due to technical reasons, namely the loss of electrodes, I was also unable to extend the overall numbers of sessions in both monkeys. However, a potential follow-up experiment would be to give the monkey the Radial-Swap decoder, or another type of decoder perturbation, during a multi-day cage experiment, to see if the continuous use of this decoder facilitates learning.

5.5 Other challenges to building clinically-viable BMIs

Beyond improving control strategies for BMI systems, there are also other practical issues that may impede their full translation to the clinic. One major challenge to contend with is the longevity of electrodes. Electrode longevity may depend on the type of the electrode, or unknown variables, perhaps related to the quality of the initial electrode insertion during surgery. One prevailing theory is that electrodes may be subject to “glial scarring”, where glial cells migrate toward the foreign array, and act as a buffer between electrode and neuron (Griffith and Humphrey 2006). Electrodes may also have to be explanted for the more practical reason of mechanical failure, or intractable infection. Despite these types of issues, Utah arrays have shown the ability to last for a number of years, though certainly not indefinitely. In a long-term study that evaluated Utah array failure modes in 78 cases, John Donoghue’s research group reported a recording duration that ranged from 0 to 5.75 years (Barrese et al. 2013). Failures could be attributed both to mechanical problems, often due to connector issues, or to biological failures. They also predicted that a Utah array would maintain signals for about eight years in the absence of acute interruptions.

Unfortunately, for a device to be clinically viable, it should reliably last more than several years. For the time being, there are a few options for extending the lifetime of electrodes. One is through electrode ‘rejuvenation’, where voltage pulses applied through array electrodes can improve neural recordings, by getting rid of cellular or acellular debris that has migrated around the recording site (Otto, Johnson, and Kipke 2006). The use of LFPs as a decoding signal may also help extend the viability of a BMI long after discriminable spikes have disappeared (Flint et al. 2012; Flint et al. 2013). Ultimately, however, the issue of electrode longevity may primarily be a biomaterials problem to solve. Future advances in biocompatible

technology will hopefully hold the key to extending the lifetime of electrodes, which will help usher BMI technologies more seriously into the clinic.

5.6 Keeping the end-user in mind

In the medical device industry, the design process necessitates that product developers continuously keep their customers in mind. This is done through surveys and other evaluations of customer needs, often resulting in the development of a "House of Quality" – a correlation matrix that explicitly depicts customer needs versus product features. On the other hand, the goals of research labs are more typically to advance knowledge, and not to directly develop a product. In our lab, however, as in most BMI labs, we are in a unique position. Our research goals are both to expand the neurophysiology knowledge base, as well as to contribute to the practical development of a BMI system. To better inform the achievement of the latter task, it is important to step outside the lab from time to time to check in with potential customers, or appropriate representatives (see also *Ethical Considerations, The unexpected resistance to new technologies*).

One way to understand customer and patient needs is through survey studies. For example, a widely cited study with respect to spinal cord injury comes from the efforts of Kim Anderson, who surveyed both paraplegics and quadriplegics to reveal their priorities for improving their quality of life (Anderson 2004). Of course, another way to understand patient needs is to talk to individual patients in person. The Shirley Ryan AbilityLab, formerly the Rehabilitation Institute of Chicago, recently made a substantial change to facilitate these kinds of interactions. Its new physical floor design puts researchers in direct daily proximity to clinicians and patients, with the hope that the various groups will naturally interact more, thereby improving the translation of research ideas to the clinic. Northwestern University has a very strong connection with this newly designed research and rehabilitation hospital, which is home to many of its biomedical engineering labs. Time will tell how the new setup will influence cross-discipline relationships and the bench-to-bedside process.

In the Miller Limb Lab, we better inform our FES experiments by keeping in touch with fellow researchers and clinicians at the Cleveland FES Center in Ohio. These individuals work directly with

patients/subjects on a regular basis, and understand both their needs as well as the practical challenges that they face when using FES devices. Other times, we go straight to the FES users themselves. For example, as part of our process to brainstorm new FES experiments, our team met over Skype with a woman named Jennifer French. French has a C6-C7 incomplete spinal cord injury, and has benefitted from an FES system from the Cleveland center that allows her to stand and walk (French 2012). She is also the co-founder of the NeuroTech Network, a nonprofit that advocates for access to neurotechnology for the impaired, and is therefore often acts as a representative for the SCI population. During our discussion with her, she stressed the importance of the restoration of bilateral function, especially for tasks such as tooth brushing and self-feeding.

While implanting our monkeys bilaterally is unfortunately not practical for our current experiments, we recently took French's advice to design a cortically-controlled FES system that facilitates self-feeding. This involved implanting and providing for the control of muscles such as pronator and supinator. This design was an improvement over our previous experiments by providing the extra degrees of freedom necessary to properly orient the hand and forearm for feeding tasks. Successful use of cortically-controlled FES for self-feeding during a median and ulnar nerve block is shown in **Figure 5-1**. While this is just a start, we hope our upcoming cage FES experiments will further demonstrate the use of our system for self-feeding, as well as for many other activities of daily living.

Figure 5-1. Successful use of cortically-controlled FES for self-feeding. In this experiment, the monkey had to use a spoon to deliver apples to his mouth using his FES system during a median and ulnar nerve block. During catch trials, where the FES system was off, he could not grasp the spoon. However, when the FES system was on, he could grasp the spoon, and control muscle activation throughout the entire trial to get the spoon and apple to his mouth.

6 Ethical considerations

This thesis would not be complete without discussion of the ethical implications of the work described herein. I firmly believe researchers have a responsibility to consider the ethical implications of their work, and to discuss these topics with their colleagues. In my time as a graduate student, I have been fortunate to interface with scientists, clinicians, and ethicists both at Northwestern and elsewhere about topics in research and clinical ethics. My experiences have involved the publication of a book chapter, leadership in organizing an ethics symposium and journal club, as well as the oversight of a pilot program to grant graduate students in ethics exposure to laboratory settings. All of these experiences have been very rich and thought provoking, and have hopefully encouraged others to keep in mind the greater implications of their everyday work. Although there are countless subtopics of ethics relevant to the work described in this dissertation, here I very briefly introduce a few of the topics that I have either presented on or written about in recent years.

6.1.1 Responsible Resource Use

Non-human primate (NHP) research remains controversial. In most of Europe, monkey research is minimal, while invasive research with chimpanzees was recently outlawed in the United States. There are also movements like The Great Ape Project, founded by Peter Singer and Paulo Cavalieri, which claim that non-human great apes are deserving of the same moral rights afforded to human beings, such as liberty and the right to life (Cavalieri and Singer 1993). This movement very decisively shuts down any possibility of non-human great ape research, especially as these apes are unable provide verbal consent to participate in experiments.

Whether or not the high extent of contention about animal research is merited should not change the fact that the ability to conduct animal research is a privilege, and should not be taken for granted. Researchers must therefore continue to ensure that they conduct non-human primate research effectively and responsibly. While NHP research is already heavily regulated, there remain ways to improve upon the current use of animals as research subjects. In accordance with the accepted research framework to Reduce, Refine, and Replace, one way to responsibly conduct research is by maximizing the scientific contribution of each animal, while still balancing this effort with the animal's overall well-being. Better use

of data ensures that the work of these animals contributes to society, and that their research lives have not been lived in vain. It may also reduce the need for more animal subjects for future studies.

Optimizing the use of data from NHPs can increase their scientific contribution, but is not always simple. It is true that in a number of labs, very large amounts of data are collected from animal subjects, but not all of these data are eventually included in a publication. This may be due to various reasons – perhaps a particular analysis did not pan out, or the data were collected without a well-defined experiment in mind, though the signals are still valid. The unpopularity of publishing negative results in well-established science journals is also a problem. Many studies that do not reveal exciting results do not get published. This is especially unfortunate because other researchers cannot learn from these efforts. It could also mean that monkey subjects may be involved in multi-year studies that do not end up contributing to societal knowledge, simply because results that are not deemed interesting enough are not written up. Fortunately, there do exist a few forums and journals that publish negative results, though these avenues are not always taken advantage of. A hope for the future is that the dissemination of negative results becomes more widely accepted so that all attempted studies can inform future endeavors.

Another way to optimize data use is by encouraging future researchers in the lab group to revisit and analyze old data. This is useful because it allows for scientific productivity without the need to use other resources, such as more animals or equipment. It helps the data go the distance, and is also useful for better using the researchers themselves as a resource. For example, for early-stage PhD students who attend classes and can't spend a lot of time in the lab, this gives them a way to be productive early on, with minimum need to spend time setting up equipment and collecting data for new experiments.

Other options for efficient data use include collaborations with computational lab groups. These latter groups could run their own specialized analyses on NHP data and perhaps come up with a scientific story that the original lab may not have thought of, or not have been interested in on their own. In the Miller Limb Lab, we implement this idea by collaborating with Konrad Kording's computational lab, among others at Northwestern. For groups that are not in close physical proximity to other labs with whom they can establish a connection, conferences are also useful for valuable networking. There also exist online platforms, like

the newly formed Rheaply (rheaply.com), which puts laboratories in contact with each other so that can establish collaborations, or trade research equipment, supplies, and even animal subjects.

In fact, collaborations where different labs can share the research primates themselves are yet another way to facilitate efficient subject use. At Northwestern University, we have the benefit of being physically close to colleagues who are doing similar research at the University of Chicago (UC), only a few miles south of our lab. We recently implemented policies that allow us to readily transfer monkey subjects between the universities, depending on need. In another instance of animal sharing, our lab has also acquired monkeys from the pharmaceutical industry. As veteran subjects, these monkeys are often already chair-trained, which means we can more quickly train the animals on our specific experimental tasks. Using the same monkey for multiple studies is helpful because it minimizes the overall number of animals that become laboratory subjects. However, it must be noted that there are regulations in place that impose limitations on how many procedures a single monkey can undergo. This limits the ability to reuse animals in numerous studies.

Finally, in addition to caring for non-human primates during their tenure in research labs, there is also the issue of their status once they are no longer useful for experiments. Interestingly, even the idea of research subject retirement is met with resistance from some groups, who feel that research monkeys should be put out of their misery at the end of experiments and put down. The rationale from these groups is that research animals, despite being provided with enrichment toys and roommates, still generally live a life in the lab that is lacking in normal socialization. They would therefore not be able to acclimate well to a sanctuary environment, which would likely put them in social situations that they would not be able to handle. Most sanctuaries, however, are aware of this concern, and incorporate therapy into their programs to encourage a smooth transition from research to sanctuary life.

For those who do not believe that euthanasia should be a default end to an animal's research life, sanctuaries are a reasonable option (McAndrew and Helms Tillery 2016). However, because they include programs such as therapy and other amenities, sanctuaries may be cost-prohibitive. The price of retiring a monkey can be $20,000. Few labs can allocate these funds for retiring animals at the end of the study. In cases where histology is not necessary, this usually means that the animal is put down simply because

there is no other viable option. In response to this need, two of my former colleagues recently founded the Research Animal Retirement Foundation (RARF, rarfoundation.org). RARF is a non-profit organization that aims to raise funds to send research primates and other animals to retirement sanctuaries. This organization sets a great example for taking action to improve the treatment of monkeys as a resource, and will retire its first four monkeys by the end of this year. A number of scientists sit on its board of directors, including me, and our hope is that more researchers take action to value both the data they get from their animal subjects, as well as the ultimate welfare of the subjects themselves.

6.1.1 Facilitating interactions between researchers and ethicists

Today's political climate in America has not been a friend to scientific pursuit, to the point of spurring a national March for Science, where citizens argued for trust in science and defended its role in society. Now perhaps more than ever, it is important for society as whole to advocate for science, and to also engage in discussions about the societal implications of research findings. This means including researchers, ethicists, medical folks, politicians, and even laymen together in a mutual discussion. As a small step toward facilitating a greater mutual understanding, my colleagues and I recently piloted a program at ASU that brought together two of these groups, researchers and ethicists (Naufel 2011).

For the pilot semester, we selected three graduate students in ethics to do a rotation in a scientific lab, where they would be assigned to help a graduate student with a small research project. This program was designed to both expose graduate students in research ethics to a real lab environment, and researchers to the ideas of these ethics trainees. The hope was to encourage naturalistic conversations between the ethics trainee and the student researcher. The benefit here was to be twofold – the ethicists could learn more about biomedical topics that would be useful for their own publications, while the researchers would have more opportunities to discuss the wider implications of their work. These discussions could also inspire the researchers to develop new strategies for conducting experiments, which could result in positive outcomes such as more responsible resource use.

I was able to help oversee this program while at Northwestern, and also traveled to ASU for a mid-semester check-in with the students and their PIs. In the end, the program was an enriching experience for

the students who were interested in it, but it was hard to motivate the others to fully engage in their project. We were, however, lucky to have identified enthusiastic research PIs who were interested in the spirit of the program. They readily welcomed the ethics trainees into their lab, and were happy to meet with us to discuss program goals. Wider implementation of this program will need to facilitate the continued identification of receptive PIs, and will also require finding ways to further incentivize the students. However, I was recently encouraged to learn that other departments around the country are implementing similar programs, and time will tell how widely this concept catches on.

6.1.2 The unexpected resistance to new technologies

What does it mean to be normal? Neuroprosthetic devices are incredible technologies, capable of restoring hearing to the deaf, sight to the blind, sensation to the paralyzed, and movement to the lame. However, a point of contention, which may be surprising to some, is that those whom society regards as disabled do not see themselves as such, and may not readily welcome technologies designed to "help" them. The Deaf community, for example, does not fully embrace cochlear implants with open arms, despite the ability of these devices to provide hearing for even the profoundly deaf. Rather, some members of the community do not want these devices or to outfit their children with them. Being Deaf is a defining part of their culture, they are proud to be Deaf, and they do not want to lose that (Tucker 1998).

In another example, ethicist Gregor Wolbring, a thalidomide baby who was born without legs, expresses his disapproval that doctors during the thalidomide era so readily prescribed prosthetic limbs, as if it were an obvious solution to a perceived "problem" (Wolbring 2003). He contends that the prostheses available at the time were primitive, not largely functional, and excluded other possibilities that were useful for getting around, such as crawling. Moreover, the thalidomide population did not want or feel the need for them. Wolbring writes, "Like most thalidomiders, I did not view my body as deficient and did not see artificial legs as a sensible solution to my primary problem: dealing with a world that saw me first and foremost in terms of my defects, and accorded me so little respect or human dignity that I was not even allowed to choose how I wanted to move around" (Wolbring 2003).

As it would seem, the assumptions unimpaired individuals make about life with impairment can greatly miss the mark. The extent of this discrepancy with respect to SCI was explicitly highlighted in a 1994 survey study from Gerhart and colleagues. In this study, uninjured emergency health professionals were asked to imagine themselves with an SCI and answer questions accordingly (Gerhart et al. 1994). These answers were compared with responses from those with a true SCI. As it turned out, the responses from the uninjured group were far more negative than the SCI group's responses. For example, while only 18% of intact individuals guessed they would be glad to be alive with a severe SCI, 92% of the SCI comparison group answered in the affirmative.

These examples of resistance to technology and inaccurate perceptions should give pause to researchers and clinicians for the way they go about designing and prescribing devices. As I discuss earlier in this dissertation, it is imperative to bear in mind the customer or patient when researching, designing, or prescribing medical devices as end-all solutions. This does not mean simply imagining the desires of the target population, because, as has been described, assumptions can be wrong and even offensive. It does, however, mean finding meaningful ways to regularly engage with the target population to address their true needs and desires.

6.1.3 Select topics in neuroethics

Neurostimulation of the brain has shown potential both for restoring capabilities, such as vision (Brindley and Lewin 1968), and for treating the symptoms of neurological disease (i.e. deep brain stimulation). To do so, these devices must intimately interface with the brain and affect neural circuitry. However, because a full understanding of how neural circuits function remains elusive, device developers do not comprehensively understand how their devices affect the complex organ that is the brain. For example, although the FDA has granted approval to devices for deep brain stimulation to treat Parkinson's disease, dystonia, and even obsessive-compulsive disorder, its effect on the brain can reach beyond treatment of these diseases. DBS in fact can cause subtle side effects like personality and behavioral changes (Castelli et al. 2006).

Importantly, the notion of personhood is challenged by these technologies that intimately interact with the brain (Naufel 2013). If a technology can affect an individual's behavior and personality, what does this mean for the person's sense of self? How does it influence the way their peers see them? Furthermore, how are they seen in the eyes of greater society, and even in the law? One major societal question with regard to DBS, for example, is how to ascribe responsibility in cases where individuals whose brain implant may have adversely affected their faculties have committed crimes (Klaming and Haselager 2017). While there are no quick answers to any of these questions and issues, these are important topics to think and even develop policy about.

****

Other topics in neuroethics include concerns about possibilities that may still be beyond the horizon. These topics include a fear of "neuro-hacking", where nefarious individuals or groups may find a way to infiltrate wireless neuroprosthetic devices in ways that can change stimulation parameters, or other device capabilities. This type of offense could effectively result in mind control, where malevolent use of the device could alter the way neurons respond to, process, and even send out information to the rest of the body. In the more distant future, neuro-hacking could even include the ability to download or alter people's memories.

While these concepts may currently seem far-fetched, the possibilities may become more tangible as BMIs and other neuroprostheses begin to branch out from the lab and into the commercial realm. Elon Musk, for example, recently launched a company called Neuralink, with the aim of connecting human brains to computers with the ultimate goal of merging the brain and artificial intelligence. Facebook is also starting to explore brain-machine interface applications. It may not be long before other companies follow suit, launching BMIs and other neurotechnologies into the mainstream. As these technologies increase in popularity, it will become important to address the ethical and society considerations that these new innovations invite.

7 References

Agarwal, Alekh, Sahand Negahban, and Martin J. Wainwright. 2012. “Noisy Matrix Decomposition via Convex Relaxation: Optimal Rates in High Dimensions.” *Annals of Statistics* 40 (2): 1171–97. doi:10.1214/12-AOS1000.

Ajiboye, A. Bolu, Frank R. Willett, Dan R. Young, WD Memberg, Beverly C Walters, J A Sweet, H A Hoyen, et al. 2017. “Restoration of Reaching and Grasping in a Person with Tetraplegia through Brain-Controlled Muscle Stimulation: A Proof-of-Concept Demonstration.” *The Lancet*, (In press). doi:10.1016/S0140-6736(17)30601-3.

Alexander, Garrett E, and Michael D Crutcher. 1990. “Preparation for Movement: Neural Representations of Intended Direction in Three Motor Areas of the Monkey.” *Journal of Neurophysiology* 64 (1). http://jn.physiology.org/content/jn/64/1/133.full.pdf.

Alon, Gad, and Keith McBride. 2003. “Persons with C5 or C6 Tetraplegia Achieve Selected Functional Gains Using a Neuroprosthesis.” *Archives of Physical Medicine and Rehabilitation* 84 (1): 119–24. doi:10.1053/apmr.2003.50073.

AM, Bryden, Kilgore KL, Kirsch RF, Memberg WD, Peckham PH, and Keith MW. 2005. “An Implanted Neuroprosthesis for High Tetraplegia.” *Topics in Spinal Cord Injury Rehabilitation* 10 (3): 38–52 15p. doi:10.1310/G9T5-CCK9-Y0WT-4714.

Anderson, Kim D. 2004. “Targeting Recovery: Priorities of the Spinal Cord-Injured Population.” *Journal of Neurotrauma* 21 (10): 1371–83. doi:10.1089/neu.2004.21.1371.

Augurelle, A.-S. 2002. “Importance of Cutaneous Feedback in Maintaining a Secure Grip During Manipulation of Hand-Held Objects.” *Journal of Neurophysiology* 89 (2): 665–71. doi:10.1152/jn.00249.2002.

Baldi, J C, R D Jackson, R Moraille, and W J Mysiw. 1998. “Muscle Atrophy Is Prevented in Patients with Acute Spinal Cord Injury Using Functional Electrical Stimulation.” *Spinal Cord* 36 (7): 463–69. doi:10.1038/sj.sc.3100679.

Barrese, James C, Naveen Rao, Kaivon Paroo, Corey Triebwasser, Carlos Vargas-Irwin, Lachlan Franquemont, and John P Donoghue. 2013. “Failure Mode Analysis of Silicon-Based Intracortical Microelectrode Arrays in Non-Human Primates.” *Journal of Neural Engineering* 10 (6): 66014. doi:10.1088/1741-2560/10/6/066014.

Berger, Denise J., Reinhard Gentner, Timothy Edmunds, Dinesh K. Pai, and Andrea D’Avella. 2013. “Differences in Adaptation Rates after Virtual Surgeries Provide Direct Evidence for Modularity.” *Journal of Neuroscience* 33 (30): 12384–94. doi:10.1523/JNEUROSCI.0122-13.2013.

Boretius, Tim, Jordi Badia, Aran Pascual-Font, Martin Schuettler, Xavier Navarro, Ken Yoshida, and Thomas Stieglitz. 2010. “A Transverse Intrafascicular Multichannel Electrode (TIME) to Interface with the Peripheral Nerve.” *Biosensors and Bioelectronics* 26: 62–69. doi:10.1016/j.bios.2010.05.010.

Borton, David a, Ming Yin, Juan Aceros, and Arto Nurmikko. 2013. “An Implantable Wireless Neural Interface for Recording Cortical Circuit Dynamics in Moving Primates.” *Journal of Neural*

Engineering 10 (2): 26010. doi:10.1088/1741-2560/10/2/026010.

Bouton, Chad E., Ammar Shaikhouni, Nicholas V. Annetta, Marcia A. Bockbrader, David A. Friedenberg, Dylan M. Nielson, Gaurav Sharma, et al. 2016. “Restoring Cortical Control of Functional Movement in a Human with Quadriplegia.” *Nature* 0 (7602): 1–13. doi:10.1038/nature17435.

Brill, N., K. Polasek, E. Oby, C. Ethier, L. Miller, and D. Tyler. 2009. “Nerve Cuff Stimulation and the Effect of Fascicular Organization for Hand Grasp in Nonhuman Primates.” *Proceedings of the 31st Annual International Conference of the IEEE Engineering in Medicine and Biology Society: Engineering the Future of Biomedicine, EMBC 2009*, 1557–60. doi:10.1109/IEMBS.2009.5332395.

Brill, Natalie. 2015. “Optimization of High Density Nerve Cuff Stimulation in Upper Extremity Nerves,” 1–115. https://etd.ohiolink.edu/!etd.send_file?accession=case1418147191&disposition=attachment.

Brindley, G S, and W S Lewin. 1968. “The Sensations Produced by Electrical Stimulation of the Visual Cortex.” *The Journal of Physiology* 196 (2): 479–93. doi:10.1113/jphysiol.1968.sp008519.

Brown, Liana E, David A Rosenbaum, and Robert L Sainburg. 2017. “Limb Position Drift: Implications for Control of Posture and Movement.” Accessed May 26. doi:10.1152/jn.00013.2003.

Buys, E J, R N Lemon, G W Mantel, and R B Muir. 1986. “Selective Facilitation of Different Hand Muscles by Single Corticospinal Neurones in the Conscious Monkey.” *The Journal of Physiology* 381 (1986): 529–49. doi:3625544.

Caminiti, R, P B Johnson, and a Urbano. 1990. “Making Arm Movements within Different Parts of Space: Dynamic Aspects in the Primate Motor Cortex.” *The Journal of Neuroscience : The Official Journal of the Society for Neuroscience* 10 (July): 2039–58. http://www.jneurosci.org/content/jneuro/10/7/2039.full.pdf.

Campbell, Patrick K., Kelly E. Jones, Robert J. Huber, Kenneth W. Horch, and Richard A. Normann. 1991. “A Silicon-Based, Three-Dimensional Neural-Interface: Manufacturing Processes for an Intracortical Electrode Array.” *IEEE Transactions on Biomedical Engineering* 38 (8): 758–68.

Carmena, Jose M., Mikhail A. Lebedev, Roy E. Crist, Joseph E. O’Doherty, David M. Santucci, Dragan F. Dimitrov, Parag G. Patil, Craig S. Henriquez, and Miguel A L Nicolelis. 2003. “Learning to Control a Brain-Machine Interface for Reaching and Grasping by Primates.” *PLoS Biology* 1 (2): E42. doi:10.1371/journal.pbio.0000042.

Castelli, L, P Perozzo, M Zibetti, B Crivelli, U Morabito, M Lanotte, F Cossa, B Bergamasco, L Lopiano, and Lorys Castelli. 2006. “Chronic Deep Brain Stimulation of the Subthalamic Nucleus for Parkinson’s Disease: Effects on Cognition, Mood, Anxiety and Personality Traits Chronic DBS of STN for Parkinson’s Disease.” *Eur Neurol* 5555. doi:10.1159/000093213.

Cavalieri, P, and P Singer. 1993. *The Great Ape Project: Equality beyond Humanity*. https://books.google.com/books?hl=en&lr=&id=29QjAwAAQBAJ&oi=fnd&pg=PR1&dq=the+great+ape+project&ots=0AA0q7s1fb&sig=RVwqiRlveqwAv3gMpTQrp1ryGAg.

Chapin, J.K, K.A Moxon, R.S Markowitz, and M.A Nicolelis. 1999. “Real-Time Control of a Robot Arm Using Simultaneously Recorded Neurons in the Motor Cortex.” *Nature Neuroscience* 2 (7): 664–70. doi:10.1038/10223.

Cheney, P D, and E E Fetz. 1980. “Functional Classes of Primate Corticomotoneuronal Cells and Their Relation to Active Force.” *Journal of Neurophysiology* 44 (4): 773–91.

http://www.ncbi.nlm.nih.gov/pubmed/6253605.

Cherian, A, M O Krucoff, and L E Miller. 2011. “Motor Cortical Prediction of EMG: Evidence That a Kinetic Brain-Machine Interface May Be Robust across Altered Movement Dynamics.” *Journal of Neurophysiology* 106 (2): 564–75. doi:10.1152/jn.00553.2010.

Chhatbar, Pratik Y., and Joseph T. Francis. 2013. “Towards a Naturalistic Brain-Machine Interface: Hybrid Torque and Position Control Allows Generalization to Novel Dynamics.” Edited by Esteban Andres Fridman. *PLoS ONE* 8 (1). Public Library of Science: e52286. doi:10.1371/journal.pone.0052286.

Cole, Jonathan. 1995. *Pride and a Daily Marathon*. MIT Press.

Collinger, Jennifer L., Brian Wodlinger, John E. Downey, Wei Wang, Elizabeth C. Tyler-Kabara, Douglas J. Weber, Angus J C McMorland, Meel Velliste, Michael L. Boninger, and Andrew B. Schwartz. 2013. “High-Performance Neuroprosthetic Control by an Individual with Tetraplegia.” *The Lancet* 381 (9866): 557–64. doi:10.1016/S0140-6736(12)61816-9.

Cutrone, A, J Del Valle, D Santos, I Delgado-Martínez, M Righi, Srikanth Vasudevan, Kunal Patel, et al. 2011. “Comparative Analysis of Transverse Intrafascicular Multichannel, Longitudinal Intrafascicular and Multipolar Cuff Electrodes for the Selective Stimulation of Nerve Fascicles.” *J. Neural Eng. J. Neural Eng* 8 (8). doi:10.1088/1741-2560/8/3/036023.

Daly, Janis J, Janice Zimbelman, Kristen L Roenigk, Jessica P McCabe, Jean M Rogers, Kristi Butler, Richard Burdsall, John P Holcomb, E Byron Marsolais, and Robert L Ruff. 2011. “Recovery of Coordinated Gait: Randomized Controlled Stroke Trial of Functional Electrical Stimulation (FES) Versus No FES, With Weight-Supported Treadmill and Over-Ground Training.” *Neurorehabilitation and Neural Repair* 25 (7): 588–96. doi:10.1177/1545968311400092.

Ethier, C, E R Oby, M J Bauman, and L E Miller. 2012. “Restoration of Grasp Following Paralysis through Brain-Controlled Stimulation of Muscles.” *Nature* 485 (7398). Nature Publishing Group: 368–71. doi:10.1038/nature10987.

Ethier, Christian, Daniel Acuna, Sara A Solla, and Lee E Miller. 2016. “Adaptive Neuron-to-EMG Decoder Training for FES Neuroprostheses.” *Journal of Neural Engineering* 13 (4): 46009. doi:10.1088/1741-2560/13/4/046009.

Evarts, E V. 1968. “Relation of Pyramidal Tract Activity to Force Exerted during Voluntary Movement.” *Journal of Neurophysiology* 31 (1): 14–27. http://eutils.ncbi.nlm.nih.gov/entrez/eutils/elink.fcgi?dbfrom=pubmed&id=4966614&retmode=ref&cmd=prlinks%5Cnpapers3://publication/uuid/F271B3A5-7208-4AC8-92B9-D2718CC139AB.

Evarts, E V, C Fromm, J Kroller, and V A Jennings. 1983. “Motor Cortex Control of Finely Graded Forces.” *Journal of Neurophysiology* 49 (5): 1199–1215. http://jn.physiology.org/content/49/5/1199.short.

Fetz, Eberhard E, and Mary Ann Baker. 2017. “Operantly Conditioned Patterns of Activity and Correlated Responses Cells and Contralateral Muscles.” Accessed May 24. http://jn.physiology.org/content/jn/36/2/179.full.pdf.

Fisher, Lee E., Michael E. Miller, Stephanie N. Bailey, John A. Davis, James S. Anderson, Lori Rhode, Dustin J. Tyler, and Ronald J. Triolo. 2008. “Standing after Spinal Cord Injury with Four-Contact Nerve-Cuff Electrodes for Quadriceps Stimulation.” *IEEE Transactions on Neural Systems and Rehabilitation Engineering* 16 (5): 473–78. doi:10.1109/TNSRE.2008.2003390.

Flesher, Sharlene N, Jennifer L Collinger, Stephen T Foldes, Jeffrey M Weiss, John E Downey, Elizabeth C Tyler-Kabara, Sliman J Bensmaia, Andrew B Schwartz, Michael L Boninger, and Robert A Gaunt. 2017. “Intracortical Microstimulation of Human Somatosensory Cortex.” Accessed May 7. http://stm.sciencemag.org/content/scitransmed/8/361/361ra141.full.pdf.

Flint, Robert D., Zachary A. Wright, and Marc W. Slutzky. 2012. “Control of a Biomimetic Brain Machine Interface with Local Field Potentials: Performance and Stability of a Static Decoder over 200 Days.” *Proceedings of the Annual International Conference of the IEEE Engineering in Medicine and Biology Society, EMBS*, 6719–22. doi:10.1109/EMBC.2012.6347536.

Flint, Robert D, Christian Ethier, Emily R Oby, Lee E Miller, and Marc W Slutzky. 2017. “Local Field Potentials Allow Accurate Decoding of Muscle Activity.” Accessed May 2. http://jn.physiology.org/content/jn/108/1/18.full.pdf.

Flint, Robert D, Eric W Lindberg, Luke R Jordan, Lee E Miller, and Marc W Slutzky. 2012. “Accurate Decoding of Reaching Movements from Field Potentials in the Absence of Spikes.” *Journal of Neural Engineering* 9 (4): 46006. doi:10.1088/1741-2560/9/4/046006.

Flint, Robert D, Eric W Lindberg, Luke R Jordan, Sergey D Stavisky, Jonathan C Kao, Paul Nuyujukian, Kelvin So, et al. 2013. “Long Term, Stable Brain Machine Interface Performance Using Local Field Potentials and Multiunit Spikes.” *J. Neural Eng* 10: 56005–11. doi:10.1088/1741-2560/10/5/056005.

Fraser, George W, Steven M Chase, Andrew Whitford, and Andrew B Schwartz. 2009. “Control of a Brain-Computer Interface without Spike Sorting.” *Journal of Neural Engineering* 6 (5): 55004. doi:10.1088/1741-2560/6/5/055004.

French, Jennifer. 2012. *On My Feet Again*. Neurotech Press. https://www.amazon.com/My-Feet-Again-Jennifer-French-ebook/dp/B009PTMHVM.

Fromm, Christoph. 1983. “Changes of Steady State Activity in Motor Cortex Consistent with the Length-Tension Relation of Muscle.” *Pfltigers Arch* 398: 318–23.

Fromm, Christoph, and Edward V. Evarts. 1977. “Relation of Motor Cortex Neurons to Precisely Controlled and Ballistic Movements.” *Neuroscience Letters* 5 (5): 259–65. doi:10.1016/0304-3940(77)90076-3.

Fu, Q. G., D. Flament, J. D. Coltz, and T. J. Ebner. 1995. “Temporal Encoding of Movement Kinematics in the Discharge of Primate Primary Motor and Premotor Neurons.” *Journal of Neurophysiology* 73 (2). http://jn.physiology.org/content/73/2/836.short.

Galvani, Luigi. 1791. “De Viribus Electricitatis in Motu Musculari Commentarius.” *De Bononiensi Scientiarum et Artium Instituto Atque Academia Commentarii* 7: 363–418.

Gandolla, Marta, Simona Ferrante, Franco Molteni, Eleonora Guanziroli, Tiziano Frattini, Alberto Martegani, Giancarlo Ferrigno, Karl Friston, Alessandra Pedrocchi, and Nick S. Ward. 2014. “Re-Thinking the Role of Motor Cortex: Context-Sensitive Motor Outputs?” *NeuroImage* 91: 366–74. doi:10.1016/j.neuroimage.2014.01.011.

Ganguly, Karunesh, and Jose M. Carmena. 2009. “Emergence of a Stable Cortical Map for Neuroprosthetic Control.” *PLoS Biology* 7 (7). doi:10.1371/journal.pbio.1000153.

Ganguly, Karunesh, Dragan F Dimitrov, Jonathan D Wallis, and Jose M Carmena. 2011. “Reversible Large-Scale Modification of Cortical Networks during Neuroprosthetic Control.” *Nature*

Neuroscience 14 (5). Nature Publishing Group: 662–67. doi:10.1038/nn.2797.

Gaunt, Robert A., and Arthur Prochazka. 2005. “Control of Urinary Bladder Function with Devices: Successes and Failures.” *Progress in Brain Research* 152 (July 2016): 163–94. doi:10.1016/S0079-6123(05)52011-9.

Georgopoulos, a P, J F Kalaska, R Caminiti, and J T Massey. 1982. “On the Relations between the Direction of Two-Dimensional Arm Movements and Cell Discharge in Primate Motor Cortex.” *J.Neurosci.* 2(11) (11): 1527–37. doi:citeulike-article-id:444841.

Georgopoulos, AP, R Caminiti, JF Kalaska, and JT Massey. 1983. “Spatial Coding of Movement: A Hypothesis Concerning the Coding of Movement Direction by Motor Cortical Populations.” *Experimental Brain Research*.

Georgopoulos, Apostolos P, John F Kalaska, Roberto Caminiti, and Joe T Massey5. 1982. “On the Relations between the Direction of Two-Dimensional Arm Movements and Cell Discharge in Primate Motor Cortex.” *The Journal of Neuroscience* 2 (11): 1527–37. http://www.jneurosci.org/content/jneuro/2/11/1527.full.pdf.

Georgopoulos, Apostolos P, A B Schwartz, and R E Kettner. 1986. “Neuronal Population Coding of Movement Direction.” *Science (New York, N.Y.)* 233 (4771): 1416–19. doi:10.1126/science.3749885.

Gerhart, Kenneth A., Jane Koziol-McLain, Steven R. Lowenstein, and Gale G. Whiteneck. 1994. “Quality of Life Following Spinal Cord Injury: Knowledge and Attitudes of Emergency Care Providers.” *Annals of Emergency Medicine* 23 (4): 807–12. doi:10.1016/S0196-0644(94)70318-3.

Gilja, Vikash, Paul Nuyujukian, Cindy A Chestek, John P Cunningham, Byron M Yu, Joline M Fan, Mark M Churchland, et al. 2012. “A High-Performance Neural Prosthesis Enabled by Control Algorithm Design.” *Nature Neuroscience* 15 (12): 1752–57. doi:10.1038/nn.3265.

Granat, M. H., B. W. Heller, D. J. Nicol, R. H. Baxendale, and B. J. Andrews. 1993. “Improving Limb Flexion in FES Gait Using the Flexion Withdrawal Response for the Spinal Cord Injured Person.” *Journal of Biomedical Engineering* 15 (1): 51–56. doi:10.1016/0141-5425(93)90093-E.

Griffith, Ronald W., and Donald R. Humphrey. 2006. “Long-Term Gliosis around Chronically Implanted Platinum Electrodes in the Rhesus Macaque Motor Cortex.” *Neuroscience Letters*. Vol. 406. doi:10.1016/j.neulet.2006.07.018.

Heckman, C. J., Carol Mottram, Kathy Quinlan, Renee Theiss, and Jenna Schuster. 2009. “Motoneuron Excitability: The Importance of Neuromodulatory Inputs.” *Clinical Neurophysiology* 120 (12): 2040–54. doi:10.1016/j.clinph.2009.08.009.

Héliot, Rodolphe, Amy L. Orsborn, Karunesh Ganguly, and Jose M. Carmena. 2010. “System Architecture for Stiffness Control in Brain-Machine Interfaces.” *IEEE Transactions on Systems, Man, and Cybernetics Part A:Systems and Humans* 40 (4): 732–42. doi:10.1109/TSMCA.2010.2044410.

Hepp-Reymond, M. C., M. Kirkpatrick-Tanner, L. Gabernet, H. X. Qi, and B. Weber. 1999. “Context-Dependent Force Coding in Motor and Promotor Cortical Areas.” *Experimental Brain Research* 128 (1–2): 123–33. doi:10.1007/s002210050827.

Hochberg, Leigh R., Daniel Bacher, Beata Jarosiewicz, Nicolas Y. Masse, John D. Simeral, Joern Vogel, Sami Haddadin, et al. 2012. “Reach and Grasp by People with Tetraplegia Using a Neurally

Controlled Robotic Arm." *Nature* 485 (7398). Nature Publishing Group: 372–75. doi:10.1038/nature11076.

Hochberg, Leigh R, Mijail D Serruya, Gerhard M Friehs, Jon A Mukand, Maryam Saleh, Abraham H Caplan, Almut Branner, David Chen, Richard D Penn, and John P Donoghue. 2006. "Neuronal Ensemble Control of Prosthetic Devices by a Human with Tetraplegia." *Nature* 442 (7099): 164–71. doi:10.1038/nature04970.

Humphrey, Donald R., and D.J Reed. 1982. "Separate Cortical Systems for Control of Joint Movement and Joint Stiffness: Reciprocal Activation and Coactivation of Antagonist Muscles." *Advances in Neurology* 39: 347–72.

Humphrey, Donald R, E M Schmidt, and W D Thompson. 1970. "Predicting Measures of Motor Performance from Multiple Cortical Spike Trains Published by : American Association for the Advancement of Science Stable URL : http://www.jstor.org/stable/1730570 Your Use of the JSTOR Archive Indicates Your Acceptance of the." *Science* 170 (3959): 758–62.

Hwang, Eun Jung, Paul M Bailey, and Richard A Andersen. 2013. "Article Volitional Control of Neural Activity Relies on the Natural Motor Repertoire." *Current Biology* 23: 353–61. doi:10.1016/j.cub.2013.01.027.

Ijzerman, Maarten J., T. S. Stoffers, F. in 't Groen, M. a. P. Klatte, G. J. Snoek, J. H. C. Vorsteveld, R. H. Nathan, and Hermie J. Hermens. 1996. "The NESS Handmaster Orthosis: Restoration of Hand Function in C5 and Stroke Patients by Means of Electrical Stimulation." *Journal of Rehabilitation Sciences*.

Ingram, H.A., P. van Donkelaar, J. Cole, J-L Vercher, G.M. Gauthier, and R.C. Miall. 2000. "The Role of Proprioception and Attention in a Visuomotor Adaptation Task." *Exp Brain Res*, no. 132: 113–26. doi:10.1007/s002219900322 RESEARCH ARTICLE H.A.

Ito, Masao. 2000. "Mechanisms of Motor Learning in the Cerebellum." *Brain Research* 886: 237–45. www.elsevier.com.

Jacobs, Barry L., Francisco J. Martín-Cora, and Casimir A. Fornal. 2002. "Activity of Medullary Serotonergic Neurons in Freely Moving Animals." *Brain Research Reviews* 40 (1–3): 45–52. doi:10.1016/S0165-0173(02)00187-X.

Jarosiewicz, Beata, Steven M Chase, George W Fraser, Meel Velliste, Robert E Kass, and Andrew B Schwartz. 2008. "Functional Network Reorganization during Learning in a Brain-Computer Interface Paradigm." *Proceedings of the National Academy of Sciences of the United States of America* 105 (49): 19486–91. doi:10.1073/pnas.0808113105.

Johnson, Michael E. 2004. "Neurotoxicity of Lidocaine: Implications for Spinal Anesthesia and Neuroprotection." *Journal of Neurosurgical Anesthesiology* 16 (1): 80–83. doi:10.1097/00008506-200401000-00017.

Jones, K E, J Wessberg, and A Vallbo. 2001. "Proprioceptive Feedback Is Reduced during Adaptation to a Visuomotor Transformation: Preliminary Findings." *Neuroreport* 12 (18): 4029–33. doi:10.1097/00001756-200112210-00035.

Kilgore, Kevin L., Harry A. Hoyen, Anne M. Bryden, Ronald L. Hart, Michael W. Keith, and P. Hunter Peckham. 2008. "An Implanted Upper-Extremity Neuroprosthesis Using Myoelectric Control." *Journal of Hand Surgery* 33 (4): 539–50. doi:10.1016/j.jhsa.2008.01.007.

Kilgore, Kevin L., P. Hunter Peckham, Michael W. Keith, and Geoffrey B. Thrope. 1990. “Electrode Characterization for Functional Application to Upper Extremity FNS.” *IEEE Transactions on Biomedical Engineering* 37 (1): 12–21. doi:10.1109/10.43606.

Kim, Hyun K., Jose M. Carmena, S. James Biggs, Timothy L. Hanson, Miguel A L Nicolelis, and Mandayam A. Srinivasan. 2007. “The Muscle Activation Method: An Approach to Impedance Control of Brain-Machine Interfaces through a Musculoskeletal Model of the Arm.” *IEEE Transactions on Biomedical Engineering* 54 (8): 1520–29. doi:10.1109/TBME.2007.900818.

Kingma, Diederik P., and Jimmy Lei Ba. 2015. “Adam: A Method for Stochastic Optimization.” *International Conference on Learning Representations 2015*, 1–15.

Klaming, Laura, and Pim Haselager. 2017. “Did My Brain Implant Make Me Do It? Questions Raised by DBS Regarding Psychological Continuity, Responsibility for Action and Mental Competence.” Accessed May 6. doi:10.1007/s12152-010-9093-1.

Krakauer, John W, Zachary M Pine, Maria-Felice Ghilardi, and Claude Ghez. 2017. “Learning of Visuomotor Transformations for Vectorial Planning of Reaching Trajectories.” Accessed May 26. http://www.jneurosci.org/content/jneuro/20/23/8916.full.pdf.

Kurtzer, Isaac, Troy M Herter, and Stephen H Scott. 2005. “Random Change in Cortical Load Representation Suggests Distinct Control of Posture and Movement.” *Nature Neuroscience* 8 (4): 498–504. doi:10.1038/nn1420.

Lackner, James R., and Paul Dizio. 1994. “Rapid Adaptation to Coriolis Force Perturbations of Arm Trajectory.” *Journal of Neurophysiology* 72. http://jn.physiology.org/content/jn/72/1/299.full.pdf.

Lago, Natalia, Ken Yoshida, Klaus P. Koch, and Xavier Navarro. 2007. “Assessment of Biocompatibility of Chronically Implanted Polyimide and Platinum Intrafascicular Electrodes.” *IEEE Transactions on Biomedical Engineering* 54 (2): 281–90. doi:10.1109/TBME.2006.886617.

Lawrence, Stephen M., Gurpreet S. Dhillon, and Kenneth W. Horch. 2003. “Fabrication and Characteristics of an Implantable, Polymer-Based, Intrafascicular Electrode.” *Journal of Neuroscience Methods* 131 (1–2): 9–26. doi:10.1016/S0165-0270(03)00231-0.

Lebedev, M. A., Jose M. Carmena, Joseph E. O’Doherty, Miriam Zacksenhouse, Craig S. Henriquez, Jose C. Principe, and Miguel A. L. Nicolelis. 2005. “Cortical Ensemble Adaptation to Represent Velocity of an Artificial Actuator Controlled by a Brain-Machine Interface.” *Journal of Neuroscience* 25 (19): 4681–93. doi:10.1523/JNEUROSCI.4088-04.2005.

Ledbetter, Noah M, Christian Ethier, Emily R Oby, Scott D Hiatt, Andrew M Wilder, Jason H Ko, Sonya P Agnew, Lee E Miller, and Gregory a Clark. 2013. “Intrafascicular Stimulation of Monkey Arm Nerves Evokes Coordinated Grasp and Sensory Responses.” *Journal of Neurophysiology* 109 (2): 580–90. doi:10.1152/jn.00688.2011.

Lee, Robert H., and Charles J Heckman. 2000. “Adjustable Amplification of Synaptic Input in the Dendrites of Spinal Motoneurons in Vivo.” *The Journal of Neuroscience : The Official Journal of the Society for Neuroscience* 20 (17): 6734–40. doi:20/17/6734 [pii].

Li, Chiang-Shan Ray, Camillo Padoa-Schioppa, and Emilio Bizzi. 2001. “Neuronal Correlates of Motor Performance and Motor Learning in the Primary Motor Cortex of Monkeys Adapting to an External Force Field.” *Neuron* 30 (2): 593–607. doi:10.1016/S0896-6273(01)00301-4.

Llinás, Rodolfo, and John P. Welsh. 1993. “On the Cerebellum and Motor Learning.” *Current Opinion in Neurobiology* 3 (6): 958–65. doi:10.1016/0959-4388(93)90168-X.

London, B.M., L.R. Jordan, C.R. Jackson, and L.E. Miller. 2008. “Electrical Stimulation of the Proprioceptive Cortex (Area 3a) Used to Instruct a Behaving Monkey.” *Neural Systems and Rehabilitation Engineering, IEEE Transactions on* 16 (1): 32–36. doi:10.1109/TNSRE.2007.907544.

Lynch, Cheryl L., and Milos R. Popovic. 2008. “Functional Electrical Stimulation.” *IEEE Control Systems Magazine*, 41–50. doi:10.1109/MCS.2007.914689.

Martin, T a, J G Keating, H P Goodkin, a J Bastian, and W T Thach. 1996. “Throwing While Looking through Prisms II. Specificity and Storage of Multiple Gaze-Throw Calibrations.” *Brain* 119 (4): 1183–98. doi:10.1093/brain/119.4.1183.

McAndrew, Rachele, and Stephen I. Helms Tillery. 2016. “Laboratory Primates: Their Lives in and after Research.” *Temperature* 3 (4): 502–8. doi:10.1080/23328940.2016.1229161.

Michel, Carine, Laure Pisella, Claude Prablanc, Gilles Rode, and Yves Rossetti. 2007. “Enhancing Visuomotor Adaptation by Reducing Error Signals: Single-Step (Aware) versus Multiple-Step (Unaware) Exposure to Wedge Prisms.” *Journal of Cognitive Neuroscience* 19 (2): 341–50. doi:10.1162/jocn.2007.19.2.341.

Moran, Daniel W, and Andrew B Schwartz. 1999. “Motor Cortical Representation of Speed and Direction During Reaching.” http://jn.physiology.org/content/jn/82/5/2676.full.pdf.

Moritz, Chet T, Steve I Perlmutter, and Eberhard E Fetz. 2008. “Direct Control of Paralysed Muscles by Cortical Neurons.” *Nature* 456 (7222): 639–42. doi:10.1038/nature07418.

Morrow, M M, L R Jordan, and L E Miller. 2007. “Direct Comparison of the Task-Dependent Discharge of M1 in Hand Space and Muscle Space.” *J.Neurophysiol.* 97 (0022–3077 (Print)): 1786–98. doi:10.1152/jn.00150.2006.

Muir, R. B., and R. N. Lemon. 1983. “Corticospinal Neurons with a Special Role in Precision Grip.” *Brain Research*. Vol. 261. doi:10.1016/0006-8993(83)90635-2.

Naufel, Stephanie. 2011. “Single-Unit Responses in Somatosensory Cortex to Precision Grip of Textured Surfaces.” https://repository.asu.edu/attachments/56992/content/Naufel_asu_0010N_10928.pdf.

Naufel, Stephanie. 2013. “Nanotechnology, the Brain, and the Future.” Edited by Sean A. Hays, Jason Scott Robert, Clark A. Miller, and Ira Bennett. Dordrecht: Springer Netherlands, 167–78. doi:10.1007/978-94-007-1787-9.

Navarro, Xavier, Thilo B Krueger, Natalia Lago, Silvestro Micera, Thomas Stieglitz, and Paolo Dario. 2017. “A Critical Review of Interfaces with the Peripheral Nervous System for the Control of Neuroprostheses and Hybrid Bionic Systems.” Accessed May 2. http://s3.amazonaws.com/academia.edu.documents/45532567/X._Navarro_T._Krger_N._Lago_S._Micera_T.20160511-27821-pgxp5y.pdf?AWSAccessKeyId=AKIAIWOWYYGZ2Y53UL3A&Expires=1493783582&Signature=NZoHvn%2BKUKQsjD4%2FDFfFXP77KvM%3D&response-content-disposition=inline%3Bfilename%3DA_critical_review_of_interfaces_with_the.pdf.

Nemati, Shamim, Nicholas G Hatsopoulos, Lee E Miller, and Andrew H Fagg. 2007. “Constructing Robust Neural Decoders Using Limited Training Data.” *Biomedical Engineering*, 1–29.

Nowak, Dennis A., Joachim Hermsdörfer, Stefan Glasauer, Jens Philipp, Ludger Meyer, and Norbert Mai. 2002. “The Effects of Digital Anaesthesia on Predictive Grip Force Adjustments during Vertical Movements of a Grasped Object.” *European Journal of Neuroscience* 14 (4): 756–62. doi:10.1046/j.0953-816X.2001.01697.x.

Oby, Emily R., A. Degenhart, E. C. Tyler-Kabara, Byron M. Yu, and Aaron P. Batista. 2015. “Network Constraints Dictate the Timescale of Learning New Brain-Computer Interfaces.” In *Society for Neuroscience*.

Oby, Emily R, Christian Ethier, and Lee E Miller. 2013. “Movement Representation in the Primary Motor Cortex and Its Contribution to Generalizable EMG Predictions.” *Journal of Neurophysiology* 109 (3): 666–78. doi:10.1152/jn.00331.2012.

Orsborn, Amy L., Siddharth Dangi, Helene G. Moorman, and Jose M. Carmena. 2012. “Closed-Loop Decoder Adaptation on Intermediate Time-Scales Facilitates Rapid BMI Performance Improvements Independent of Decoder Initialization Conditions.” *IEEE Transactions on Neural Systems and Rehabilitation Engineering* 20 (4): 468–77. doi:10.1109/TNSRE.2012.2185066.

Otto, Kevin J., Matthew D. Johnson, and Daryl R. Kipke. 2006. “Voltage Pulses Change Neural Interface Properties and Improve Unit Recordings with Chronically Implanted Microelectrodes.” *IEEE Transactions on Biomedical Engineering* 53 (2): 333–40. doi:10.1109/TBME.2005.862530.

Overstreet, C K, J D Klein, and S I Helms Tillery. 2013. “Computational Modeling of Direct Neuronal Recruitment during Intracortical Microstimulation in Somatosensory Cortex.” *J. Neural Eng.*, no. 10: 1–15. doi:10.1088/1741-2560/10/6/066016.

Paninski, Liam, Matthew R Fellows, Nicholas G Hatsopoulos, and John P Donoghue. 2017. “Spatiotemporal Tuning of Motor Cortical Neurons for Hand Position and Velocity.” Accessed May 1. doi:10.1152/jn.00587.2002.

Pavlides, C, E Miyashita, and H Asanuma. 1993. “Projection from the Sensory to the Motor Cortex Is Important in Learning Motor Skills in the Monkey.” *Journal of Neurophysiology* 70 (2): 733–41. doi:10.1016/j.neuron.2011.07.029.

Peckham, P. Hunter, Michael W. Keith, Kevin L. Kilgore, Julie H. Grill, Kathy S. Wuolle, Geoffrey B. Thrope, Peter Gorman, et al. 2001. “Efficacy of an Implanted Neuroprosthesis for Restoring Hand Grasp in Tetraplegia: A Multicenter Study.” *Archives of Physical Medicine and Rehabilitation* 82 (10): 1380–88. doi:10.1053/apmr.2001.25910.

Peckham, P. Hunter, and Jayme S. Knutson. 2005. “Functional Electrical Stimulation for Neuromuscular Applications*.” *Annual Review of Biomedical Engineering* 7 (1): 327–60. doi:10.1146/annurev.bioeng.6.040803.140103.

Peckham, P Hunter, E Byron Marsolais, and J Thomas Mortimer. 1980. “Restoration of a Key Grip and Release in the C6 Tetraplegic Patient through Functional Electrical Stimulation.” *International Journal of Smart Engineering System Design*. doi:10.1016/S0363-5023(80)80076-1.

Perlmutter, Joel S, and Jonathan W Mink. 2006. “Deep Brain Stimulation.” doi:10.1146/.

Pohlmeyer, Eric A., Luke R. Jordon, Peter Kim, and Lee E. Miller. 2009. “A Fully Implanted Drug Delivery System for Peripheral Nerve Blocks in Behaving Animals.” *Journal of Neuroscience Methods* 182 (2): 165–71. doi:10.1016/j.jneumeth.2009.06.006.

Pohlmeyer, Eric A., Emily R. Oby, Eric J. Perreault, Sara A. Solla, Kevin L. Kilgore, Robert F. Kirsch, and Lee E. Miller. 2009. “Toward the Restoration of Hand Use to a Paralyzed Monkey: Brain-Controlled Functional Electrical Stimulation of Forearm Muscles.” *PLoS ONE* 4 (6): e5924. doi:10.1371/journal.pone.0005924.

Pohlmeyer, Eric A, Sara A Solla, Eric J Perreault, and Lee E Miller. 2008. “Prediction of Upper Limb Muscle Activity from Motor Cortical Discharge during Reaching” 4 (4): 369–79. doi:10.1088/1741-2560/4/4/003.Prediction.

Polasek, Katharine H., Harry A. Hoyen, Michael W. Keith, and Dustin J. Tyler. 2007. “Human Nerve Stimulation Thresholds and Selectivity Using a Multi-Contact Nerve Cuff Electrode.” *IEEE Transactions on Neural Systems and Rehabilitation Engineering* 15 (1): 76–82. doi:10.1109/TNSRE.2007.891383.

Polasek, Katharine H., Matthew A. Schiefer, Gilles C. Pinault, Ronald J. Triolo, and Dustin J. Tyler. 2007. “Intraoperative Evaluation of the Spiral Nerve Cuff Electrode for a Standing Neuroprosthesis.” *Proceedings of the 3rd International IEEE EMBS Conference on Neural Engineering* 66005: 89–92. doi:10.1109/CNE.2007.369619.

Popovic, Milos R, Dejan B Popovic, and Thierry Keller. 2002. “Neuroprostheses for Grasping.” *Neurological Research* 24 (5): 443–52. doi:10.1179/016164102101200311.

Prochazka, Arthur, Michel Gauthier, Marguerite Wieler, and Zoltan Kenwell. 1997. “The Bionic Glove: An Electrical Stimulator Garment That Provides Controlled Grasp and Hand Opening in Quadriplegia.” *Archives of Physical Medicine and Rehabilitation* 78 (6): 608–14. doi:10.1016/S0003-9993(97)90426-3.

Quallo, M M, A Kraskov, and R N Lemon. 2012. “The Activity of Primary Motor Cortex Corticospinal Neurons during Tool Use by Macaque Monkeys.” *The Journal of Neuroscience* 32 (48): 17351–64. doi:10.1523/JNEUROSCI.1009-12.2012.

Ragnarsson, K T. 2008. “Functional Electrical Stimulation after Spinal Cord Injury: Current Use, Therapeutic Effects and Future Directions.” *Spinal Cord* 46 (4): 255–74. doi:10.1038/sj.sc.3102091.

Rasmussen, Robert G, Andrew Schwartz, and Steven M Chase. 2017. “Dynamic Range Adaptation in Primary Motor Cortical Populations.” *eLife* 6: 1–20. doi:10.7554/eLife.21409.

Sachs, Nicholas A, Ricardo Ruiz-Torres, Eric J Perreault, and Lee E Miller. 2016. “Brain-State Classification and a Dual-State Decoder Dramatically Improve the Control of Cursor Movement through a Brain-Machine Interface.” *Journal of Neural Engineering* 13 (1). IOP Publishing: 16009. doi:10.1088/1741-2560/13/1/016009.

Sadtler, Patrick T., Kristin M. Quick, Matthew D. Golub, Steven M. Chase, Stephen I. Ryu, Elizabeth C. Tyler-Kabara, Byron M. Yu, and Aaron P. Batista. 2014. “Neural Constraints on Learning.” *Nature* 512 (7515). Nature Publishing Group: 423–26. doi:10.1038/nature13665.

Scheidt, Robert A, and Claude Ghez. 2017. “Separate Adaptive Mechanisms for Controlling Trajectory and Final Position in Reaching.” Accessed May 26. doi:10.1152/jn.00121.2007.

Schenker, M., M. K O Burstedt, M. Wiberg, and R. S. Johansson. 2006. “Precision Grip Function after Hand Replantation and Digital Nerve Injury.” *Journal of Plastic, Reconstructive and Aesthetic Surgery* 59 (7): 706–16. doi:10.1016/j.bjps.2005.12.004.

Schieber, Marc H. 2011. “Dissociating Motor Cortex from the Motor.” *The Journal of Physiology* 589 (Pt 23): 5613–24. doi:10.1113/jphysiol.2011.215814.

Schiefer, Matthew, Daniel Tan, Steven M Sidek, and Dustin J Tyler. 2016. “Sensory Feedback by Peripheral Nerve Stimulation Improves Task Performance in Individuals with Upper Limb Loss Using a Myoelectric Prosthesis.” *Journal of Neural Engineering* 13 (1). IOP Publishing: 16001. doi:10.1088/1741-2560/13/1/016001.

Schwartz, Andrew B. 1992. “Motor Cortical Activity During Drawing Movements: Single-Unit Activity Uring Sinusoid Tracing.” *Journal of Neurophysiology* 68 (2). http://jn.physiology.org/content/jn/68/2/528.full.pdf.

Schwartz, Andrew B. 1993. “Motor Cortical Activity during Drawing Movements: Population Representation during Sinusoid Tracing.” *Journal of Neurophysiology* 70 (1): 28–36. doi:citeulike-article-id:449884.

Schwartz, Andrew B, and Daniel W Moran. 2000. “Arm Trajectories and Representation of Movement Processing in Motor Cortical Activity” 12: 1851–56.

Schwarz, David a, Mikhail a Lebedev, Timothy L Hanson, Dragan F Dimitrov, Gary Lehew, Jim Meloy, Sankaranarayani Rajangam, et al. 2014. “Chronic, Wireless Recordings of Large-Scale Brain Activity in Freely Moving Rhesus Monkeys.” *Nature Methods* 11 (6). Nature Research: 670–76. doi:10.1038/nmeth.2936.

Serruya, Mijail D., Nicholas G. Hatsopoulos, Liam Paninski, Matthew R Fellows, and John P Donoghue. 2002. “Instant Neural Control of a Movement Signal.” *Nature* 416 (6877): 141–42. doi:10.1038/416141a.

Shadmehr, R, and F a Mussa-Ivaldi. 1994. “Adaptive Representation of Dynamics during Learning of a Motor Task.” *The Journal of Neuroscience* 14 (5): 3208–24. doi:8182467.

Shelley, Mary Wollstonecraft. 1818. *Frankenstein, Or, The Modern Prometheus*. New York: Oxford University Press.

Shenoy, KrishnaV, and JoseM Carmena. 2014. “Combining Decoder Design and Neural Adaptation in Brain-Machine Interfaces.” *Neuron* 84 (4): 665–80. doi:10.1016/j.neuron.2014.08.038.

Snoek, G. J., M. J. IJzerman, F. A. in ’t Groen, T. S. Stoffers, and G. Zilvold. 2000. “Use of the NESS Handmaster to Restore Handfunction in Tetraplegia: Clinical Experiences in Ten Patients.” *Spinal Cord* 38 (4): 244–49. doi:10.1038/sj.sc.3100980.

Strick, P L, and J B Preston. 1982. “Two Representations of the Hand in Area 4 of a Primate. II. Somatosensory Input Organization.” *Journal of Neurophysiology* 48 (1): 150–59. http://jn.physiology.org/content/48/1/139.short%5Cnpapers3://publication/uuid/73BB7766-41D5-42D7-9040-6479709246FC.

Strick, Peter L., and James B. Preston. 1978a. “Multiple Representation in the Primate Motor Cortex.” *Brain Research* 154 (2): 366–70. doi:10.1016/0006-8993(78)90707-2.

Strick, Peter L., and James B. Presto. 1978b. “Sorting of Somatosensory Afferent Information in Primate Motor Cortex.” *Brain Research* 156 (2): 364–68. doi:10.1016/0006-8993(78)90520-6.

Suminski, A. J., D. C. Tkach, A. H. Fagg, and N. G. Hatsopoulos. 2010. “Incorporating Feedback from

Multiple Sensory Modalities Enhances Brain-Machine Interface Control." *Journal of Neuroscience* 30 (50): 16777–87. doi:10.1523/JNEUROSCI.3967-10.2010.

Suminski, AJ, FR Willett, AH Fagg, M. Bodenhamer, and NG Hatsopoulos. 2011. "Continuous Decoding of Intended Movements with a Hybrid Kinetic and Kinematic Brain Machine Interface." In *Proceedings of the Annual International Conference of the IEEE Engineering in Medicine and Biology Society, EMBS*, 5802–5806. doi:10.1109/EMBC.2013.6609817.

Tan, D. W., M. A. Schiefer, M. W. Keith, J. R. Anderson, J. Tyler, and D. J. Tyler. 2014. "A Neural Interface Provides Long-Term Stable Natural Touch Perception." *Science Translational Medicine* 6 (257): 257ra138-257ra138. doi:10.1126/scitranslmed.3008669.

Tan, Daniel, Matthew Schiefer, Michael W. Keith, Robert Anderson, and Dustin J. Tyler. 2013. "Stability and Selectivity of a Chronic, Multi-Contact Cuff Electrode for Sensory Stimulation in a Human Amputee." *International IEEE/EMBS Conference on Neural Engineering, NER* 12 (2). IOP Publishing: 859–62. doi:10.1109/NER.2013.6696070.

Taylor, Dawn M., Stephen I. Helms Tillery, and Andrew B. Schwartz. 2002. "Direct Cortical Control of 3D Neuroprostheticdevices." *Science* 296 (5574): 1829–32. doi:10.1126/science.1070291.

Thach, W T. 1978. "Correlation of Neural Discharge with Pattern and Force of Muscular Activity, Joint Position, and Direction of Intended Next Movement in Motor Cortex and Cerebellum." *Journal of Neurophysiology* 41 (3). doi:10.220.33.2.

Thrasher, T.A., H.M. Flett, and M.R. Popovic. 2006. "Gait Training Regimen for Incomplete Spinal Cord Injury Using Functional Electrical Stimulation." *Spinal Cord : The Official Journal of the International Medical Society of Paraplegia* 44 (6): 357–61. doi:10.1038/sj.sc.3101864.

Tkach, D., J. Reimer, and N. G. Hatsopoulos. 2007. "Congruent Activity during Action and Action Observation in Motor Cortex." *Journal of Neuroscience* 27 (48): 13241–50. doi:10.1523/JNEUROSCI.2895-07.2007.

Todorova, Sonia, Patrick Sadtler, Aaron Batista, Steven Chase, and Valérie Ventura. 2014. "To Sort or Not to Sort: The Impact of Spike-Sorting on Neural Decoding Performance." *Journal of Neural Engineering* 11 (5). IOP Publishing: 56005. doi:10.1088/1741-2560/11/5/056005.

Tucker, Bonnie Poitras. 1998. "Deaf Culture, Cochlear Implants, and Elective Disability." *The Hastings Center Report* 28 (4): 6. doi:10.2307/3528607.

Tyler, Dustin J., and Dominique M. Durand. 2002. "Functionally Selective Peripheral Nerve Stimulation with a Flat Interface Nerve Electrode." *IEEE Transactions on Neural Systems and Rehabilitation Engineering* 10 (4): 294–303. doi:10.1109/TNSRE.2002.806840.

Velliste, M, S Perel, M C Spalding, a S Whitford, and a B Schwartz. 2008. "Cortical Control of a Robotic Arm for Self-Feeding." *Nature* 453 (June): 1098–1101. doi:10.1038/nature06996.

Venugopalan, L., P. N. Taylor, J. E. Cobb, and I. D. Swain. 2015. "Upper Limb Functional Electrical Stimulation Devices and Their Man–machine Interfaces." *Journal of Medical Engineering & Technology* 39 (8): 471–79. doi:10.3109/03091902.2015.1102344.

Vogel, J., S. Haddadin, B. Jarosiewicz, J. D. Simeral, D. Bacher, L. R. Hochberg, J. P. Donoghue, and P. van der Smagt. 2015. "An Assistive Decision-and-Control Architecture for Force-Sensitive Hand-Arm Systems Driven by Human-Machine Interfaces." *The International Journal of Robotics*

Research 34 (6): 1–18. doi:10.1177/0278364914561535.

Wahnoun, Remy, Jiping He, and Stephen I Helms Tillery. 2006. “Selection and Parameterization of Cortical Neurons for Neuroprosthetic Control.” *Journal of Neural Engineering* 3: 162–71. http://iopscience.iop.org/1741-2552/3/2/010.

Wei, Kunlin, Joshua I Glaser, Linna Deng, Christopher K Thompson, Ian H Stevenson, Qining Wang, Thomas G Hornby, Charles J Heckman, and Konrad P Kording. 2014. “Serotonin Affects Movement Gain Control in the Spinal Cord.” *J. Neurosci.* 34 (38): 12690–700. doi:10.1523/JNEUROSCI.1855-14.2014.

Werner, W, E Bauswein, and C Fromm. 1991. “Static Firing Rates of Premotor and Primary Motor Cortical Neurons Associated with Torque and Joint Position.” *Exp Brain Res* 86: 293–302.

Wessberg, J, Christopher R. Stambaugh, Jerald D. Kralik, Pamela D. Beck, Mark Laubach, John K. Chapin, Jung Kim, S. James Biggs, Mandayam A. Srinivasan, and Miguel A. L. Nicolelis. 2000. “Real-Time Prediction of Hand Trajectory by Ensembles of Cortical Neurons in Primates.” *Nature* 408: 361–65.

Wessendorf, Martin W., Herbert K. Proudfit, and Edmund G. Anderson. 1981. “The Identification of Serotonergic Neurons in the Nucleus Raphe Magnus by Conduction Velocity.” *Brain Research*. Vol. 214. doi:10.1016/0006-8993(81)90449-2.

Wilson, Blake S, and Michael F Dorman. 2017. “Cochlear Implants: A Remarkable Past and a Brilliant Future.” Accessed May 12. doi:10.1016/j.heares.2008.06.005.

Wodlinger, B., J. E. Downey, E. C. Tyler-Kabara, A. B. Schwartz, M. L. Boninger, and J. L. Collinger. 2015. “Ten-Dimensional Anthropomorphic Arm Control in a Human Brain−machine Interface: Difficulties, Solutions, and Limitations.” *Journal of Neural Engineering* 12 (1): 16011. doi:10.1088/1741-2560/12/1/016011.

Wolbring, Gregor. 2003. “Confined to Your Legs.” In *Living with the Genie*, 139–57.

Yin, Ming, David A. Borton, Jacob Komar, Naubahar Agha, Yao Lu, Hao Li, Jean Laurens, et al. 2014. “Wireless Neurosensor for Full-Spectrum Electrophysiology Recordings during Free Behavior.” *Neuron* 84 (6): 1170–82. doi:10.1016/j.neuron.2014.11.010.

Yoshida, K and Horch K. 1993. “Selective Stimulation of Peripheral Nerve Fibers Using Dual Intrafascicular Electrodes.” *IEEE Transactions on Biomedical Engineering* 40 (5): 492. http://dx.doi.org/10.1109/10.243412.

Zarzecki, P., and H. Asanuma. 1979. “Proprioceptive Influences on Somatosensory and Motor Cortex.” *Progress in Brain Research* 50 (C): 113–19. doi:10.1016/S0079-6123(08)60812-2.

8 Appendix

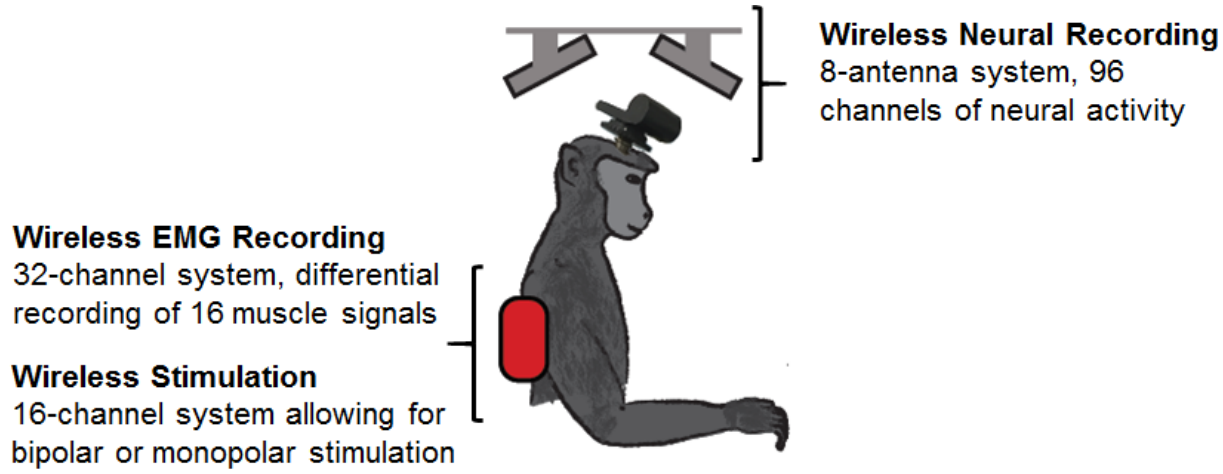

Figure 8-1. Wireless FES setup. This figure delineates the major components for wireless FES: wireless neural recording, EMG recording, and stimulation. Wireless neural recording requires a neural transmitter that attaches to the electrode array pedestal on the head, as shown here (not to scale). The EMG recording and stimulation components are housed in a backpack the monkey wears (shown in red).

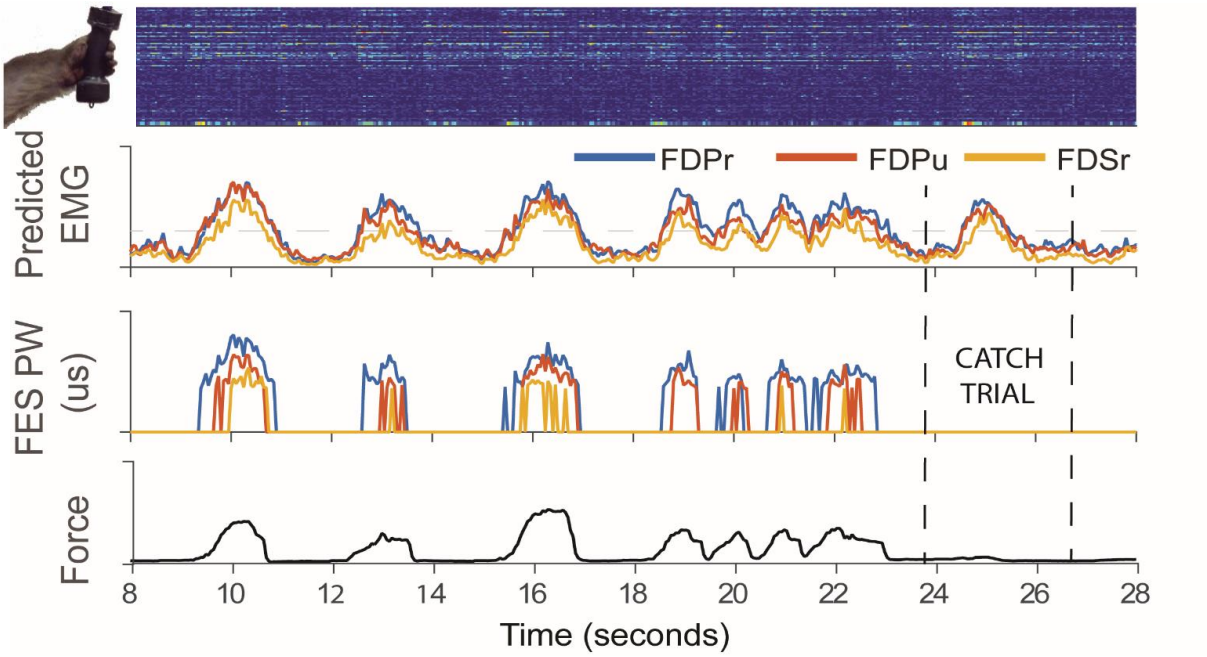

Figure 8-2. Wireless FES in the lab. The monkey was able to use the wireless system to restore functional grasp of finger flexors during a median nerve block. This figure demonstrates the ability to control a power grasp to squeeze a pneumatic tube and generate varying levels of force. During a catch trial, the stimulator was turned off, and despite the monkey's attempts, he was unable to generate force with his paralyzed flexors.

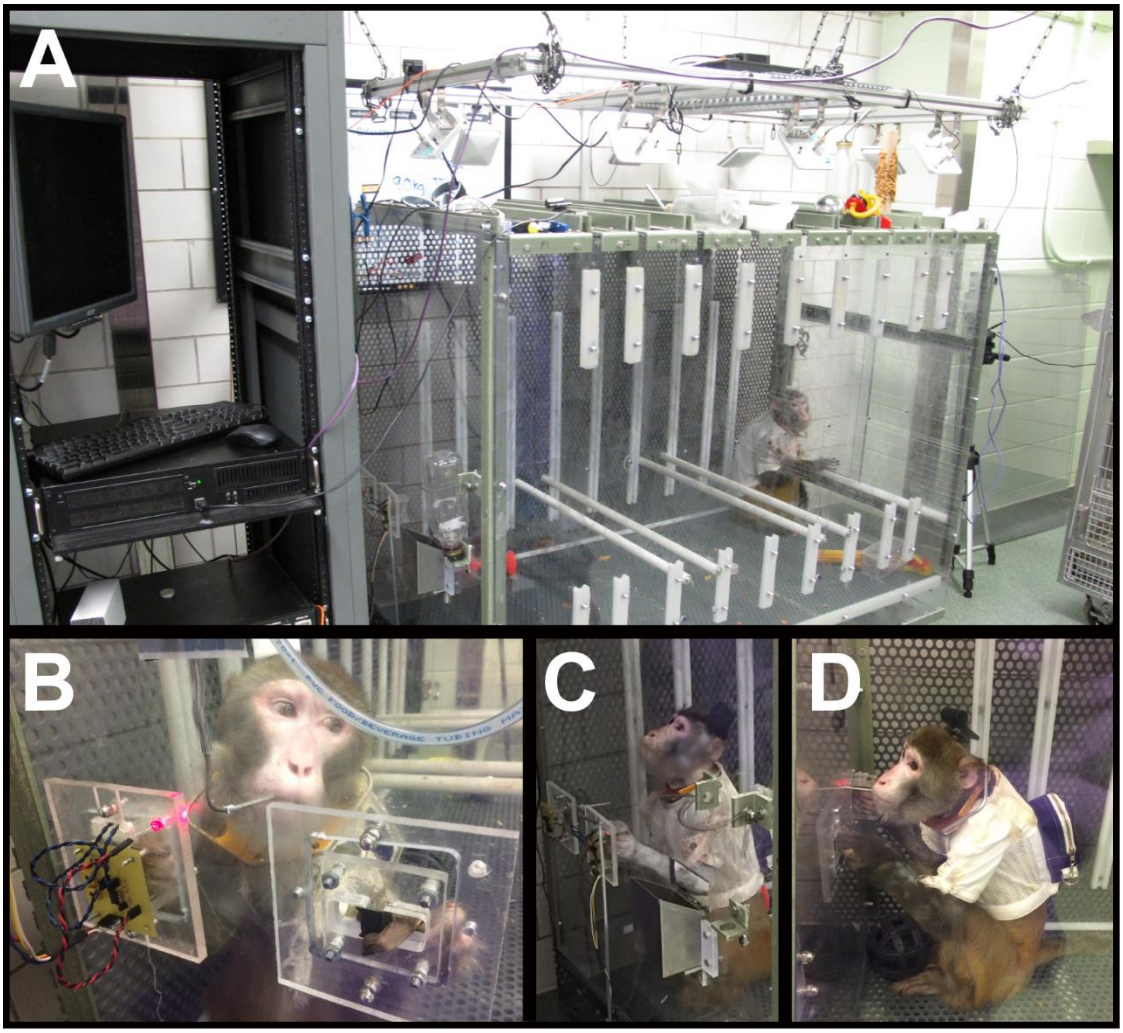

Figure 8-3. Wireless cage setup. During wireless FES experiments, the monkey is housed in a plastic cage (A) surrounded by antennas for wireless neural data acquisition. The cage includes holes through which the experimenter can give the monkey treats. There is also a bimanual grasp task set up at one end of the cage (B-D), with interchangeable manipulanda for pinch, key, or power grasp.

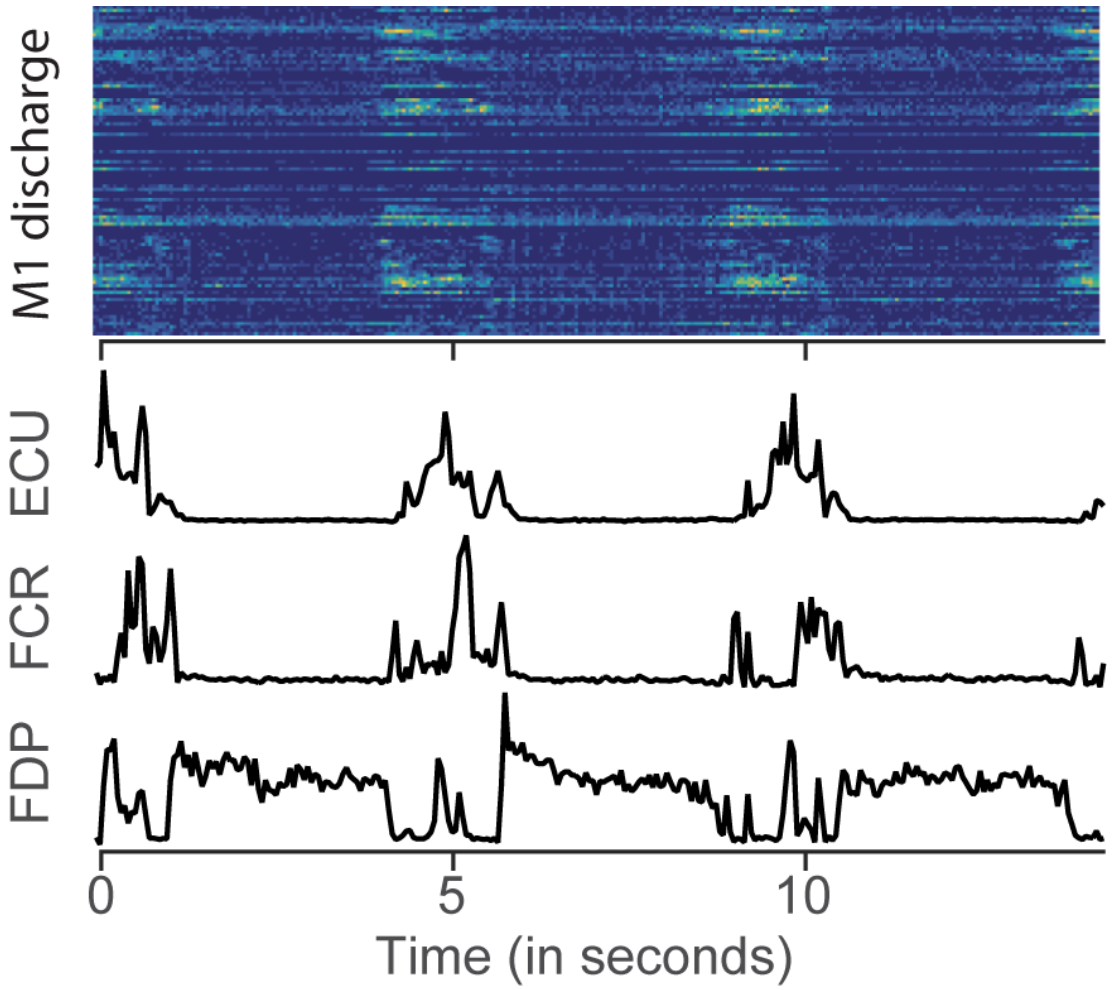

Figure 8-4. Example of wireless in-cage recordings of neural activity and EMG. This figure demonstrates the ability to wirelessly record neural activity and EMG activity in the monkey's home cage. These data were collected while the monkey performed a series of three power grasps using a manipulandum installed on one of the cage walls.